NASA Technical Memorandum 4007
DOE/SR/14075-1

Airborne Lidar Experiments at the Savannah River Plant

June 1985

William B. Krabill
Goddard Space Flight Center
Wallops Flight Facility
Wallops Island, Virginia

Robert N. Swift
EG&G Washington Analytical Services Center
Wallops Island, Virginia

National Aeronautics
and Space Administration

**Scientific and Technical
Information Office**

1987

TABLE OF CONTENTS

EXECUTIVE SUMMARY

Results are presented from a series of studies conducted at the Department of Energy (DOE) Savannah River Plant (SRP) with the NASA Airborne Oceanographic Lidar (AOL). These studies included a topographic survey of a ~1000 acre lake basin (presently designated L Lake) which had been excavated for use as a cooling pond for L Reactor; a study of the movement of discharged cooling water in Pond C and the warm arm of Par Pond using Rhodamine WT dye as a tag; initial baseline studies of the vegetation cover of the Steel Creek corridor (through which the outflow of L Lake is carried to the Savannah River); and a demonstration of potential forestry applications of the AOL. These investigations were conducted over a 3-day period in June 1985.

The AOL is an advanced airborne laser system capable of making temporal or time history measurements of laser backscatter (bathymetry mode) or spectral measurements of laser induced fluorescence from waterborne constituents (fluorosensing mode). The AOL is flown together with auxiliary instruments and camera systems on board a four engine P-3A aircraft. Recent modifications to the AOL allow in-flight changes between the two basic operational modes of the instrument which permitted the topographic study to be conducted on the same flights as the fluorescent dye study.

The L Lake topographic survey represents a state-of-the-art demonstration of airborne laser surveying capability. As expected, aspects involving real-time navigation and post-flight positioning represented the major problems associated with the investigation. Real-time navigation was accomplished using tethered weather balloons and fluorescent ground tarps as visual targets for the pilots. Post-flight positioning was determined from a combination of time-tagged aerial photographs and recognizable vertical features in the laser ranging records. The application of these techniques, coupled with data handling procedures developed by NASA for this project, resulted in completing a successful and internally consistent survey of the upper portion of L Lake. Contour and 3-dimensional isometric projections of the topographic relief of the lake bed are presented.

The AOL was used to measure the horizontal distribution of the dye in Pond C. Passes were flown over Par Pond and Pond C at several time intervals following the initial release of the dye. This time-series of dye surveys permits an assessment of the movement of the cooling water within the pond system for use in hydraulic models. The advantages of various forms of graphical representation of the data are discussed. Data is also presented on the vertical measurement of the dye within the water column. This latter application of the laser system is confined to the upper several meters of the water column due to the strong attenuation of the 580 nm dye fluorescence by the pond water.

The 1985 investigations of vegetation in the Steel Creek corridor were restricted to ranging and reflectivity measurements due to the relatively low output power of the laser transmitter. Measurements of plant height and reflectivity are used to characterize the vegetation along two flight lines. Future laboratory and airborne studies are planned which utilize higher power laser excitation at a wavelength of 355 nm. This arrangement would permit the measurement of laser induced fluorescence from the vegetation in addition to the height and reflectivity characteristics measured in the 1985 study.

The forestry investigations, which were not included in the joint study agreement between NASA and DOE, were conducted as a matter of opportunity and mutual interest at no extra cost to the project. Certain of the passes flown in conjunction with the L Lake survey were located over forested areas (representative of larger stands at SRP) which were easily truthed with ground surveys. A graduate student affiliated with the project is using the data for his doctoral dissertation. The results will be provided as soon as the dissertation is approved.

JUNE 1985 AIRBORNE LIDAR EXPERIMENTS AT THE SAVANNAH RIVER PLANT

W. B. Krabill
NASA Goddard Space Flight Center
Wallops Flight Facility
Wallops Island, VA 23337

and

Robert N. Swift
EG&G Washington Analytical Services Center
Wallops Island, VA 23337

1.0 INTRODUCTION

The NASA Airborne Oceanographic Lidar (AOL) was used in a series of experiments at the Department of Energy (DOE) Savannah River Plant (SRP), located in the vicinity of Aiken, South Carolina. These investigations, which were conducted in June 1985 were designed to determine the potential of an airborne lidar system for meeting environmental monitoring activities associated with plant operations. These facilities, which include nuclear reactors, separation facilities, cooling ponds, and other related structures, are spread over an area in excess of 770 square kilometers (km^2). Thus, due to the size of the facility as well as the nature of the operation, considerable advantage can be made of new sensors and methods for acquiring the monitoring information from remote sensing platforms, such as aircraft and satellites.

The AOL has proven to be a versatile instrument, capable of performing a number of seemingly unrelated investigations. The applications of the AOL which were of interest in the SRP studies include measurements of aquatic and terrestrial chlorophyll concentrations; fluorescent tracer dye; tree height, forest inventory and wetlands characterization; and topographic surveying. Improvements

to the basic lidar system during the past two years have allowed rapid reconfiguration of the instrument between the fundamental bathymetry (temporal) and fluorosensing (spectral) modes of operation. In addition, for certain applications, the sensor can acquire simultaneous temporal and spectral measurements. The fluorescence mode includes the simultaneous observation of both laser induced fluorescence (LIF) and upwelling passive solar spectra. The investigations at the SRP site took advantage of these new capabilities.

Investigations conducted during June 1985 included (1) the topographic mapping of a recently cleared stream valley which was in preparation for use as a cooling pond (L Lake); (2) hydraulic studies of discharged cooling water in Pond C and Par Pond using Rhodamine WT as a fluorescent tracer dye; (3) baseline mapping of wetlands in the Steel Creek area below L Lake; (4) timber volume estimates and related forestry applications; and (5) aquatic chlorophyll and photopigment measurements.

The basic study sites are shown in Figure 1. Due to the proximity of the various areas to be investigated and the nature of the studies, it was possible to devise a sampling plan which took maximum advantage of the aircraft sensors on the two major flight operations. Specifically, the hydraulic study, involving the use of fluorescent Rhodamine WT dye, was conducted in the Pond C and Par Pond system. These cooling ponds were also part of the aquatic chlorophyll and photopigment study. It was necessary to complete the studies related to the algae in these ponds prior to the introduction of dye that could potentially interfere with the active and passive spectral signatures from which information on chlorophyll and other algal pigments is determined. Thus, approximately one-half of the topographic investigation of the L Lake construction area was conducted during one mission along with the algal study from the Par Pond System. On the following day, the other half of the topographic mission was completed along with the dye study. During the latter mission, sets of passes were made over the Pond C and Par Pond system at four separate times during the course of the flight. Between each of the sets of dye passes, a number of topographic mapping passes were conducted. In this way, the temporal separation required

between the dispersing dye observations was realized in a cost effective manner.

The results from these investigations are discussed in separate sections following a brief discussion of the airborne lidar (AOL) instrumentation and techniques used to extract information from the backscattered laser radiation and/or resulting fluorescent emission from various ground targets. The Results Section will be followed by a discussion of new instrument capabilities developed since the SRP missions. These improvements and added techniques are expected to be of significant benefit in future applications designed to address remote sampling needs at SRP.

2.0 INSTRUMENTATION

Although the AOL has been in operation since 1977, the system has been continuously upgraded and improved as new technology has become available. During this time, the instrument has proven to be an extremely flexible tool capable of performing a broad range of applications in widely separated areas of marine and, more recently, terrestrial sciences. Originally designed to provide feasibility demonstrations and technology transfer to a number of interested federal agencies[1], the instrument has developed into a permanent facility at the NASA Wallops Flight Facility of the Goddard Space Flight Center. A number of the lidar applications thus far investigated are briefly reviewed below. More complete discussions of each of these applications can be found in the identified reference list.

2.1 Previous Instrument Investigations

The AOL has two basic modes of operation. In the bathymetry mode, either the backscattered laser pulse or a specific laser stimulated response is temporally resolved. The most obvious application of this mode is airborne laser hydrography where depth measurements are determined from the time separation between return pulses from the water surface and bottom. An extensive series of field tests of the instrument for this application was conducted by NASA during 1977 in cooperation with the Naval Ocean Research and Development Activity (NORDA) and the National Ocean Survey (NOS).

These results, which have been reported by NASA[2] (as well as by NOS in a series of internal publications), served in large part as the basis for the design of the NAVY's Hydrographic Airborne Laser Sounder (HALS). The AOL has also been used in joint hydrographic investigations with the U.S. Army Corps of Engineers and most recently the sensor package was reconfigured to test individual transmitter and receiver components of the HALS system. An additional application which utilized techniques developed in the hydrographic investigations has been the development of capabilities for overland surveying in forest covered areas[3] and for timber volume measurements[4].

The second basic mode of operation of the AOL is that of fluorosensing. Here the laser induced responses including the Raman backscatter from the water volume and fluorescence from waterborne constituents are spectrally resolved. Demonstrated applications include airborne mapping of deployed fluorescent dye[5], measuring the distribution of chlorophyll and other photopigments contained in phytoplankton[6], and delineating the boundaries of marine fronts[7].

Common to both the bathymetry and fluorosensing mode is the capability to provide altimetry data in which the slant range (laser pulse transit time) between the aircraft and the surface target is measured.

2.2 AOL System Description

The AOL hardware configuration has been described for the bathymetry[2] and fluorosensing[8] modes of operation. These modifications are discussed in detail in the next section. The basic system layout is shown schematically in Figure 2 which should be referred to during the discussion below. The transmitter and receiver portion of the system are contained in a three-tier optical table which has been ruggedized for an aircraft operational environment. The laser transmitter, together with beam forming lenses and steering mirrors, is situated on the upper tier. The second tier contains the receiver telescope, the return backscatter reforming optics, the photomultiplier tube (PMT), fluorosensing spectrometer and power supply. The

third tier consists of one last folding mirror and the scan mirror/ off nadir adjustment mount.

2.2.1 Transmitter

Part of the unique flexibility built into the AOL is the relative ease in which different laser transmitters can be exchanged to provide specific wavelengths or other special characteristics of a particular laser for a desired application. During the past eight years, nine different lasers have been utilized as the transmitter on the AOL at various times. In some experiments two lasers have been utilized at the same time by firing them successively on alternating pulses[9]. In the 1985 SRP studies, an experimental model of a frequency doubled Nd:YAG laser (532 nm output wavelength) was utilized as the transmitter. This laser was especially developed as an operational prototype by the AVCO-Everett Corporation under contract with the U.S. Navy. The pertinent specifications for the laser are provided in Table 1.

TABLE 1. HALS LASER SPECIFICATIONS

Output Energy	2 mJoules peak pulse energy
Pulse Duration	12 nanoseconds
Pulse Repetition Rate	400 pulses per second
Beam Divergence (variable)	5 mrad used
Emission Wavelength	532 nm

The high pulse repetition rate, narrow pulse width, and moderate pulse power make this laser especially attractive for surveying applications. Although this laser performed quite well for the L Lake topographic survey and the fluorescent dye studies, which were viewed as the primary investigations, internal timing problems related to operating the laser at peak power levels prevented the acquisition of any pigment data in the algal studies. A different approach with a more powerful laser transmitter was utilized for the 1986 investigations. This aspect will be expanded in Section 4.

The transmitter portion of the instrument includes the beam forming and steering optics. The beam size was controlled with a beam expander and collimation lens assembly which was located just outside of the laser head. For reasons of "eye-safety" the beam collimation was set at 5 mrad which corresponds to a laser "footprint" diameter of approximately 1.5 m at the 300 m flight altitude maintained for most of the survey work. The dye studies were conducted from a somewhat lower altitude of 170 m which provided a "footprint" diameter of 0.85 m. Dielectric mirrors, especially coated for a 45° incidence angle at a wavelength of 532 nm, were used to fold the beam from the upper tier downward through a diplexer mirror which is positioned immediately in front of the collecting telescope. The diplexer mirror is designed to allow co-alignment of the transmitter and receiver paths. The outgoing beam passes through a hole bored through the center of the mirror, whereas the expanded backscattered light is primarily reflected into the telescope. The two remaining mirrors are shared between the transmitter and receiver portions of the instrument.

The two mirrors are used in combination to control the off-nadir incidence angle of the laser beam. The first of these is a simple front surface folding mirror set at 45° from horizontal. This mirror folds the beam 90° to the angle adjustable scan mirror which can be controlled to provide incidence angle settings at 0, 5, 10, and 15°. A 15° setting was utilized for all of the experiments at SRP. The mirror is locked in an aft-pointing position when profiling data is desired. To provide scanning data, the mirror is motor driven at five revolutions per second. The rotational position of the scanning mirror is provided by a shaft-mounted scan azimuth encoder which is digitized and recorded along with the laser related information. The resulting scan pattern is roughly elliptical in shape and has a diameter equal to approximately 50 percent of the altitude at the 15° mirror setting. This sampling pattern will be readily apparent in some of the figures presented with the results from the dye mapping investigations.

2.2.2 Receiver

The arrangement of the receiver optical components is shown in Figure 2. A 30 cm diameter Cassegrainian telescope is used to collect the backscattered light from the surface target. Additional beam collimating and steering optics are shown in the upper portion of the schematic illustration. The receiver field-of-view (FOV) is controlled by a pair of operator adjustable knife-edges. The FOV is controllable between 0.1 and 20 mrad. During these experiments the FOV was maintained at slightly larger than the 5 mrad divergence setting of the transmitted laser beam.

During the topographic survey investigation, all of the captured backscattered laser light was focused on a 12-stage photomultiplier tube (PMT) located at the end of the optical assembly. Ambient light rejection was accomplished with a 10 nm wide, narrow band filter centered on the 532 nm laser transmitter wavelength. The signal from the "bathymetry" PMT is linearly amplified by a factor of 100 and routed from the optics table to the system control racks. There, the signal is electronically fanned out or reproduced 36 times and routed to separate LeCroy 2249SG charge digitizers (CD's). The temporal aperture of the CD's is set to provide an integration window of ~4 nsec. Individual channels are separated by 2.5 nsec yielding some overlap which is useful for relatively fine (< 30 cm) distance determinations. For more coarse applications such as tree height measurements where distances greater than 12 m must be spanned, a 5 nsec separation between the CD's is utilized. The signal from the bathymetry PMT is also used to measure the transit time (slant range) of the laser pulse between the aircraft and the ground target.

During the fluorosensing investigations, a split mirror is inserted in front of the system spectrometer shown in the upper portion of Figure 2. A small amount of the returning signal is allowed to continue through to the above bathymetry PMT in order to provide slant range measurement and timing for the digitization of the laser-induced signal by the spectrometer. The backscattered signal passing into the spectrometer is spectrally dispersed with a diffractive grating. The dispersed light falls on 36 individual light guides (of which only 32 are currently calibrated) arranged in

the focal plane of the spectrometer. The on-wavelength laser radiation is rejected from channels redder than 532 nm with wafers (individually cut from Kodak #22 long-pass filters) placed immediately in front of the light guides. The light guides are connected to individual PMT's with fiber-optical cables. The voltage (and thus the sensitivity) of each of the PMT's is maintained with a programmable 32-channel power supply under control of the system computer.

The signal from passive solar upwelling radiation is separated from the wide bandwidth laser induced signal by straightforward electronic filtering. This aspect, together with procedures developed for the calibration of the spectrometer using an illuminated calibration sphere, have recently been described in detail[10,11]. The digital output from the CD's and the slant range timer is then interfaced through a CAMAC crate to a Hewlett-Packard 1000 E-series computer where (along with other ancillary digital information) it is recorded on standard nine-track computer tapes.

2.2.3 Real-time Software and Data Handling

The development of a flexible real-time software and data handling package has evolved during the past 8 years and continues to improve as other applications are addressed. The present system is able to accommodate the simultaneous operation of two lasers. Many aspects related to the acquisition and recording of data are presently under computer control. These aspects include regulation of voltage to the bathymetry PMT (or multiple PMT's in the fluorosensing mode), setting laser pulse repetition rate, adjusting receiver gating and delay, buffering and recording laser return waveform data, and recording information from auxiliary components connected with AOL operation. Switching between the bathymetry and fluorosensing modes of operation is now done under computer control (except for the insertion of the split mirror in front of the spectrometer). In addition to the primary HP 1000 E-series computer, other microprocessors are tasked to preprocess incoming data and to run the real-time displays used by the operators for quality control.

2.2.4 Ancillary Measurement Capability

Information from a number of auxiliary components and instruments is captured and recorded along with the other AOL data. A Litton LTN-51 Inertial Navigation System (INS) provides continuous updates on aircraft pitch and roll and samples heading, track angle, ground speed, and position information every 250 msec. Water surface temperature from a Barnes PRT-5 infrared radiometer is collected and recorded with each laser pulse. A 35 mm flight research camera controlled by an intervalometer is operated with the instrument package to assist in post-flight horizontal positioning of the lidar data. An inset within each camera frame photographs an LED display of time of day which is slaved to the same digital time controller sampled by the AOL computer. An event flag triggered by the intervalometer is recorded in the AOL data stream, thus allowing further registration of the laser data with the photographic records.

3.0 EXPERIMENT DESCRIPTION AND DISCUSSION OF RESULTS

The various sites for the AOL studies at SRP are shown in Figure 1. A total of four missions were flown in conjunction with the investigations. The initial mission consisted of two photographic passes over the L Lake and Steel Creek sites at the end of the transit flight to SRP on June 12, 1985. The aerial photographs, which were acquired with a 9-inch format T-11 photogrammetry compatible camera from an altitude of 1830 m (6000 ft), were taken to document the ground cover at the time of the flight and to assist in horizontal control. On June 13, approximately half of the L Lake topography passes were flown along with two passes over Par Pond, Pond B and Pond C to assess information on the distribution of algal pigment concentrations in those water bodies. The topographic measurements of the L Lake site were completed on June 13 as were the first four sets of time-study dye distribution passes over Par Pond and Pond C. Two of the L Lake passes were extended through the Steel Creek corridor to gather baseline information on wetlands vegetation. Additionally, several of these passes were located in areas of interest to SRP for demonstrating the capability of the AOL for acquiring useful forest management information. Finally, an addi-

tional set of passes were flown over Par Pond and Pond C on the morning of June 15 to complete the dye study prior to beginning the transit flight back to the Wallops Flight Facility. The results from these individual studies are described separately below.

3.1 L Lake Topographic Mapping

The largest task undertaken as part of the 1985 SRP investigations in terms of both flight time and subsequent reduction and analysis was the topographic survey of the excavated Steel Creek flood plain located adjacent to the L Reactor. The project served as an ideal opportunity for NASA to provide a practical, large-scale demonstration of techniques previously developed in joint projects with the U.S. Army Corps of Engineers[3,13] and the U.S. Forestry Service (results not published). Based on these results and the need for improved topographic information, DOE requested NASA to survey the upper half of the lake. The topographic information, in both digital form and in contoured diagrams, was needed by engineering personnel at SRP for future hydraulic modeling of the flow patterns.

This portion of the final report is intended to document the techniques utilized to acquire the airborne topographic data and methods used in the subsequent processing and analysis of the information to produce useful mapping products. The most difficult aspect related to this application is associated with horizontal and vertical control. Careful planning and real-time coordination was necessary to provide the navigation control, on the scale required (±30 m of the intended ground track) to ensure that complete coverage was obtained from a minimum number of passes which were arranged with ~20% overlap. Moreover, previously developed techniques for the horizontal registration and vertical control of the laser ranging information had to be refined to provide the resolution required for the survey products.

L Lake is now a 1000 acre cooling pond for L Reactor at the Savannah River Plant. Figure 3 shows the extent of L Lake in the stippled area, and cultural features in existence prior to construction. At the time of the 1985 AOL mission to SRP, the majority of the lake was cleared, and construction of the dam was under way.

During the planning of the 1985 mission, it was determined that data to provide the survey of the entire lake could be collected by simply extending many of the flight lines by an additional 30 seconds. As a result, the data set needed to map the entire lake (with the exception of the area around the dam, which was under construction) was collected, and has been 90% processed. The topography of the upper half of the lake basin, in the form of contour maps and a digital image on computer tape has been finalized.

The requirements and constraints of conducting laser mapping for an area the size of L Lake are many and varied. The state-of-the art in navigation/positioning systems available to the AOL project at that time was the most extensive limitation. Our data requirements dictated complete laser scanning coverage of the entire lake. However, to accomplish the necessary vertical and horizontal control, it was necessary to extend the mapping lines to include coverage of areas adjacent to the L Lake site which were associated with identifiable features useful for registration. Four passes were reoccupied with the scanner turned off to provide high density profile data for additional control. The selected set of lines are shown in Figure 4 (every other line is actually drawn) and the resultant coverage is provided in Figure 5.

The real-time navigation requirements were met through use of a series of weather balloons tethered just above tree-top level along various roadways. A ground team pre-surveyed and marked each balloon location on the day before the mission. Typically, three balloons were deployed on each flight line. Each balloon was manned by two people, and constant radio contact was maintained between the aircraft and the ground parties. At the immediate conclusion of each data pass, the Project Scientist would make a determination whether or not the navigation for the desired line was adequate. If the line was satisfactory, the ground teams would then proceed to deploy the balloons at the pre-surveyed positions for the next line. The passes were accomplished by flying in a race track pattern which required 6 to 8 minutes per line. This allowed adequate time for each ground crew to occupy the new flight line and deploy balloons. The technique worked so well that none of the 26 passes needed to be repeated.

3.1.1 Base Map Registration Data

The positioning associated with the raw data is relative to the trajectory of the aircraft. For practical utilization, the laser measurements must eventually be registered to a satisfactory ground coordinate system on a pass-by-pass basis. SRP has developed a coordinate system for local use which is related to North American Datum by a rotation of 36°, 22 minutes. Since SRP has a large number of map products based on this system, it was the choice for the base map on which to register the laser data. SRP supplied the AOL project with a series of engineering maps called "3302's" which had been produced for the entire plant area in the 1950's and periodically updated. These maps were contoured in five-foot intervals at a horizontal scale of 1:1200 and were further annotated with cultural features. For each of the 3302's in the study area, the horizontal location at which each contour line crossed the crown of a roadway was digitized and annotated with the corresponding vertical value. Thus a detailed set of comparison/referencing data was compiled. SRP also provided NASA with a computer tape containing a digitized ground survey of the 190-foot contour for the L Lake area (which was the planned water level). These two digital data sets formed the basis for horizontal and vertical referencing of the laser data.

3.1.2 Data Processing and Analysis

A combination of sensors, data types, and algorithms was utilized in the process of post-flight positioning. The specific instruments and their respective data types are given in Table 2. The LTN-51 Inertial Navigation System (INS) utilized by the Wallops Flight Facility P-3 aircraft has especially modified software to provide a subset of the normal digital data stream at a higher data rate (four samples per second), which is more suitable for integration into a continuous trajectory. The vertical acceleration data was sampled and recorded at the pulse repetition frequency (PRF) of the laser, in this case 400 Hz. Aircraft attitude parameters (pitch and roll) were also recorded at the laser PRF. Time of day was supplied onboard the aircraft to a precision of one millisecond.

TABLE 2.

Sensor	Make/Model	Measurement/Data
Accelerometer	Columbia Model 100	vertical acceleration
Inertial Navigation System	Litton LTN-51	track angle, horizontal velocity, heading, attitude
Video Camera and Recorder		video record of ground track
Flight Research Camera		35mm record of ground track

Vertical control for each pass was accomplished utilizing a technique involving the integration of vertical accelerometer data. In post-mission analysis, the acceleration data is integrated twice, and combined with three or more known reference points. These reference points are typically laser ranges which can be associated with recognizable features in the data, such as the crown of a road, or to a flat area where horizontal position adjustments of the laser footprint would produce negligible vertical changes. The resultant vertical trajectory is subsequently evaluated for the altitude of the aircraft corresponding to each laser range measurement. The accuracy of the technique is a function of the geometry of the reference point locations (equal spacing is best), and a function of wind gusts. Assuming light winds and well-distributed reference points, the resultant trajectory is of the same accuracy as that of the reference points. This technique has been described in detail by Krabill and Martin[12].

Horizontal control was primarily obtained from the aircraft INS. The horizontal information from the INS is considered to be precise in a relative sense for short time periods of one to several minutes. Thus, once the time-position of one point in a pass is known, the entire pass is then registered horizontally.

Registration of the laser data was an iterative, "boot-strapping" process. The analyst processing the data needed reasonably good horizontal control in order to determine areas of known vertical position in the laser data. However, a reasonably good vertical

trajectory was frequently needed in order to recognize horizontal features. Initial estimates of the position of the aircraft as it crossed major roads were obtained from the 35 mm flight research camera prints, or from the down-looking video recording. Using this estimate of horizontal position, the pass of data was processed through algorithms which integrated the positioning information to reference the horizontal location of the footprint for each laser measurement. This initial referencing iteration was next compared to existing survey information on the surrounding area. This task was facilitated by utilizing digitized versions of the registration data supplied by SRP, which permitted an automated comparison with a computer.

The software developed by the AOL project team for the registration task was used to compare each point in the laser data file with the available digitized survey data. The observations were "ranked" according to the X coordinate in the SRP system prior to the comparison in order to minimize computer time for this and other subsequent processing. The software extracted corresponding samples from the two data sets which were within a selectable horizontal distance apart, and produced a computer file. This file could be analyzed graphically or examined manually for quality control, or selection of new points for vertical control to be incorporated into the next iteration.

Part of the bootstrapping technique involved the utilization of previously registered laser data to assist in referencing each new pass. The detail available in the laser data, particularly in profiling, provided considerable strength in the registration process. To initiate the registration process, the principal profile pass (18/2) which was located in the center of the upper part of the lake (Figure 6), was subjected to very intensive analysis. Detailed plots of this pass were made at the various road crossings. An example of this analysis is shown in Figures 7, 8, and 9. Figure 7 is a "stick diagram" showing a portion of pass 18/2 in the vicinity of the intersection of Road B with Road C. Each individual stick represents a discrete elevation measurement. The base of the stick indicates the location of the measurement in x and y coordinates while the length

of the stick indicates the relative height obtained at that location. A second "stick diagram" (shown in Figure 8) provides an expanded view of the Road B crossing shown in Figure 7. The finer resolution available at this scale permits the recognition of features within the laser elevation profile. Road B consists of two individual pavements separated by a grass strip as illustrated in Figure 8. The rounded surfaces of each of the pavements as well as the depressed grass covered area are quite apparent in the "stick figure."

The road features are even more apparent in the cross-sectional plot shown in Figure 9 where the individual laser elevation measurements are plotted as a function of distance along the x-axis. Notice, in particular, the five "+" symbols that lie approximately 10-15 cm above the remaining observations acquired between pixel location 1549 and 1551. The location of these elevated measurements correspond to two bright, sand covered patches along the berm of the road and to the painted lines (along both sides of the roadway as well as a line which separates the roadway into two lanes). The large backscattered laser return from these very reflective targets cause the range tracking hardware to trigger early resulting in the apparent 10 cm to 15 cm offset seen in the cross-section in Figure 9. The other road crossings were similarly examined and were found to have a sufficient number of unique features in the laser topographic profile to provide horizontal positioning at an accuracy of one to two meters. Given this level of horizontal control, flat areas of known elevation were able to be selected with sufficient reliability to provide vertical reference points accurate to within 20-40 cm. Pass 18/2 thus became the foundation for positioning the rest of the data set.

The next step in processing the topographic data was to register pass 18/1, which was the scanning pass repeated over the same line as 18/2. Because of commonality of formats, we were able to use information from the already registered 18/2 in the intercomparison software along with the SRP survey data to position 18/1. According to our original design, pass 18/2 also had a considerable overlap with both scanning passes 17/1 and 19/1. In like fashion, we were able to register these two passes using the survey data and pass 18/2. The

coverage provided by the resultant data set is illustrated in Figure 10. The ground track of pass 18/2 (profiling) can be seen as connected "squares" surrounded by the swath coverage associated with the three scanning passes. The extent of the scan coverage is indicated by the distribution of the small symbols. Intercomparisons between corresponding pixels from 18/2 and two of the scanning passes are shown in Figures 11 and 12. In these figures, the individual elevation measurements from the pass 18/2 (profile) are shown as small "dots" while the elevation determined for each pixel from the respective scanning passes is shown as a solid, connected line. As can be seen in the figures, there is quite good agreement except in the areas covered by the trees.

3.1.3 Terrain Correlation Analysis

The processing described thus far has involved the preprocessing stage, i.e., integration of vertical and horizontal positioning, ranking the data according to position, and intercomparison with other data sets and available SRP survey information. The next step was to place the individual samples collected with the conical scanner of the AOL into a rasterized, evenly gridded format. At this stage additional adjustment and verification of horizontal positioning was accomplished via a statistical technique, whereby the coefficient of correlation was calculated for the overlapping portions of two rasterized data sets. As the data is passed through the program, the indices are sequentially offset by typically ±1, 2, and 3 pixels in both coordinates, thereby creating a 7 X 7 matrix of coefficients for analysis. Table 3 is an example of the correlation analysis of pass 18/1 with 17/1. In Table 3, the first 7 x 7 group is the number of samples in the overlap area, for the given set of indices. The second group is the corresponding coefficient of correlation. The software can provide either a comparison of two individual passes, or of an individual pass and a composite made by merging several other passes. This algorithm became a powerful tool in the processing and merging of the remaining data passes. Thus, as each new pass was registered and amalgamated into the base map, more information became available to position the remaining data. Table 4 shows the final

correlation coefficients obtained by way of verifying the quality of the horizontal control. Note that no coefficients are present for passes which did not overlap.

TABLE 3. NUMBERS OF SAMPLES AND CORRELATIONS BETWEEN THE OVERLAP PORTIONS OF PASSES 18/1 AND 17/1

	-3	-2	-1	0	1	2	3
-3	3411	3686	3866	3887	3867	3853	3784
-2	3405	3638	3804	3891	3868	3827	3719
-1	3545	3802	3990	3982	3945	3887	3800
0	3520	3742	3910	3967	3907	3808	3694
1	3624	3903	4001	3984	3931	3861	3747
2	3563	3779	3879	3923	3852	3735	3623
3	3641	3906	3908	3902	3843	3747	3623

	-3	-2	-1	0	1	2	3
-3	.916	.920	.930	.935	.936	.931	.924
-2	.926	.940	.949	.953	.951	.946	.936
-1	.939	.934	.960	.970	.967	.958	.943
0	.946	.964	.977	.982	.974	.956	.937
1	.948	.964	.975	.974	.960	.947	.930
2	.946	.954	.956	.951	.945	.931	.918
3	.929	.931	.932	.930	.926	.918	.910

TABLE 4. CORRELATIONS BETWEEN ADJACENT PASSES IN THE UPPER PART OF THE LAKE.

	16/1	17/1	18/1	19/1	20/1	18/2
15/1	.98	.99				
16/1		.98	.98			
17/1			.98	.97		.98
18/1				.96		.98
19/1					.97	.99

The gridding and merging process places each sample into an evenly gridded format, keeping track of the mean and the total number of samples in each pixel. Principally because of computer memory restrictions, a ten meter pixel size was chosen for this data set. The resultant matrix, or Digital Terrain Model (DTM), is the product

of merging over 500,000 individual spot elevations from the laser system, covering all of L Lake and parts of the surrounding area.

Following the assessment of data quality, the combined base map was then processed through a program which "filled" pixels containing no observations. Values to fill the empty pixels were calculated from the surrounding elements using the inverse square of the distance between the respective pixel centers as a weighting factor. The resultant "filled" base map in this form is suitable for computational purposes including the calculation of volume or use for flow models. The utilization of the topography data (now bathymetry) for estimating the flow of cooling water from the reactor is, of course, beyond the scope of this paper. However, the filled base map is not suited for direct use in programs to create isometric or contour projections unless the particular software package that is used has provisions for locally smoothing the data. For practical utilization in our contour package we found that smoothing each pixel with values from the surrounding pixels produces more satisfactory results. The smoothing computation consisted of independently averaging each pixel with the mean value from the eight surrounding pixels. Figure 13a is an isometric projection of the northern part of the lake bed. Figure 13b is a contoured map of the same area with elevations given in meters. Several features are apparent in the figures. These features include (1) a depressed discharge canal in the upper portion of the lake where the heated water from L Reactor is introduced; (2) an elevated dome-shaped area, a portion of which is positive and forms an island in the lake which is currently filled; and (3) an area covered by trees which appears as very high, jagged region in the isometric projection. The locations of these features are labelled within the figure.

The mapping of the L Lake cooling pond at SRP with a scanning airborne laser system has produced results that we feel are consistent with the present state-of-the-art in topographic mapping. This project afforded a relatively ideal setting for evaluating the sensor for this application. The area to be surveyed was surrounded by roads which were reasonably discernible in the laser ranging data, especially in the non-scanning passes. Moreover, comparatively

detailed surveys of the surrounding roads and the 190' contour of the lake were also readily available for use in registering the passes. As expected, the greatest difficulty in conducting this project, and ultimately the largest source of error, was the establishment of horizontal control.

3.2 Par Pond and Pond-B Dye Studies

A total of eight passes were flown over the Par Pond system (Figure 14) following the release of the dye on June 14. Six passes were flown during the June 14 mission and another two prior to transiting to Wallops Flight Facility on the morning of June 15. The temporal distribution of the passes is provided in Table 5. The initial set of two passes and the first pass of the second set were not successful due to a delay setting inadvertently left in the AOL digitization subsystem. This delay setting, which was recently put under computer control, was necessary for the metric surveying of L Lake but should have been changed to acquire the fluorescence signal from the deployed dye. The remaining sets of passes, however, were

TABLE 5. PAR POND/POND C DYE PASSES

PASS #	DATE (1985)	TIME	ELAPSED TIME (from release of the dye	DATA SET #
1	JUNE 14	16:39:29	2:22:29	1
2	JUNE 14	16:44:25	2:27:25	1
3	JUNE 14	17:47:58	3:30:58	2
4	JUNE 14	17:53:29	3:36:29	2
5	JUNE 14	19:03:38	4:46:38	3
6	JUNE 14	19:08:42	4:51:42	3
7	JUNE 15	10:14:15	19:57:15	4
8	JUNE 15	10:20:28	20:03:28	4

of high quality and are adequate for evaluating the potential of an airborne fluorosensor for dye mapping applications. For discussion in this report, only the results from the mission flown on June 15 are shown. These are the most useful for descriptive purposes since the dye was distributed and observed over the entire portion of Pond C and was detected in the warm arm of Par Pond.

The general flight track used during the dye studies extended from Par Pond, across the dam of Pond C at the "bubble-up", and then up the main axis of Pond C. The ground tracks of the aircraft on the last two sets of passes are shown in Figures 14 and 15. The AOL was operated in a scanning mode during all of these passes. The width of the AOL sampling swath was approximately 100 m or about 50% of the altitude of the aircraft above the surface of the ponds. The intent of the sampling strategy was to make observations up the middle portion of Pond C, as well as the warm arm of Par Pond rather than to provide complete coverage since it was recognized that this swath diameter was insufficient for full coverage in just two passes. On each of the sets of two passes an attempt was made to provide as much coverage as possible by offsetting the passes to opposite sides of the center of the dam at the bubble-up.

The AOL was configured in the fluorosensing mode during the entire series of dye passes. Laser-induced fluorescence (LIF) data were recorded with the spectrometer adjusted to acquire spectra in 32 contiguous channels over a 360 nm interval between 370 nm and 730 nm. Figure 16 is a sample airborne LIF spectrum obtained on the initial June 15 pass and is typical of those obtained on the other passes. Figure 17 is a laboratory LIF spectrum procured in the Wallops Laser Laboratory from a sample provided by SRP personnel during the airborne dye study. Spectral peaks have been labelled in both figures. Several important aspects can be seen when comparing the two spectra. The finer resolution in the laboratory spectrum is apparent. The broad spectral peak from the Rhodamine WT dye LIF (centered near 580 nm) is easily seen in both spectra as is the on-wavelength laser backscatter at 532 nm. Notice that the strong laser backscattered signal is spread over a number of channels bluer than the 532 nm laser wavelength in the airborne spectra while it remains relatively narrow in the laboratory spectrum. The strong on-wavelength laser backscatter is rejected from redder channels in the AOL spectrometer through the use of Kodak #22 long pass filters covering each of the light guides of the longer wavelength channels.

The lack of a water Raman backscatter line (located near 645 nm) is obvious in both the aircraft and laboratory spectra. The Raman

signal provides a built-in reference for normalizing the LIF signals to compensate for variations in water attenuation properties. The Raman signal provides a built-in reference for normalizing the remaining LIF signals to compensate for variations in water attenuation properties. The utility of normalizing chlorophyll LIF with the water Raman signal has been demonstrated in experiments conducted over marine[6] as well as fresh[14] bodies of water. The laboratory spectrum, in particular, indicates a problem which must be addressed when using a 532 nm laser excitation source to study Rhodamine WT dye. Notice that, at a sensitivity setting sufficient to provide a fluorescence signal that spans most of the 1024 count field (available with 10 bit resolution), no measurable Raman signal is present around 645 nm. The concentration of dye utilized to generate the spectrum shown in Figure 17 was determined by SRP support personnel to be 71.7 ppb. If the sensitivity of the laboratory spectrometer were increased to a point where the Raman signal were to become measurable, the dye fluorescence would, of course, become too large to be digitized within the allowable resolution span. This problem remains even at concentration levels well below 10 ppb. Changing to a shorter wavelength laser excitation source appears to satisfactorily resolve this problem. In our laboratory investigations, which were conducted using a 337 nm nitrogen laser, we were able to resolve separate Raman and dye peaks at 385 nm and 590 nm, respectively. However, the attenuation of 337 nm by the pond water is very strong, and accordingly it would not provide a useful transmitter wavelength for depth resolving the dye concentration. In recently completed investigations at SRP, 355 nm from a frequency tripled Nd:YAG laser was used successfully to stimulate the dye and Raman backscatter. This aspect will receive further treatment in the final section of this report.

Although the presence of the Raman signal will ultimately be required in order to make the use of an airborne lidar for operational mapping of entrained fluorescent dye, the lack of a Raman signal in the airborne data is not considered particularly serious for the interpretation of this initial data set and for the evaluation of the potential of an airborne laser fluorosensor for this

application. In the interpretation of subsequent results, it will be assumed that the water attenuation properties were approximately the same throughout Pond C and the warm arm of Par Pond. This is a fairly reasonable assumption since there was no high run-off during the week prior to the experiment and since considerable mixing is apparent in Pond C when the reactor is in operation.

Results of recent flight tests conducted at Wallops have indicated that the failure to acquire a measurable water Raman signal with the Navy's HALS laser is due to the relatively low peak pulse power of that transmitter and due to the relatively high dynamic range difference between the signal strength of the dye fluorescence and the water Raman signal at dye concentrations above ~5 ppb. The use of a more powerful Nd:YAG laser such as the one used to successfully acquire a Raman signal in marine investigations[9] was precluded in the SRP investigations for eye safety considerations. This problem is common to the investigations aimed at measuring concentrations of algal pigments at SRP which are discussed in another portion of this section. Discussion on the use of a higher power laser operated at 355 to resolve this problem will be expanded in Section 4. Near visible, UV wavelengths have considerably higher permissible eye exposure limits.

Water surface temperature data was acquired along with the LIF spectra. Information from a calibrated PRT-5 infrared radiometer was recorded with each laser pulse. The radiometer sensor head is mounted in a separate port near the AOL scan mirror assembly. The radiometer sensor is stationary and nadir-looking, thus the water surface temperature cannot be associated with each individual laser point when the AOL is operated in a scanning mode. Moreover, the range over which the instrument was set to operate was not sufficient to allow recovery of thermal information from the warmest portion of Pond C. Independent findings at SRP as well as in the Wallops Laser Laboratory indicate that water temperature significantly lowers the fluorescence quantum efficiency of Rhodamine WT dye. The results, presented in Figure 18, are not in agreement in either magnitude or in the shape of the curve. The figure shows both sets of data plotted as a function of fluorescence signal versus temperature. The

SRP results are linear and indicate a lower dependence of fluorescence on temperature than are shown in the results from the Wallops Laser Laboratory on several successive runs. The SRP results were obtained with a continuous wave (CW) source in a standard laboratory spectrometer while the Wallops results were obtained with a short pulse nitrogen laser source and viewed with a time gated spectrometer. Presently, however, no explanation has been offered for this discrepancy in results. This disparity remains as an issue to be investigated during future studies. Figure 18 also shows dissolved organic fluorescence plotted as a function of temperature. These results, obtained in the Wallops Laser Laboratory indicate that the reduction in the quantum efficiency of the dissolved organic matter due to an increase in temperature is considerably lower.

The fluorosensing scanning data were processed through essentially the same software package developed to register the L Lake topographic survey data. Likewise, a combination of 35 mm aerial photography, INS data, and unique features found in the AOL digital record were used to establish the horizontal position of each laser "footprint". Owing to the lower data acquisition altitude and resulting higher data density, a five square meter pixel size was selected for use in data registration.

A number of different presentations of the data are possible. Each of these types of presentations has unique advantages. The most useful method for viewing the data depends, of course, on the potential application for which the data is sought. In order to illustrate the potential of these varied data products that are possible with the scanning data, we have selected the results obtained on the final set of dye observations acquired on June 15. At that time, the dye plume had reached the Pond C dam and had begun to enter the warm arm of Par Pond, thus these data sets allow a more complete illustration of data types. The ground track of the flight line (shown in Figure 15) should be referred to during the following discussion.

A profile of the fluorescence signal in the 580 nm spectral band from Pass 1 (June 15) is shown plotted as a function of time in Figure 19. The data had not been processed through the gridding program prior to plotting. Instead the fluorescence signal is

plotted in the chronological order in which it was acquired. The 5 Hz modulation in the fluorescence signal, which is obvious, especially near the beginning of the pass, results as the laser spot is swept alternately into and out of the dye plume by the scanner. Later in the pass, around second 6-7, the entire scan fell within the dye patch and accordingly the modulation is less pronounced. This type of plot is useful for making an initial assessment of the signal strength in the fluorescence channels, however, it is not satisfactory for quantitatively assessing the spatial distribution of the dye. Following this initial processing, the data were passed through the same gridding software that was utilized in the topographic mapping, which placed each of the laser fluorescence measurements into an evenly spaced matrix of 5 X 5 meter pixels. Options in the gridding software allow the filling in of pixels where no laser samples fell with a value obtained from surrounding pixels using the inverse square of the distance for weighting the values found in the surrounding pixels. The routine also allows smoothing of the data to remove any sharp local variability in concentration for ease in interpreting the overall distribution of the dye.

Several types of presentations for the evenly gridded data are presented in the following figures. Figure 20 is a color composite of the same pass presented in Figure 19 in which only the pixels containing laser samples are shown (note the overlapping elipses characteristic of the conical scanner used by the AOL). The color of each of the pixels is determined by the signal strength of the fluorescence in the 580 nm channel and is scaled according to the color bars presented at the top of the figure. Only the portion of each pass containing discernible levels of dye are shown in the figure. In this figure, as well as on the other color composites, the swath shown at the upper portion of the figure is continued at the bottom, such that the progression of the data along track is top left-to-right, connecting to bottom left, continuing to the right. This type of data presentation allows an "eye-ball" assessment of the distribution of dye and is useful for gauging the validity of the final filled and smoothed data product. This format does not, however, provide quantitative products.

Figure 21 is a color composite of the same pass in which the pixels not containing laser observations have been filled and the resulting matrix has been smoothed. The effect of changes in aircraft roll as the pilots adjusted the flight track of the aircraft along the desired course is apparent in this figure as the edges of the scan swath can be seen to undulate in response to apparent changes in aircraft attitude. The color composites in Figures 20-21 have been shown projected relative to the local heading of the aircraft; however, the individual pixels are registered in the standard true north coordinate system. This method of registration facilitates comparing and combining individual passes. The filled and smoothed data sets from the two passes acquired on the June 15 mission are shown as a combined color composite in Figure 22. As would be expected from the plot of the two flight tracks in Figure 15, the flight lines in the color composite separate in the vicinity of the dam breast and then reconverge toward the northern part of Pond C.

The image in Figure 22 indicates that, on a gross scale, the near surface concentration of the dye in Pond C was distributed into several large, distinct patches some 19 hours after the introduction of the dye into the pond system. This aspect can perhaps be seen better in Figure 23(a-c) which shows along-track density slices sampled from the filled matrix near the west, center, and east portion of the scan swath from Pass 1 (see Figure 21). By contrast, the sample-to-sample variability within each patch is considerably lower. The sample to sample consistency can also be seen in the Figure 20 image (unfilled and unsmoothed) where the individual points appear to gradually increase or decrease as the scan is swept through the patch.

The combined color composite image in Figure 22 encompasses the bubble-up area of the warm arm of Par Pond and goes directly over the containment dam of Pond C. As would be expected, any dye beginning to pass from Pond C and into Par Pond would be strongest in the vicinity of the bubble-up. The presence of the dam is obvious within these figures as a dark blue band crossing the scan swath. Immediately before the dam a few lighter blue and white pixels can be seen

near the center of the swath indicating the presence of some dye in the near surface region of the water column. The apparent concentration of the dye in the warm arm is considerably lower than was encountered in Pond C. Figure 24 shows dye concentration values obtained by SRP personnel at the bubble-up plotted as a function of elapsed time in minutes measured from the release of dye on June 14 at 2:17 PM EDT. The approximate time of the two June 15 passes are denoted in the figure by an arrow. These measurements indicate that dye began entering the warm arm of Par Pond approximately 400 minutes (6.66 hours) after deployment. The maximum concentration flowing through the bubble-up was 4.9 ppb. Since dye patches were detectable below the bubble-up, this concentration fixes a maximum boundary of the lower limit of the AOL sensitivity at the time of the June 1985 investigations. It is quite likely that the sensitivity of the system was somewhat below this figure since the outflow would have been diluted by ambient water within this portion of the Par Pond.

Several other methods for displaying results from the combined passes were prepared to aid in the interpretation of the dye distribution. Perhaps a more quantitative assessment of the dye distribution measurements can be seen in cross-track density slices extracted at regular intervals in the along track direction. In Figure 25, a collection of such cross-sections in the form of "stick" diagrams was projected onto an outline of the pond complex which provides a perspective of the dye distribution relative to local features.

The most useful form of the data for most applications is a contour plot. The results from the set of passes acquired on June 15 are shown in Figure 26. Sections where the passes do not overlap have been contoured with dashed lines. The general outline of the pertinent portion of the pond complex has been projected onto the contour plot to facilitate interpretation.

A secondary objective in the 1985 dye investigations, but a requirement for future airborne laser studies of dye movement in the cooling ponds, was to assess the vertical distribution of Rhodamine WT dye. The preceding portion of the discussion has centered on analysis of the horizontal distribution of the entrained dye within the surface layer. This measurement was made by integrating the

backscattered return over a 30 nsec period. Through gating and delaying techniques this measurement is set to begin 5 nsec prior to the arrival of the laser beam at the water surface and to continue for some 30 nsec, thus providing an integration over the upper 2.5 m of the water column. However, due to the high attenuation characteristics of the watermasses involved, especially in the 580 nm region where peak Rhodamine WT fluorescence occurs, the actual measurement is heavily weighted toward the water surface and, for all practical purposes, is confined to the upper 1 m of the water column.

During the passes conducted on June 15, the shorter wavelength channel adjacent to the 580 nm channel (peak laser-induced fluorescence from Rhodamine WT) was set to be temporally digitized with the LeCroy 2249SG charge digitizers (CD's) instead of the normal on-wavelength laser backscatter which is normally time-resolved. As described in Section 2, the temporal aperture of the CD's is set to provide an integration window of ~4 nsec each. Individual channels are separated by 2.5 nsec yielding some overlap which is useful for relatively fine (< 30 cm) distance determinations. These tests represented the first attempt (ever) to capture temporal measurements from one of the AOL fluorosensor channels. Accordingly, the initial pass on June 15 was consumed attempting to optimize the voltage of the PMT channel used in the digitization process.

On the second pass, encouraging results were obtained. Profiles of dye fluorescence obtained at the surface, 1, 2, and 3 m are shown on Figure 27(a-d), respectively. Notice that variations in signal amplitude are easily observed from depths 0 to 2 m, and variability is not apparent from a depth of 3 m. The lack of measurable signal from 2 m is, of course, not an indication that no dye was present from this depth. Rather, that the exponential decay in the transmission of light in water in the 580 nm spectral region, where Rhodamine WT fluoresces, has precluded the meaningful detection of backwelling signal. Although the timing, digitizer resolution, and signal strength were less than optimal, the time waveforms did reveal distinct variability in signal strength at different depths below the water surface and thus provide an indication of the potential for the measurement of Rhodamine WT dye in near surface cooling pond water

with an airborne lidar system. System improvements aimed at optimizing the AOL for depth resolution of Rhodamine WT dye are described in the final section of this report along with some preliminary results from the 1986 experiments. It should be recognized, however, that the high attenuation at 580 nm within the SRP cooling pond water masses virtually preclude measurement of dye concentrations at depths beyond the upper 4-5 m of the water column.

The potential of airborne laser induced fluorescence for tracer dye mapping was adequately demonstrated through the series of passes flown on June 14 and 15. Interpretation of hydraulic aspects of the data sets is, of course, beyond the scope of this report. The results have, however, been sent on computer compatible magnetic tape to SRP where they can potentially be valuable in checking presently used flow models.

3.3 Steel Creek Wetlands Investigations

Part of the 1985 airborne laser studies at SRP involved gathering preliminary baseline information on the vegetative cover in the Steel Creek corridor. The purpose for the investigations in the Steel Creek wetlands area is to determine the extent to which the airborne laser ranging measurements can be utilized to assist in characterizing particular vegetative types. The utility of the application would be to remotely recognize any systematic changes in the plant assemblages comprising the wetlands. An evaluation of the potential of the airborne laser system for this application is expected to involve interpretation of the laser data set along with passive spectral observations, information obtained by biologists on the ground, and from fluorosensing and laboratory investigations accomplished as part of the 1986 follow-on studies. Such a study will involve corroboration with other groups and is beyond the scope of this report. This report is instead intended to provide a description of the data set and a preliminary evaluation of the measurements relative to the gross vegetative cover types found within the study area.

Two passes flown during the L Lake topographic investigations were extended down the Steel Creek corridor to the Savannah River.

During both of these passes the AOL was operated in a non-scanning, profiling mode. The two passes are labelled in Figure 28 which shows their location relative to L Lake and Steel Creek. The purpose of this investigation was to obtain baseline remote sensing information on the wetlands prior to initiating the operation of the L Lake reactor.

Pass 6/2 was collected with the system operated in the bathymetry or temporal measurement mode which was utilized for all but one of the passes in the topographic investigations. Pass 5/2 was collected with the system configured in the fluorosensing mode which was also used to acquire the dye measurements in Pond B and Par Pond. The fluorosensing configuration was utilized to determine whether laser induced fluorescence signatures could be acquired from the indigenous wetlands vegetation in the corridor. Unfortunately, this part of the experiment was not successful due to the relatively low output power of the Nd:YAG laser transmitter operated in the experiment. Moreover, the voltage (or gain) of the fluorosensor photomultiplier tubes was set too high to allow recovery of useful passive irradiance information. The elevated voltage levels were employed on Pass 5/2 in an attempt to acquire the weak chlorophyll fluorescence data. Recent tests conducted in the vicinity of Wallops Flight Facility as well as at SRP (May, 1986) with a 355 nm frequency tripled Nd:YAG laser loaned to the project by SRP, successfully obtained fluorescence from an assortment of overland vegetation, including some varieties found in the Steel Creek wetlands. This aspect will be amplified in Section 4. Metric and reflectivity measurements of the wetlands vegetation were successful on both passes and should provide a usable baseline from which to detect changes due to the operation of the L Reactor. These results are presented below.

The laser data were obtained at a pulse repetition rate of 200 pps on both of the passes. At the nominal 100 m/sec velocity of the aircraft, this results in an independent observation every 0.5 m along the ground track. A 5 mrad laser beam divergence was utilized on both passes. This divergence setting provided a footprint spot diameter approximately .75 m on pass 5/2 which was flown at an alti-

tude of 150 m above local terrain and a diameter of approximately 1.5 m on pass 6/2 which was flown at an altitude of 300 m above local terrain. A profile of the slant range between the aircraft and ground is provided for both passes in Figure 29. For ease of interpretation, a value greater than the longest slant range measurement on each pass has been subtracted from each individual slant range and the result has been inverted. Thus, vegetation such as shrubs and trees will appear graphically above the surrounding terrain. No attempt has been made to remove any vertical aircraft motion from these data sets. The vertical scale has been exaggerated to allow for improved recognition of features.

The slant range is measured by timing the difference between the laser start pulse and the surface return pulse generated when the backscattered laser radiation from any surface target exceeds the threshold of the tracking discriminator. Accordingly, the profile describes the uppermost canopy in areas where there is sufficient biomass present to reflect a significant number of the laser pulses. Notice that in some sections nearly all of the laser pulses were reflected by the overlying vegetation while along other sections of the flight line a significant number of laser pulses penetrated directly through openings in the canopy to the ground. This is one measure of canopy closure which is important in vegetation and tree-related studies.

Although some parameters such as laser penetration can adequately be represented for an entire flight line of approximately 12 km in length, most of the detail available is lost due to the high data density relative to the gross scale of the plots. In this report we have selected a number of 2 km sections representing different vegetation cover types for detailed presentation. In classifying cover types found within each of the 2 km sections, an attempt was made to be consistent with that given in the EG&G (Las Vegas) Land Classification Report.[15] In processing the data from each of the selected cover types, each 2 km section was treated separately. Initially, a best-fit ground reference line was drawn through the data. This line was then digitized on an 18-inch Tektronix digitizing tablet. Following this step, the resulting data was processed

through a computer program designed to separate canopy, sub-canopy, and ground measurements. The results of this analysis are presented below for both of the lines.

The information derived from Pass 6/2 is presented in Figures 30-34 and that from Pass 5/2 is presented in Figures 35-39. These figures display the inverted slant range as a function of along-track distance. The ground cover type is identified in each of the figures. The ground reference line has been plotted along with the inverted slant range data. The combination of the inverted slant range profile and ground reference profile can be used to gauge the cross-sectional height of the vegetation.

The vegetative cover types within each of the above 2 km profiles were analyzed to determine the distribution of vegetation height and reflectivity measurements. In forest covered areas, the distribution of height and reflectivity observations were also determined for the upper canopy as a potential indication of canopy shape and closure. The results of the height distribution measurements for the upper canopy of the forest covered sections are provided in Figures 40 and 41 for Flight Lines 6/2 and 5/2, respectively. Additional statistical information relative to the various vegetation cover types is given in Table 6. The significance of these indices for potentially detecting environmental changes to the various vegetation cover types found within the Steel Creek Corridor is not known on the basis of these two passes. Nonetheless, the 1986 missions that were flown down the Steel Creek Corridor should help in establishing the natural variability of these parameters to the individual cover types involved.

The investigations in the Steel Creek corridor which were begun in 1985 have been continued into 1986. The aircraft field mission is briefly discussed in Section 4.0. In addition to the aircraft observations, a series of laboratory experiments were conducted as part of the 1986 joint NASA/DOE studies at SRP. These laboratory observations concentrated on determining the feasibility of utilizing laser induced fluorescence to differentiate between plant types. The analysis and interpretation of this data set is currently being performed by NASA. An independent study utilizing the 1985 AOL data

TABLE 6. STEEL CREEK CORRIDOR LAND CLASSIFICATION STATISTICS

PASS 5/2

Coverage		Canopy Topography (m)		Canopy Penetration (%)		Canopy Reflectivity (Relative Counts)	
		Mean	St.Dev.	Upper	Ground	Mean	St.Dev.
1	Shrub/Scrub	6.7	3.0	35.2	31.6	126.0	43.1
2	Evergreen Forest	14.5	6.2	30.0	24.6	128.9	45.7
3	Bottomland Hardwood	19.0	5.1	8.2	3.4	126.7	43.8
4	Scrub/Shrub	7.5	3.3	25.7	16.9	101.9	34.3
5	Deciduous Swamp	17.6	5.3	13.6	9.2	143.3	57.3

PASS 6/2

Coverage		Canopy Topography (m)		Canopy Penetration (%)		Canopy Reflectivity (Relative Counts)	
		Mean	St.Dev.	Upper	Ground	Mean	St.Dev.
1	Mixed*	13.5	4.1	24.4	20.5	234.8	84.7
2	Evergreen Forest	17.4	3.0	24.3	21.1	236.1	87.6
3	Evergreen Forest	15.1	3.4	32.7	31.9	211.9	75.3
4	Bottomland Hardwood	14.3	3.1	28.5	21.1	195.2	76.3
5	Scrub/Shrub	3.4	1.7	35.9	32.9	227.5	70.0
6	Deciduous Swamp	16.4	5.5	13.9	9.6	250.9	82.0
7	Deciduous Swamp	16.8	5.8	12.1	6.4	209.2	69.5

* Mixed Swamp Hardwood and Evergreen

acquired over SRP as well as contemporaneous passive spectral data from a scanning spectroradiometer is underway at the University of South Carolina. Thus, although the significance of the airborne laser observations over the Steel Creek for characterizing the wetlands vegetation has not yet been established, the more complete coverage afforded by the 1986 flights, coupled with the laboratory and corroborative information from the passive imagery are expected to provide baseline criterion essential to monitoring changes in the natural vegetative cover of the corridor.

3.4 Forestry Inventory and Applications Results

The L Lake topographic surveying investigation discussed in Section 3.1 provided an opportunity to demonstrate and further evaluate the application of an airborne laser system to furnish forest management related information. Although not called for in the Statement of Work between DOE and NASA, it was determined that portions of a number of flight lines occupied in connection with the L Lake topographic survey passed directly over particular stands of trees which could be readily truthed and which were representative of more extensive forested areas within SRP. The analysis of these data sets was undertaken because (1) a number of instrument improvements had been made to the AOL since the earlier forestry investigations; (2) Gordon Maclean, a doctoral candidate at the University of Wisconsin (Madison Campus) who was a consultant on the SRP investigations, had interest in pursuing the analysis and reporting of results from the SRP study at no cost to the project; and considerable interest for future research in this area had been expressed for this application by personnel at SRP. It is because of this interest, and because the data was collected (incidentally) as a part of this project, that these preliminary results are presented herein.

Several significant applications of the AOL in the field of forestry were first tested at SRP in the summer of 1985. These include: (1) new hardware for tracking ground beneath tree cover; (2) the use of the return signal in the 36 temporal channels for analysis of tree foliage; and (3) estimation of merchantable timber volume through geographic extension of equations established elsewhere.

Through previous agreements, the analysis and interpretation of forestry applications data is being undertaken by Gordon Maclean. Although progress is being made on the data set, results suitable for inclusion in the Final Report along with the other research activities are only available for application (1), above. (The results from the remaining two investigations are being reported in Maclean's dissertation which is expected to be completed on or before June 1987. At that time copies of the dissertation and data will be made available to both SRP and NASA).

3.4.1 Estimation of Foliar Biomass

The estimation of tree foliage or leaf biomass through the interpretation of backscattered laser signal represents a new application of an airborne lidar system. A reliable and reasonably reproducible method for remotely determining leaf biomass would serve as an extremely useful tool for assessing year-to-year changes in the foliage cover. Positive changes could be due to growth and maturation while negative changes may be due to stress of one kind or another. Should this airborne lidar application be successful, it would be a practical method for monitoring various forest covered habitats at SRP such as the Steel Creek corridor which is discussed above. Analysis of data for this investigation requires the modification of existing computer programs and the design of new software. This software has been developed and is now being tested at the University of Wisconsin. The theoretical basis for this study is that the amount of light reflected is proportional to the amount of foliar biomass present in the canopy. In this technique, signals from the 36 temporal channels are processed to quantify foliar aspects of the canopy. Preliminary analysis indicates that the AOL temporal waveform hardware may represent a significant improvement over other techniques for gauging canopy characteristics.

3.4.2 Timber Volume Estimation

The research project related to the estimation of merchantable timber volume is focused on certain plots located near the L-Reactor which were overflown as extensions of flight lines required for the L

Lake topographic survey. The location of these lines are provided on Figure 42. The plots are delineated within the figure. Previous studies, which used algorithms developed from test plots in the vicinity of Wallops Flight Facility, have shown that a high correlation exists between AOL measurements of the canopy and terrain surface profiles and ground measurements of merchantable timber volume. Algorithms developed to make timber volume estimates on similar indigenous tree species at another site located near Bainbridge, Georgia, will be applied to the airborne lidar data acquired at SRP. These results will then be tested for validity using ground truth results obtained during a site visit to SRP during October 1985. An example of the data available from the October 1985 ground truthing is provided in Table 7.

TABLE 7. Example of Surface Truth Survey Data

SPECIES	HEIGHTS (nearest 5 ft.)			
	D.B.H (nearest 0.1")	TOTAL	MERCHANT	LIVE CROWN
Longleaf Pine	11.3	122	91	36
Longleaf Pine	9.9	112	97	57
Longleaf Pine	12.0	121	94	61
Water Oak	3.9	80	0	22
Water Oak	3.0	60	0	5
Longleaf Pine	9.8	127	95	47
Longleaf Pine	10.2	92	74	45
Loneleaf Pine	13.1	95	65	32
Longleaf Pine	9.8	92	74	39
Longleaf Pine	12.3	96	84	45
Longleaf Pine	10.0	98	77	56
Water Oak	4.6	66	0	15
Water Oak	4.5	67	0	15
Longleaf Pine	14.7	91	75	25
Water Oak	5.0	135	0	37
Water Oak	3.1	85	0	20
Water Oak	3.3	64	0	10
Water Oak	5.0	105	0	15

3.4.3 Hardware Terrain Tracker Evaluation

One of the objectives of the forestry investigations conducted at SRP was to attempt a new method of measuring tree heights using a device which operates in real-time on the analog signal. The suc-

cessful demonstration of this new method for determining foliage height would represent a major improvement in the hardware configuration of the AOL for forestry applications. The capability to utilize the reflected laser waveform to determine the height of vegetation has been established for a number of years.[3,4] In all prior studies performed with the AOL, the height measurements were extracted from recorded digital waveforms during post-flight analysis using algorithms previously developed for hydrographic applications of the airborne lidar system. The digital waveform method required recording 36 or more channels of temporal waveform information, thus necessitating the use of a large computer-compatible tape handler. The waveform method also requires considerable computer manipulation of the digital information in order to make consistent determinations of the ground location beneath the foliage canopy. This combination of problems has severely hampered more widespread utilization of airborne lidar systems for forest management applications. A hardware component capable of reliably tracking the ground beneath forested areas would substantially reduce both the amount of data necessary to record in real-time and further would alleviate the need for sophisticated waveform manipulation software.

The hardware device utilized in the AOL system for these investigations was a LeCroy Model 4208, 8 channel "Multistop." In principal, the device functions as an extended time interval counter in that it measures the elapsed time between a start pulse which "arms" the timer and a subsequent stop pulse determined from a discriminator through which the amplified signal from the PMT is routed. The major difference between the Multistop and a time interval counter is that the Multistop can store the elapsed time between the start pulse and up to eight stop pulses from targets intercepted by the laser beam. The device has the potential for measuring the return from the ground surface as well as from intermediate targets between the crown and ground level such as would be provided by an understory or subcanopy. The threshold of the Multistop is under operator control and can be optimally adjusted during a short pass over a forested site prior to beginning the actual survey. During the SRP experiment, the elapsed time measured by the first register of the Multistop was generally

found to be the backscatter from the first folding mirror, the second register usually contained a measurement associated with the return from the crown of the canopy. The measurement recorded from the third register was most often determined to be from the forest carpet in stands which were relatively clear of understory development. In stands where a denser understory development was noted during ground truth investigations, numerous returns from intermediate targets were often found instead of the return from the ground. In cases where an intermediate target was intercepted, there was seldom sufficient remaining signal to capture the location of backscatter from the forest floor. The significance of this finding has not yet been established. Perhaps more operator experience with threshold settings will allow the recovery of both understory and ground information on future investigations with the Multistop.

The present precision of the Multistop is one nanosecond, effectively limiting the measurement capability to a granularity of approximately 30 cm. This is not considered a severe limitation for the forestry management application. The practical advantage realized through the use of the Multistop goes beyond the simplification of the data processing procedure and the reduction of components necessary to capture and record the needed data. The Multistop is not limited in the range over which trees can be measured. By contrast, the waveform method is restricted to temporal period covered by the available analog-to-digital converters. The AOL is currently configured with 36 digitizer channels. Each of these channels can be separated by either 2.5 or 5 ns depending on the vertical resolution requirements of the experiment. Even with the more coarse, 5 ns channel separation, the measurement window extends only to approximately 26 m. For gauging trees taller than 26 m, a delay or gap must be placed before the first digitizer, thereby extending the measurement window. However when this is done, smaller trees and shrubs falling within the gap are effectively excluded, potentially compromising the experiment objectives. When operating in areas of high or moderate relief, the effective height determination range is further reduced. With the LeCroy Multistop it is possible to measure a giant redwood on one pulse and an aspen sapling on the next.

Results acquired on a portion of Flight Line 18/2 (Figure 42) have been selected for presentation in this report. These results are typical of the findings obtained on the other flight lines. A profile of the slant range between the aircraft and ground is shown in Figure 43. For ease of interpretation, a vector greater than the longest slant range measurement has been subtracted from each individual value and this difference has been inverted. Thus, vegetation such as shrubs and trees appear graphically above the surrounding terrain. No attempt has been made to remove any aircraft motion from these data sets. Notice that the vertical scale has been exaggerated to allow the improved recognition of features. The laser data was obtained at a pulse repetition rate of 400 pps. At the nominal 100 m/sec velocity of the aircraft, this amounts to an independent observation every 0.25 m and the distance covered in the 60-second portion of the pass plotted in Figure 43 is ~6 km.

The slant range is a measurement of the time difference between the laser start pulse and the surface return pulse generated when the backscattered laser radiation from any surface target exceeds the threshold of the tracking discriminator. Accordingly, the profile describes the uppermost canopy in areas where there is sufficient biomass present to reflect a significant number of the laser pulses. In data acquired over forest covered terrain, relatively few pulses manage to penetrate directly through the canopy to the ground. Occasionally, the leafed foliage in the upper canopy is sufficiently solid to almost completely block any laser radiation falling within the ~1.8 m laser footprint (at 300 m). More often a potentially measurable portion of the radiation goes through micropores in the canopy structure. Some of the laser beam that penetrates the canopy strikes intermediate targets such as supporting branches or a subcanopy and finally a part of the beam may strike the forest floor. It is this relatively small parcel of the initial laser energy that was used to establish the ground location relative to the canopy.

The measurements obtained with the Multistop on Flight Line 18/2 are shown in Figure 43(b) as small symbols. The inverted slant range profile shown in Figure 43(a) has been repeated to aid in interpretation. Notice that in the area with thicker canopy cover (0 to 2

seconds) a number of Multistop values did not reach ground, but instead were intercepted by targets between the upper canopy structure and ground. In the section which the ground truth investigation indicated less understory development was present (between 2 and 4 seconds), the Multistop measurement generally defined ground targets rather than intermediate targets.

The results available at this time are only qualitative. Little data was acquired at SRP in which the instrument was configured to yield concurrent waveform and Multistop information from which a quantitative comparison could be made. The finer (2.5 channel separation) setting was used on the AOL digitizers during the SRP topographic surveying investigation. The finer resolution setting reduces the temporal measurement span to 90 ns (~13 m), effectively preventing the capture of backscatter from both the canopy and ground within the same temporal waveform. However, during an experiment conducted several days prior to the SRP missions at the International Paper Corporation (IP) holdings near Bainbridge, Georgia, the AOL was operated with the coarser (5 ns) digitizer separation. This configuration allowed the capture of temporal waveforms which can be directly compared with the Multistop information. Analysis of the IP data set, which is currently being performed by Maclean, is expected to furnish a comparison between the Multistop and waveform methods of determining tree height for several different forest cover types. The findings from the IP study are expected to yield accuracy bounds which are considered sufficient for forest inventory purposes. More rigorous accuracy tests of the hardware terrain tracker measurements for surveying purposes remain for a future flight where conventional ground surveying or other truthing techniques are available.

4.0 SENSOR DEVELOPMENTS SINCE THE JUNE 1985 INVESTIGATIONS

The investigations conducted during June 1985 (presented in the preceding section) cover a wide range of the total instrument capabilities available at that time. The topographic mapping and forestry applications required the instrument to be operated in the bathymetry (or temporal) mode; the algae and overland studies utilized the fluorosensing (or laser induced spectral) modes of the

instrument; and the tracer dye experiment involved the simultaneous operation of the sensor in both modes. The degree of difficulty posed by these applications also varied considerably. Some were relatively proven, others were questionable to an extent, and a few involved aspects that had never been tested in similar settings. Nonetheless, the overall assessment of the combined results is considered to have been successful. The primary goals for the 1985 studies were achieved. These included the topographic mapping of the upper portion of L Lake, demonstrating tracer dye mapping capability, and gathering baseline metric measurements of vegetation in the Steel Creek corridor and delta. Some of the other investigations that were considered as secondary objectives aimed at establishing feasibility were less successful. However, considerable information, essential for the future success of an airborne laser fluorosensor for these applications, was acquired during the SRP overflights.

The operation of the instrument for acquiring topographic information was a well established and proven capability. The only known problems here were associated with real-time navigation, post-flight positioning, and establishing vertical control. Likewise, the instrument requirements for the mapping of surface layer dye concentration had been previously determined and demonstrated and thus presented no significant difficulty. The investigations related to the measurement of fluorescence from algae and overland vegetation was a different matter. The AOL has been utilized to collect information on algae and associated photopigment concentration on numerous occasions since the application was first demonstrated in 1979. These previous investigations, however, were conducted over open ocean sites with a laser that provided output power levels for pigment excitation that were considerably above ANSI approved allowable eye exposure limits. The rather confined cooling lakes associated with the SRP operation precluded the use of laser sources which were above the ANSI approved standards. Likewise, the overland fluorosensing investigations that had previously been demonstrated were largely conducted with the same high power laser over a test site which had been secured from public access. Finally, the transmission properties of the ponds under investigation were known

to be considerably below any that had been encountered on comparable studies where the techniques had been demonstrated.

During the year separating the 1985 flights from the recently completed 1986 missions, a number of instrument changes had been implemented which have resulted in the successful demonstration of several of the applications sought during the earlier study. The results obtained during the 1986 field experiment will, however, require some time to fully document and report. We are, therefore, including a brief description of the recent results in this section to more fully represent the present state of the instrument at the time of the submission of this report.

The problems identified during the 1985 field experiments were largely associated with the lack of adequate laser transmitter power and the insufficient temporal resolution necessary to quantify relatively small changes in the backscattered fluorescence signal strength associated with vertical dye distribution. The laser transmitter problem was resolved in early spring 1986 when SRP loaned a Quanta Ray model DCR-2A Nd:YAG laser to the project. During the two months preceding the 1986 flights, the laser was engineered into the AOL system and was subsequently tested in the vicinity of Wallops Flight Facility. The particular feature that makes the model DCR-2A Nd:YAG laser of considerable advantage in the remote sensing investigations at SRP is the capability of tripling the primary 1064 nm IR output wavelength of the Nd:YAG laser to 355 nm. Fortunately, the power of the laser is sufficiently high to deliver a 100 μjoule peak pulse at 355 nm despite rather substantial energy losses during the tripling process. The fluid of the cornea is essentially opaque to 355 nm radiation. Therefore, ANSI standards allow significantly higher eye exposure levels at 355 nm than are permitted anywhere within the visible and near-infrared spectral regions. Thus full advantage can be taken of the high output power of the model DCR-2A Nd:YAG laser which was approximately a factor of 50 times stronger than the relatively modest two μjoule peak pulse power of the Navy's HALS laser utilized during the 1985 mission. Moreover, the pigments involved in the algae study and the overland vegetation studies are induced to fluoresce nearly as efficiently at 355 nm as can be

achieved at 532 nm where most of the previous AOL investigations have been conducted.

The problem of increased temporal resolution needed to measure vertical dye distribution was solved by adding a subsystem to the AOL which was capable of recording waveform signals from a Tektronix R-7912 digitizer. The temporal resolution R-7912 digitizer is adjustable down to a practical limit of 200 psec per channel where it was operated during the SRP 1986 field experiment. Although the ultimate aim is to incorporate the operation and recording from the unit directly into the AOL operating system, the subsystem was found to perform adequately during the dye study.

Preliminary results have been obtained for several of the passes flown in connection with the dye investigation. The data from two of these passes is plotted in Figure 44. A profile showing the horizontal (surface layer) distribution of the entrained dye is plotted in Figure 45a. The signal from the dye recovered from depths of 1, 2, and 3 meters are shown for the same profile in Figure 45 (b-d) respectively. It is hoped that rigorous analysis of the temporal waveforms from all of the numerous passes available from the 1986 investigations will reveal valuable information about the steady-state flow characteristics within L Lake.

Some initial results have also been obtained for the passes flown in connection with monitoring the Steel Creek corridor. The additional power provided by the model DRC-2A Nd:YAG laser (operating at 355 nm) enabled the acquisition of fluorescence spectra from various plant types growing in the corridor. The trajectories of the passes were specifically selected by SRP personnel to furnish data which would complement the metric information gathered during the 1985 passes flown over the wetland area as well as some more recent passive imagery. Pass ST-3 was selected for preliminary presentation in this report. Profiles of inverted slant range, laser reflectivity, and laser induced fluorescence (685 nm) are provided in Figure 46. The data were obtained at 20 pps. At the nominal aircraft velocity of 100 m/sec, this amounts to an observation every 5 m along the flight line. The inverted slant range data in Figure 46 (a) are raw, unaveraged observations. The reflectivity and chloro-

phyll fluorescence data presented in Figure 46 (b) and (c), respectively, have been averaged over a one second (or 100 m) interval. This averaging was done in the initial processing in order to indicate trends in different areas of the corridor. Adjacent pulses, separated by approximately 5 m, often strike different plant types oriented in different aspects. Accordingly, the pulse-to-pulse variability in the raw data is too high to allow interpretation on a scale as gross as that utilized in Figure 46. The figure is, however, useful for indicating the relationship of laser induced fluorescence to laser reflectivity and both of these measurements to plant topography. Notice that dense vegetation in the marsh and scrub/shrub area has relatively low albedo (at the laser wavelength) while yielding relatively high fluorescence when compared to adjacent tree-covered areas. Detailed studies of the fluorescence spectra are to be initiated near the time of the completion of this Final Report. Laboratory-based investigations involving plant species growing within the corridor are to be conducted prior to the end of FY-86. The results of these controlled tests are expected to be extremely helpful in aiding in the interpretation of these results.

ACKNOWLEDGMENTS

The authors wish to thank the staff of the Savannah River Plant for their outstanding cooperation and support. In particular, H. Mackey (SRL) and D. Hayes (SRL) were instrumental in the planning and ground truth measurement facets of the investigation. Also, the assistance and support of other individuals including E. Goodson (DOE-SR), J. Corey (SRL), and R. Malstrom is gratefully acknowledged.

REFERENCES

1. Goodman, L. R., Ed., "Laser Hydrography User Requirements Workshop Minutes," NASA Report TMX-73274 by NOAA for NASA Wallops Flight Center (Jan 1975).
2. Hoge, F. E., Swift, R. N., and Frederick, E. B., "Water Depth Measurements Using an Airborne Pulsed Neon Laser System", Applied Optics, 19, No. 6, 871 (1980).
3. Krabill, W. B., Collins, J. C., Link, L. E., and Butler, M. L., "Airborne Laser Topographic Mapping Results from Joint NASA/U. S. Army Corps of Engineers Experiments", Photogrammetric Engineering and Remote Sensing, 50, No. 6, 685 (1984).
4. Nelson, R., Krabill, W., and Maclean, G., "Determining Forest Canopy Characteristics Using Airborne Laser Data", Remote Sensing of Environment, 15, (1984).
5. Hoge, F. E. and Swift, R. N., "Absolute Tracer Dye Concentration Using Airborne Laser Induced Water Raman Backscatter", Applied Optics, 20, No. 7, 1191 (1981).
6. Hoge, F. E. and Swift, R. N., "Airborne Mapping of Laser-Induced Fluorescence of Chlorophyll a and Phycoerythrin in a Gulf Stream Warm Core Ring", in Mapping Strategies in Chemical Oceanography, (Alberto Zirino, ed)., Advances in Chemistry Series No. 209, American Chemical Society, Washington, D.C., 353-372 (1985).
7. Hoge, F. E. and Swift, R. N., "Delineation of Estuarine Fronts in the German Bight Using Airborne Laser-Induced Water Raman Backscatter and Fluorescence of Water Column Constituents", Int. J. Remote Sensing, 3, No. 4, 475 (1982).
8. Hoge, F. E. and Swift, R. N., "Airborne Simultaneous Spectroscopic Detection of Laser-Induced Water Raman Backscatter and Fluorescence from Chlorophyll a and Other Naturally Occurring Pigments", Applied Optics, 20, No. 20, 3197 (1981).
9. Hoge, F. E. and Swift, R. N., "Airborne Dual Laser Excitation and Mapping of Phytoplankton Photopigments in a Gulf Stream Warm Core Ring", Applied Optics, 22, No. 15, 2272 (1983).

10. Hoge, F. E., Berry, R. E., and Swift, R. N., "Active-Passive Airborne Ocean Color Measurement. 1: Instrumentation", Applied Optics, 25, No. 1, 39 (1986).
11. Hoge, F. E., Swift, R. N., and Yungel, James K., "Active-Passive Airborne Ocean Color Measurement. 2: Applications", Applied Optics, 25, No. 1, 48 (1986).
12. Krabill, W. B. and Martin, C. F., "Analysis of Aircraft Vertical Positioning Accuracy Using a Single Accelerometer", NASA TM 84417, February 1983.
13. Krabill, W. B. et al., "Airborne Laser Topographic Mapping Results from Initial Joint NASA/U.S. Army Corps of Engineers Experiment", NASA TM 73287, June 1980.
14. Bristow, M. P. F. et al., "Airborne Laser Fluorosensor Survey of the Columbia and Snake Rivers: Simultaneous Measurements of Chlorophyll, Dissolved Organics and Optical Attenuation", International Journal of Remote Sensing, 6, No. 11, November 1985.
15. Ezra, C. E., "Steel Creek Land Cover Data Base Update Savannah River Plant Aiken, South Carolina", DOE/ONS-8512, September 1985.
16. Bristow, Bundy, Edmonds, Froy, Ponto and Small, "Airborne Laser Survey of the Columbia and Snake Rivers: Simultaneous Measurements of Chlorophyll, Dissolved Organics and Optical Attenuation", Int. Journal of Remote Sensing, 6, No. 11, November 1985.

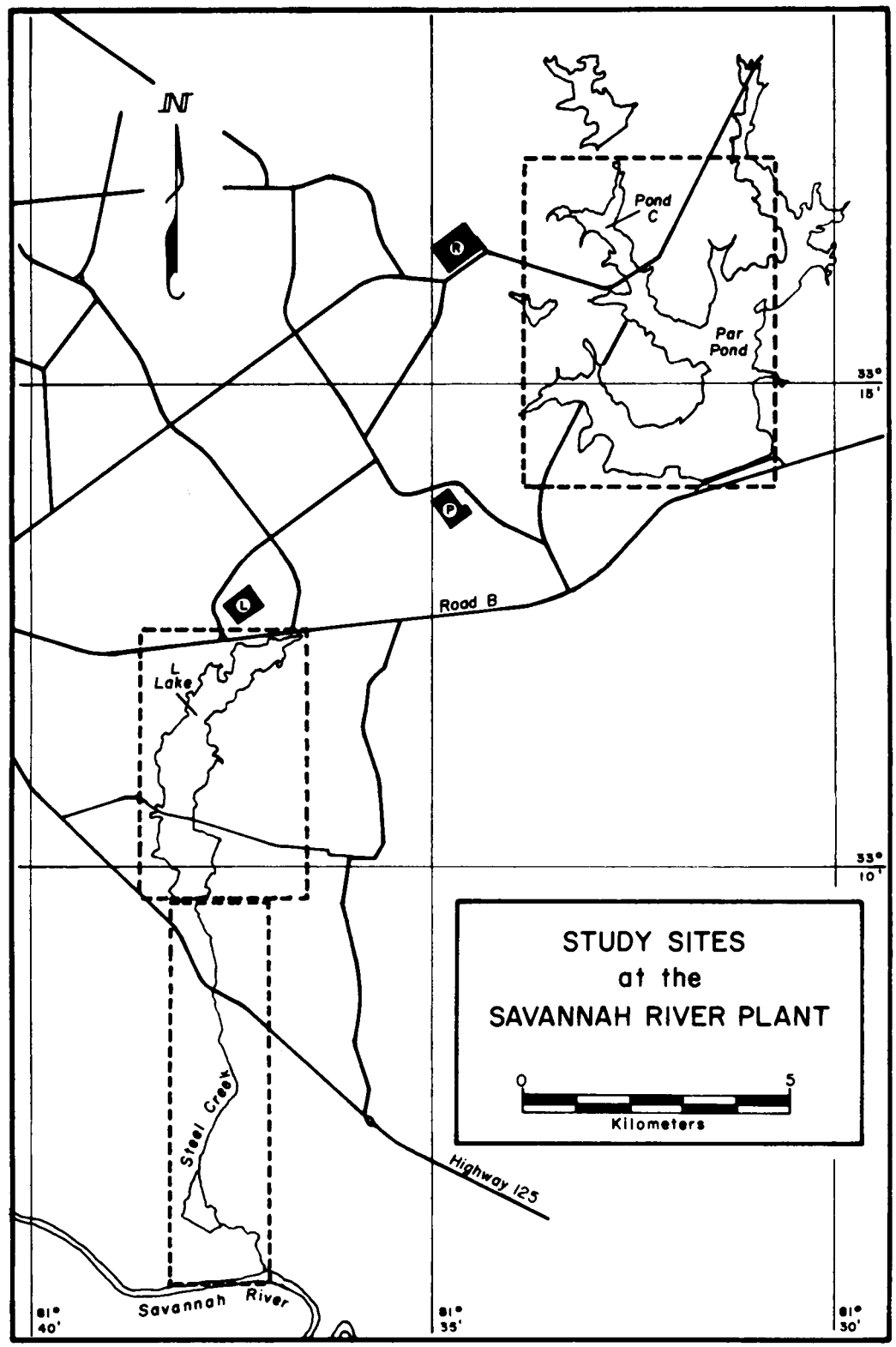

Figure 1. Map showing the three primary sites studied during the 1985 NASA Airborne Oceanography Lidar investigations at SRP.

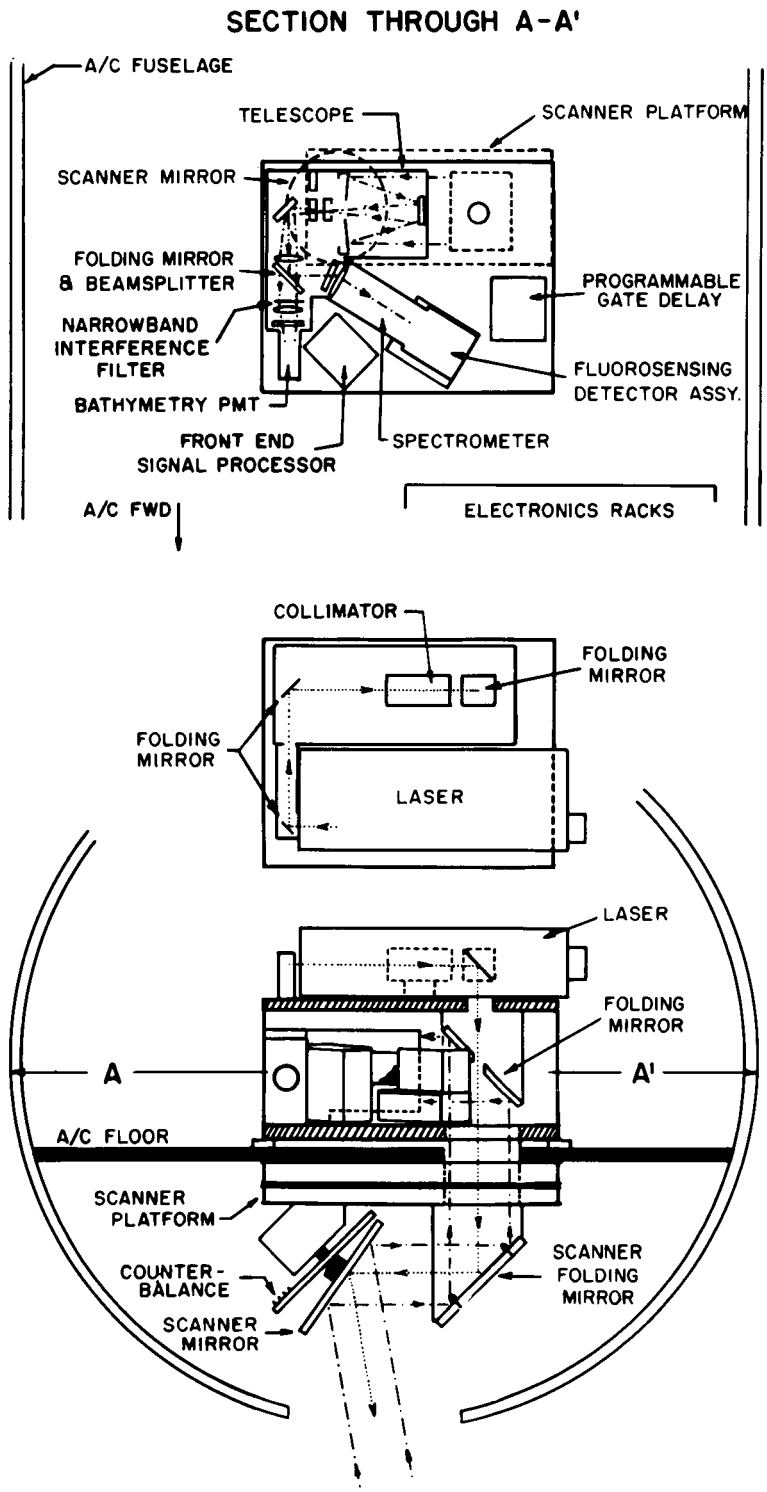

Figure 2. Elevation and plan view of the AOL illustrating the electro-optical components as configured for the 1985 NASA Airborne Oceanography Lidar investigations at SRP.

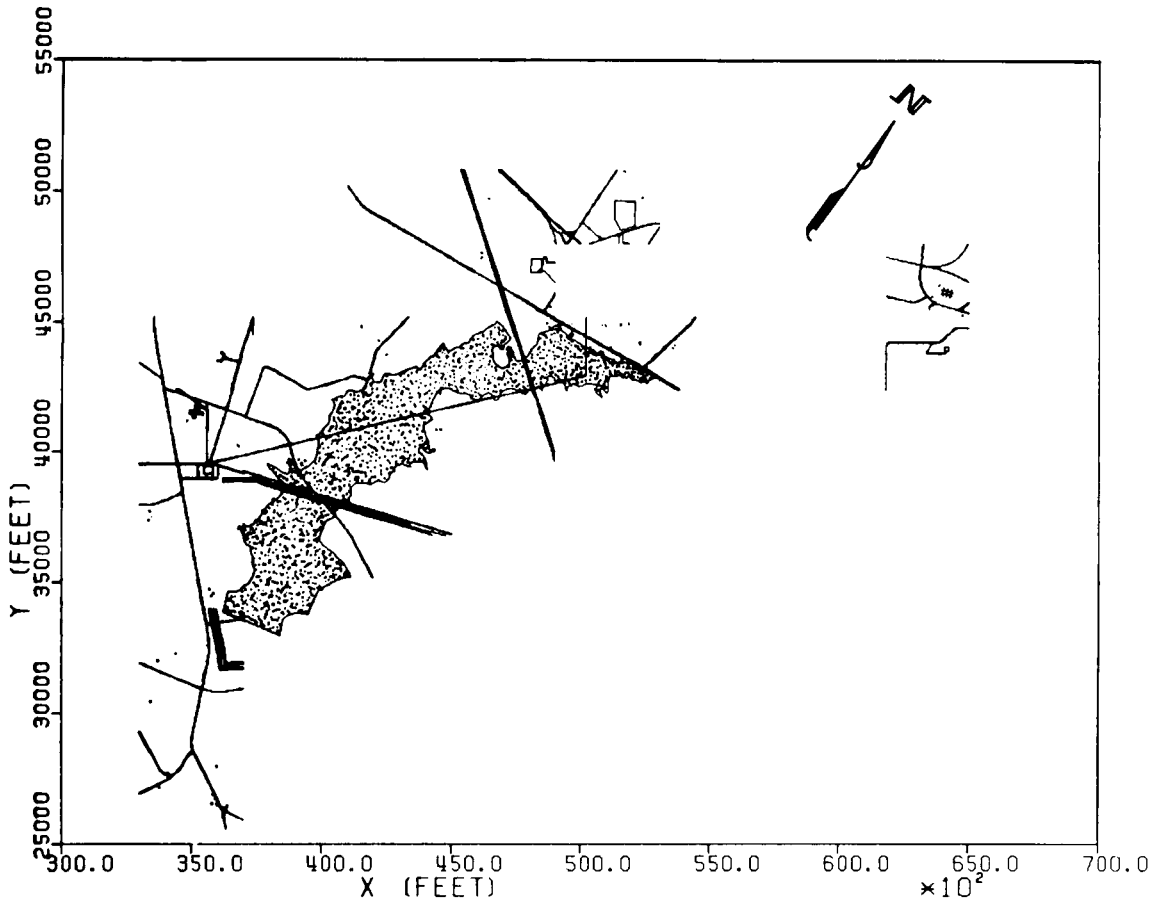

Figure 3. A map of the L-Lake study area plotted in the SRP coordinate system. The shaded area indicates the survey coverage undertaken with the AOL. Major cultural features are shown.

ORIGINAL PAGE
COLOR PHOTOGRAPH

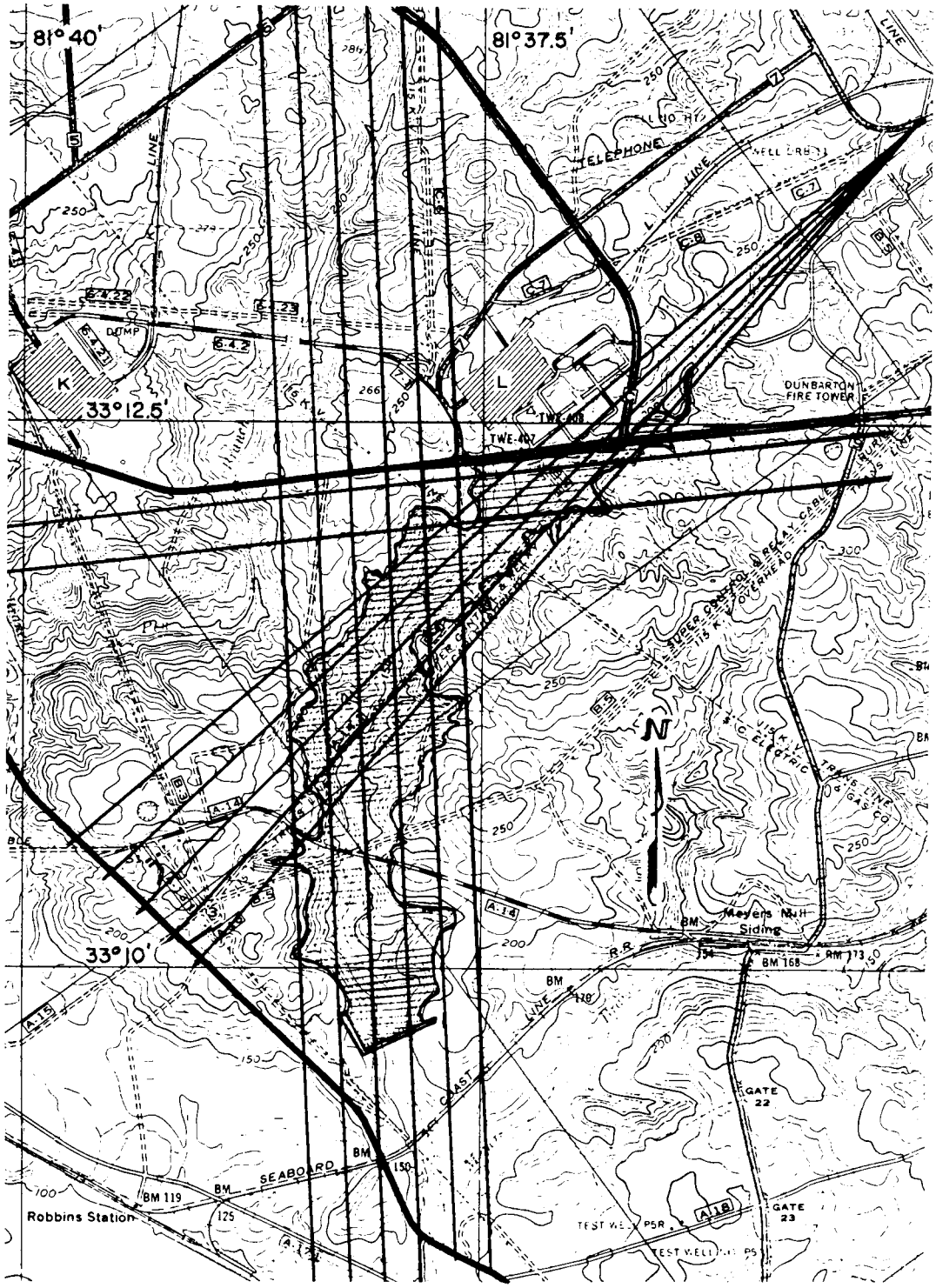

Figure 4. A map from the Pre-flight Mission Plan illustrating the intended flight lines for the topographic mapping survey of the L-Lake area.

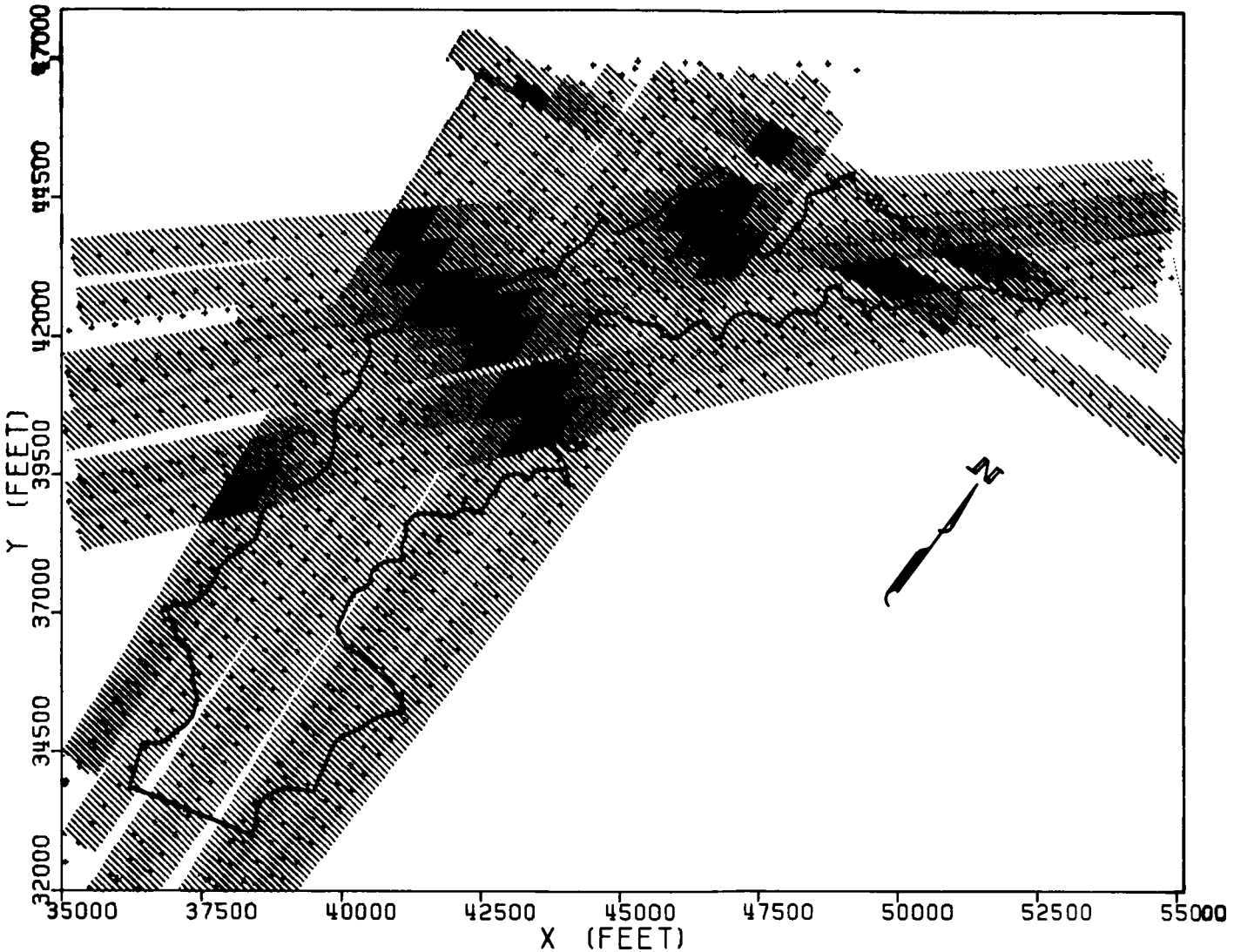

Figure 5. A plot of the actual scan swath coverage from NASA Airborne Oceanographic Lidar topographic mapping survey of the L-Lake area. The outline of the 180 ft contour is shown.

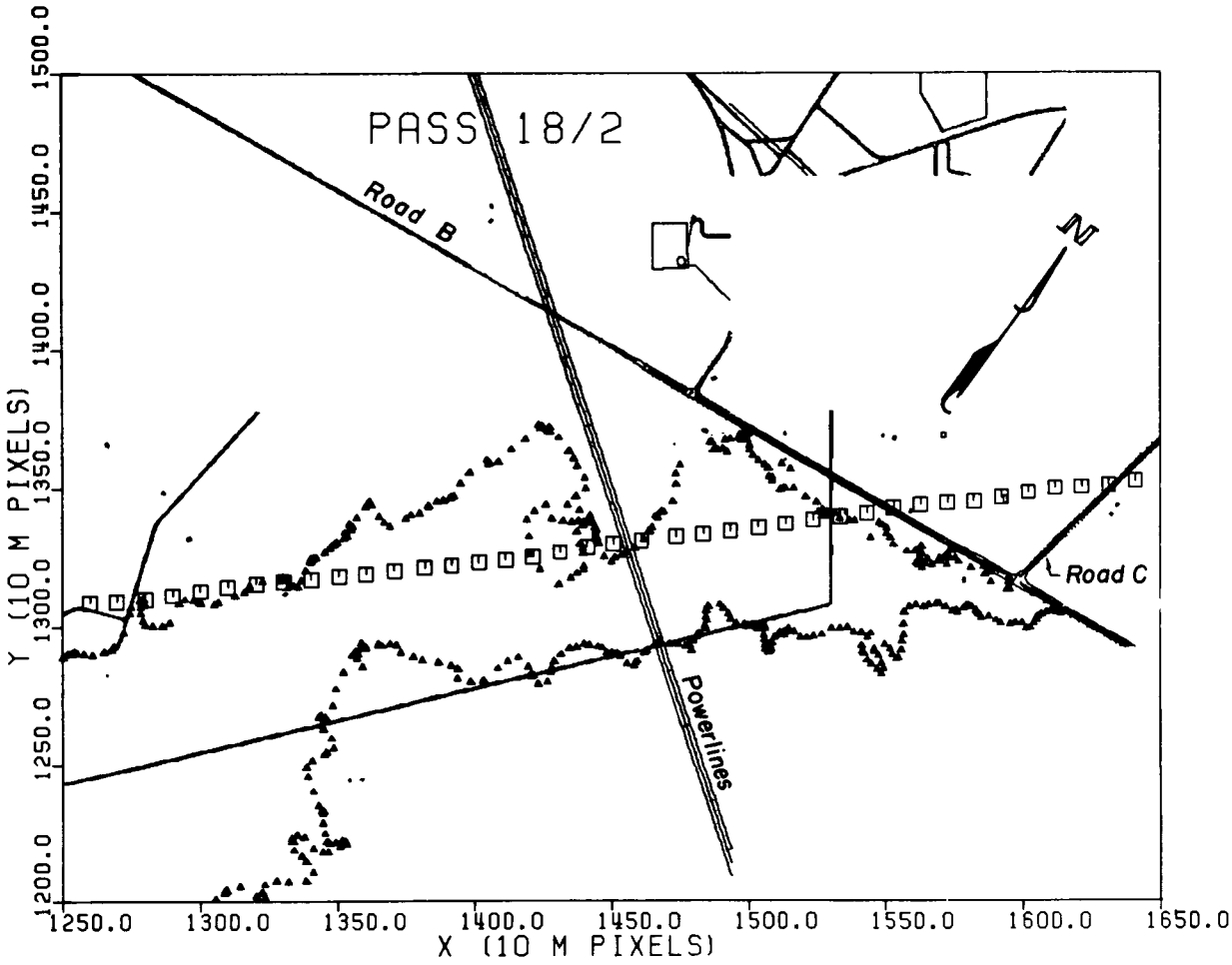

Figure 6. A map showing the ground track of the aircraft on Pass 18/2 as indicated by the small unconnected squares. Also shown in the figure are the major cultural features used in registering the flight line.

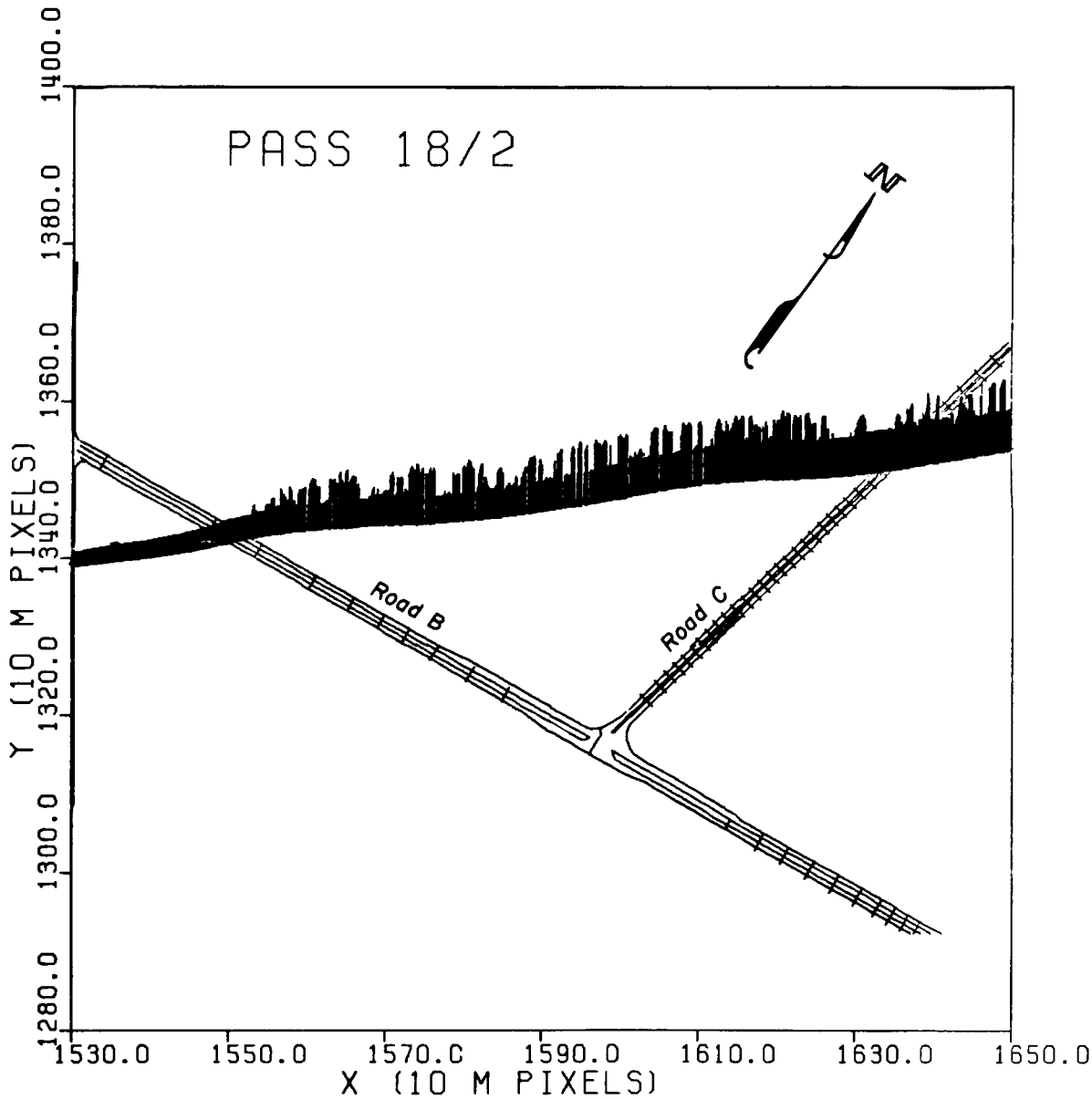

Figure 7. An enlargement of a portion of Pass 18/2 near the intersection of Roads B and C. The relative elevation of each of the laser measurements is provided by the length of a small stick plotted normal to the aircraft trajectory. Such illustrations were useful in the initial registration of the AOL profiling passes.

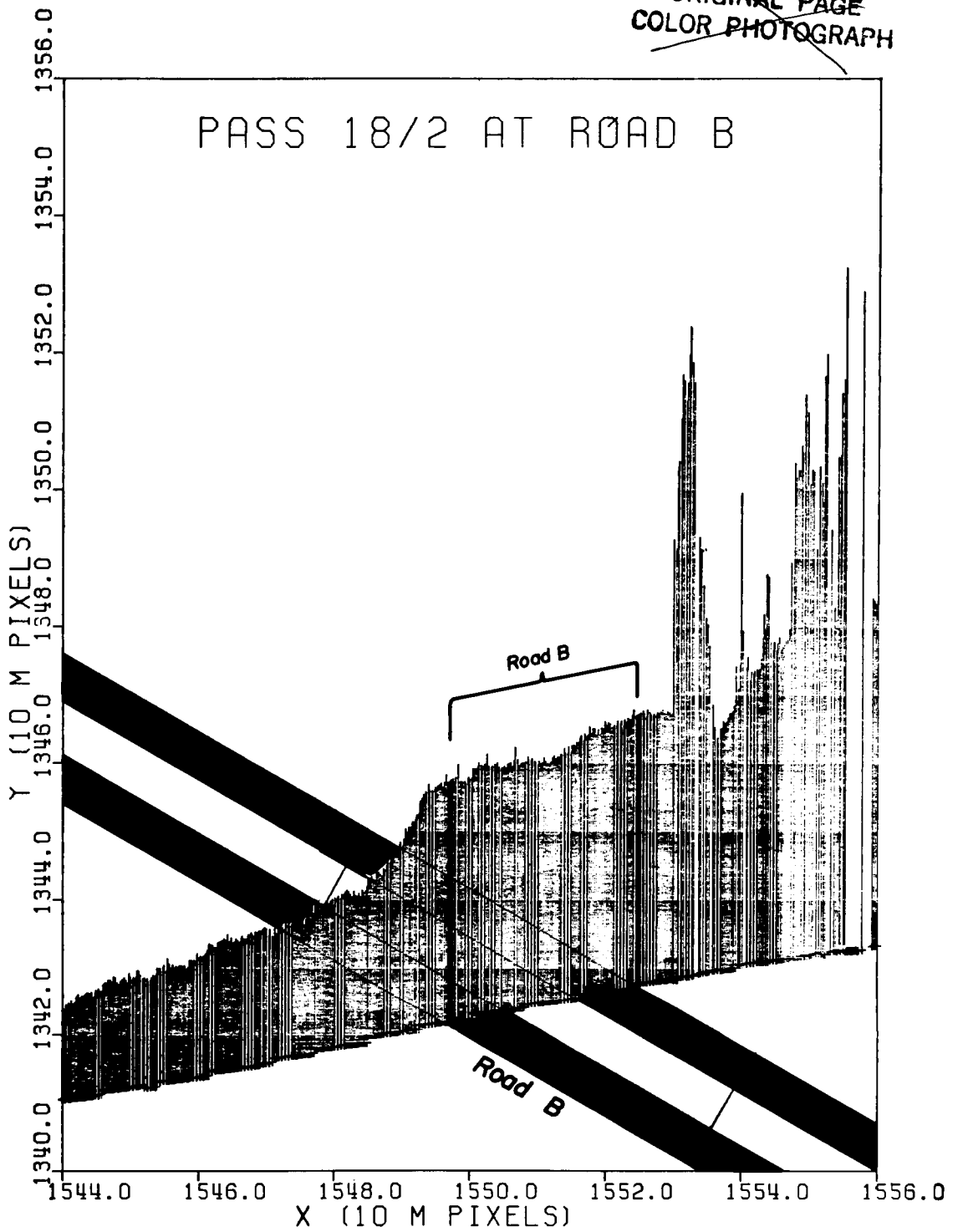

Figure 8. An enlargement of a portion of Pass 18/2 in the vicinity of Road B. The relative elevation of each of the laser measurements is provided by the length of a small stick plotted normal to the aircraft trajectory. Notice the two roadway pavements which are apparent in the diagram.

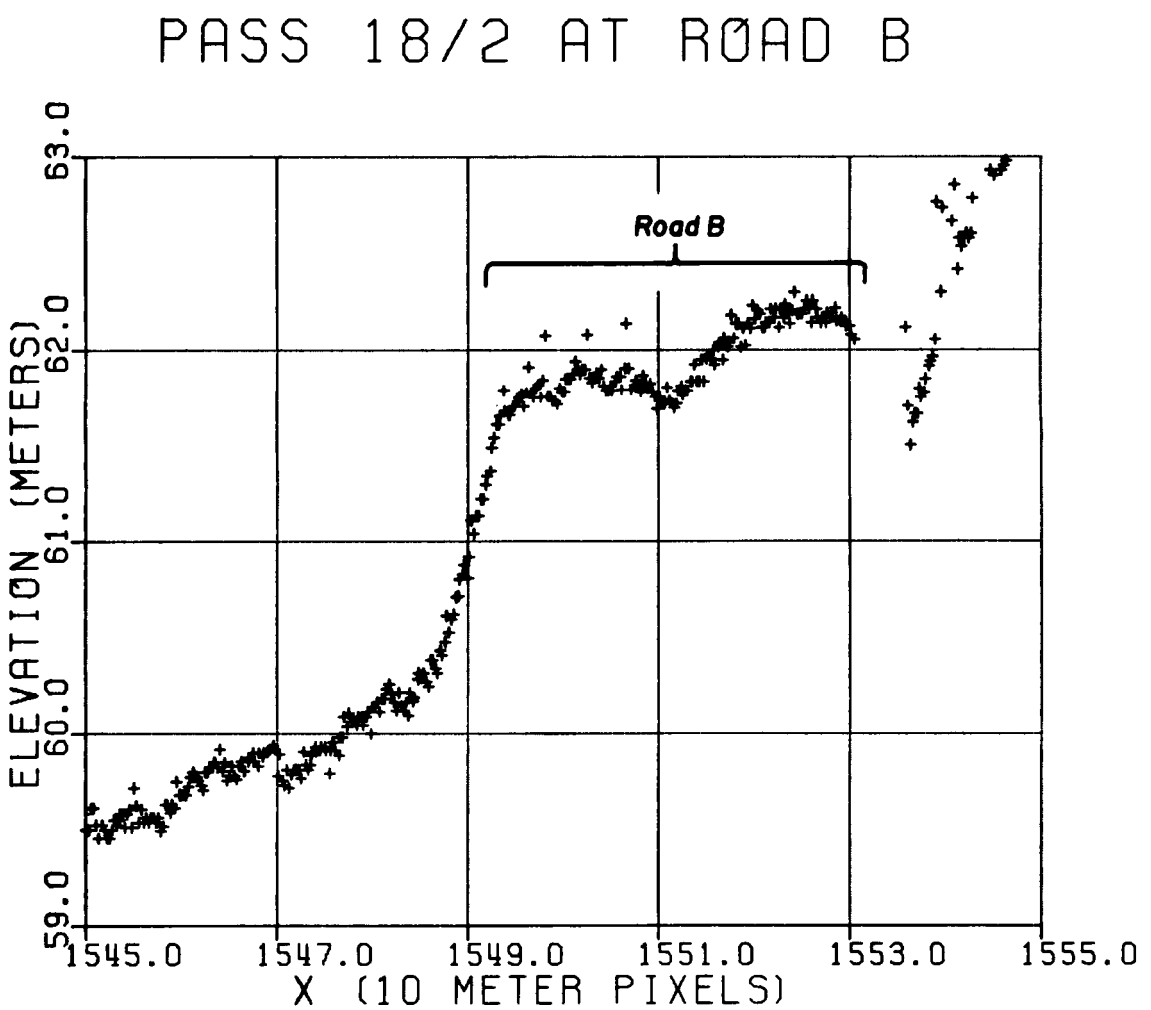

Figure 9. An enlargement of a portion of Pass 18/2 in the vicinity of Road B. The elevation of each individual laser measurements is indicated by a small "+". Notice the two roadway pavements which are apparent in the diagram.

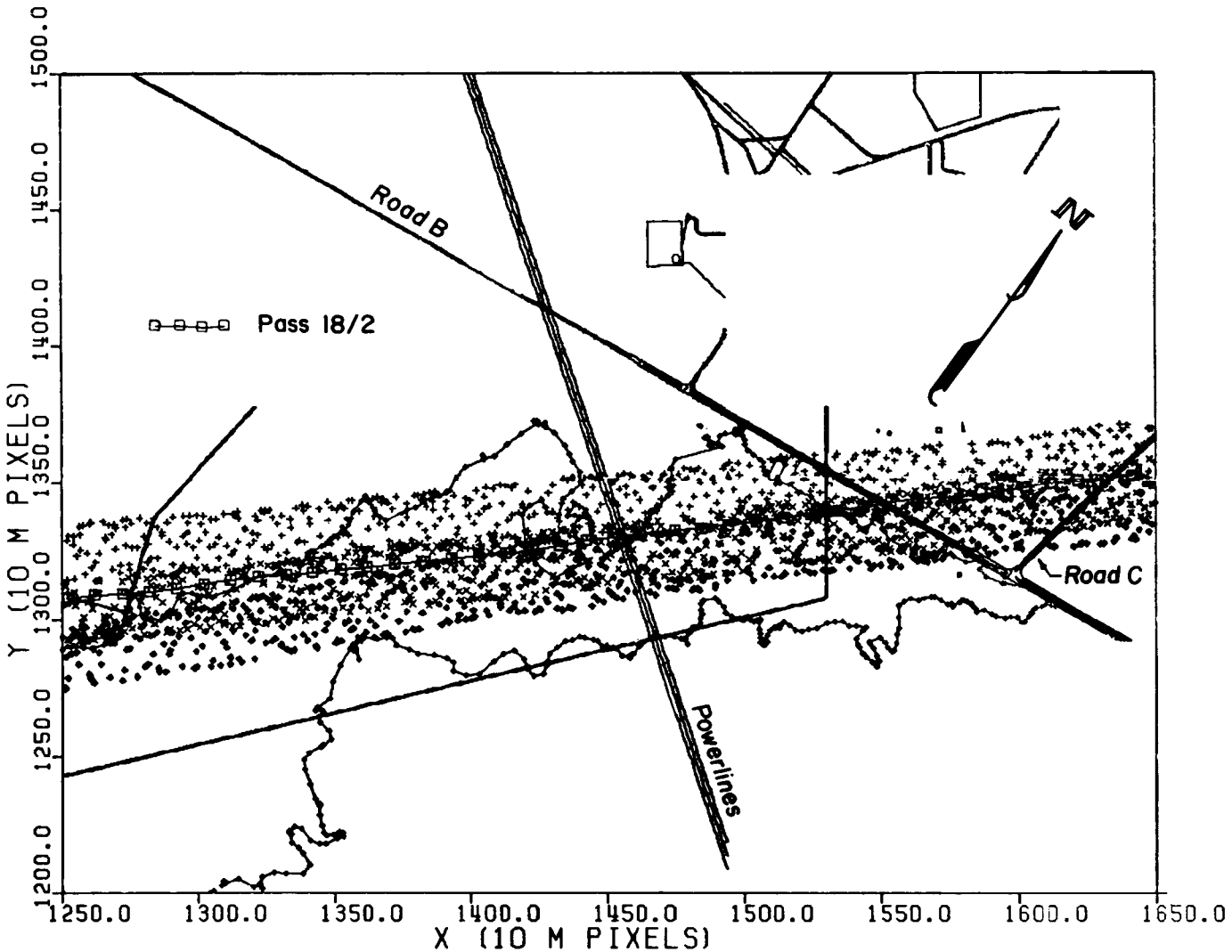

Figure 10. A diagram showing the swath coverage on passes 18/1 and 19/1. The ground track of the aircraft on Pass 18/2 is indicated by the small connected squares. The figure illustrates the common coverage of the three passes which facilitated registration.

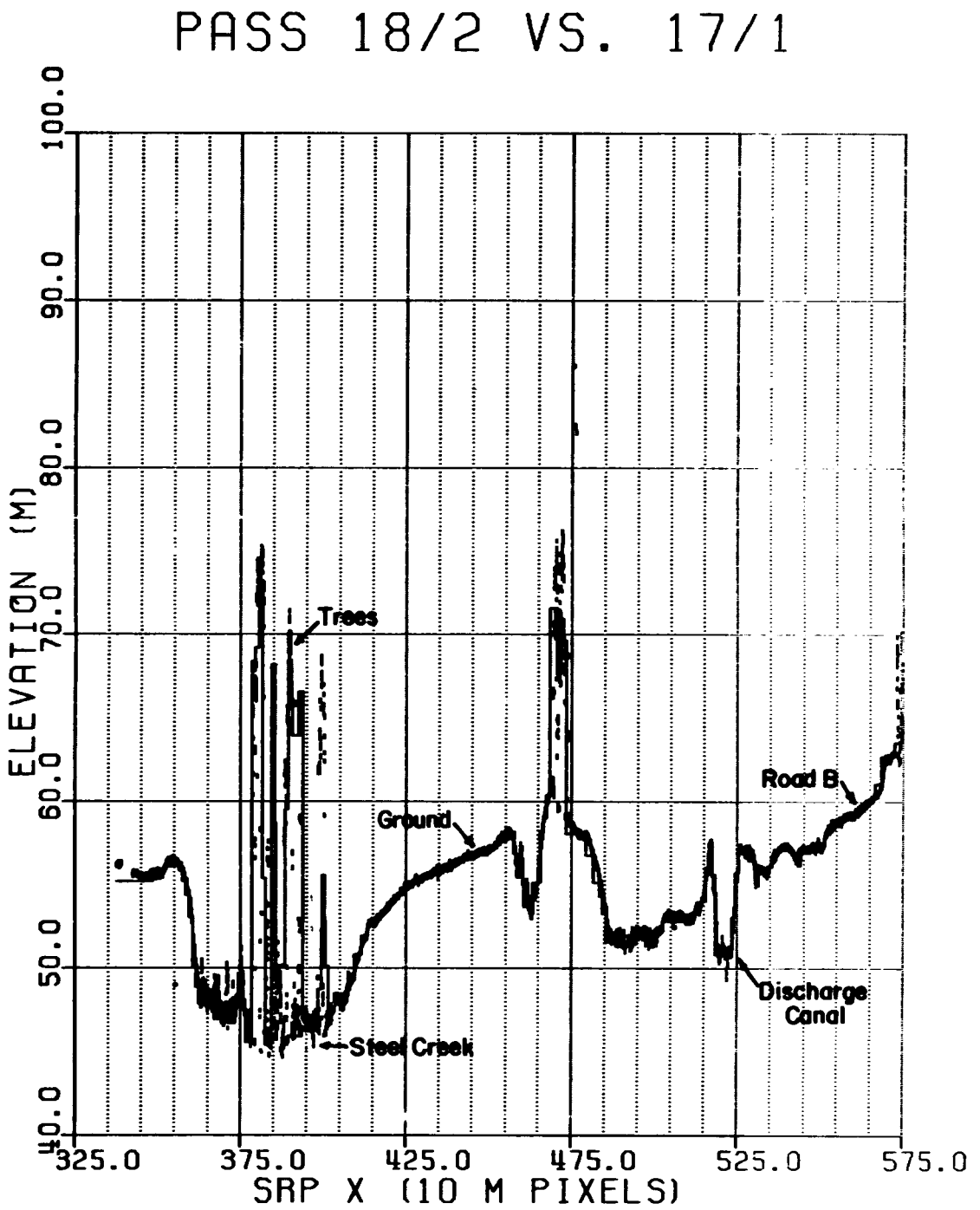

Figure 11. A plot comparing an elevational cross-section from profiling pass 18/2 (short vertical lines) with a profile extracted from scanning pass 17/1 (continuous connected line) after leveling and processing into evenly gridded pixels. Various features are labelled in the figure.

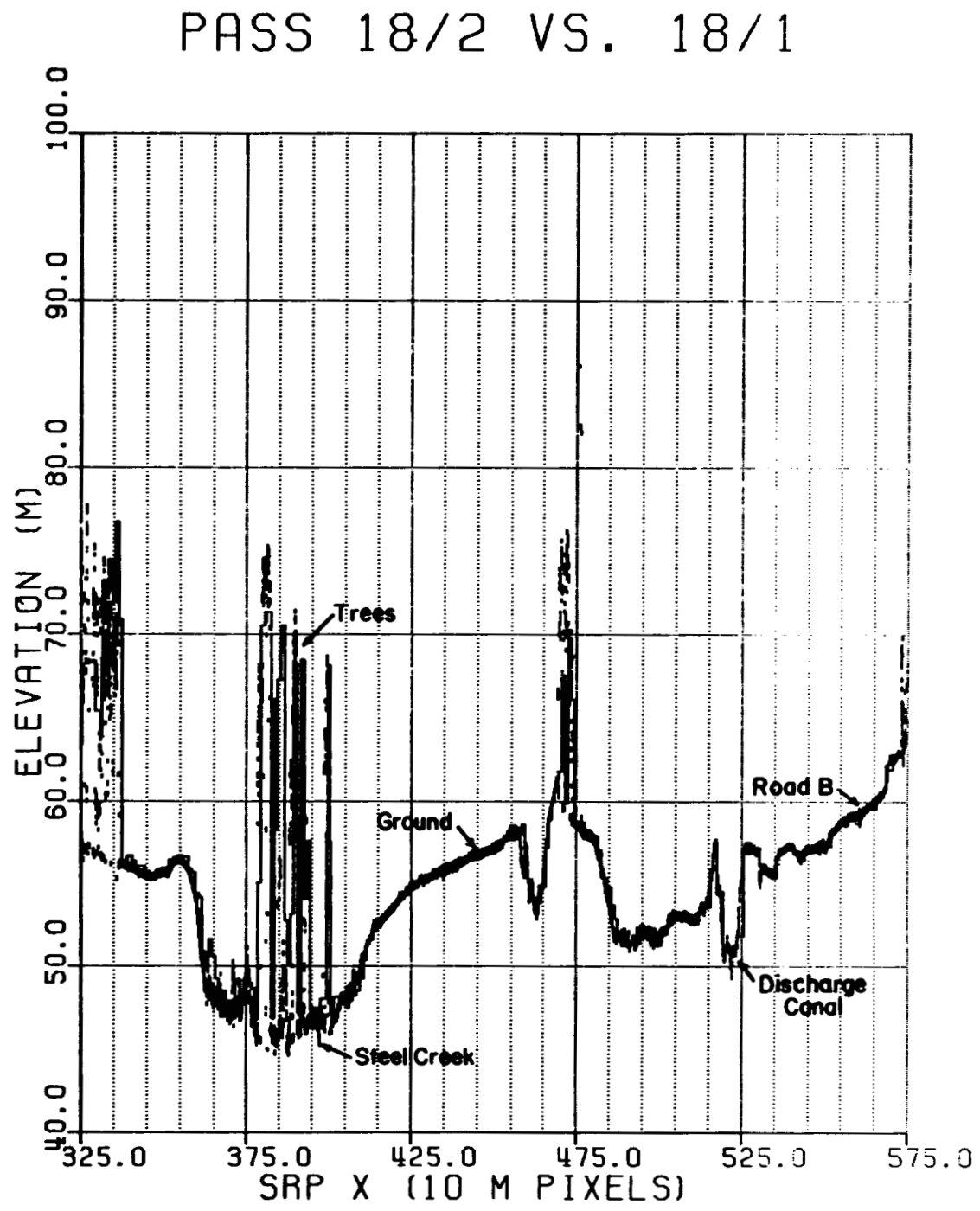

Figure 12. A plot comparing an elevational cross-section from profiling pass 18/2 (short vertical lines) with a profile extracted from scanning pass 18/1 (continuous connected line) after leveling and processing into evenly gridded pixels. Various features are labelled in the figure.

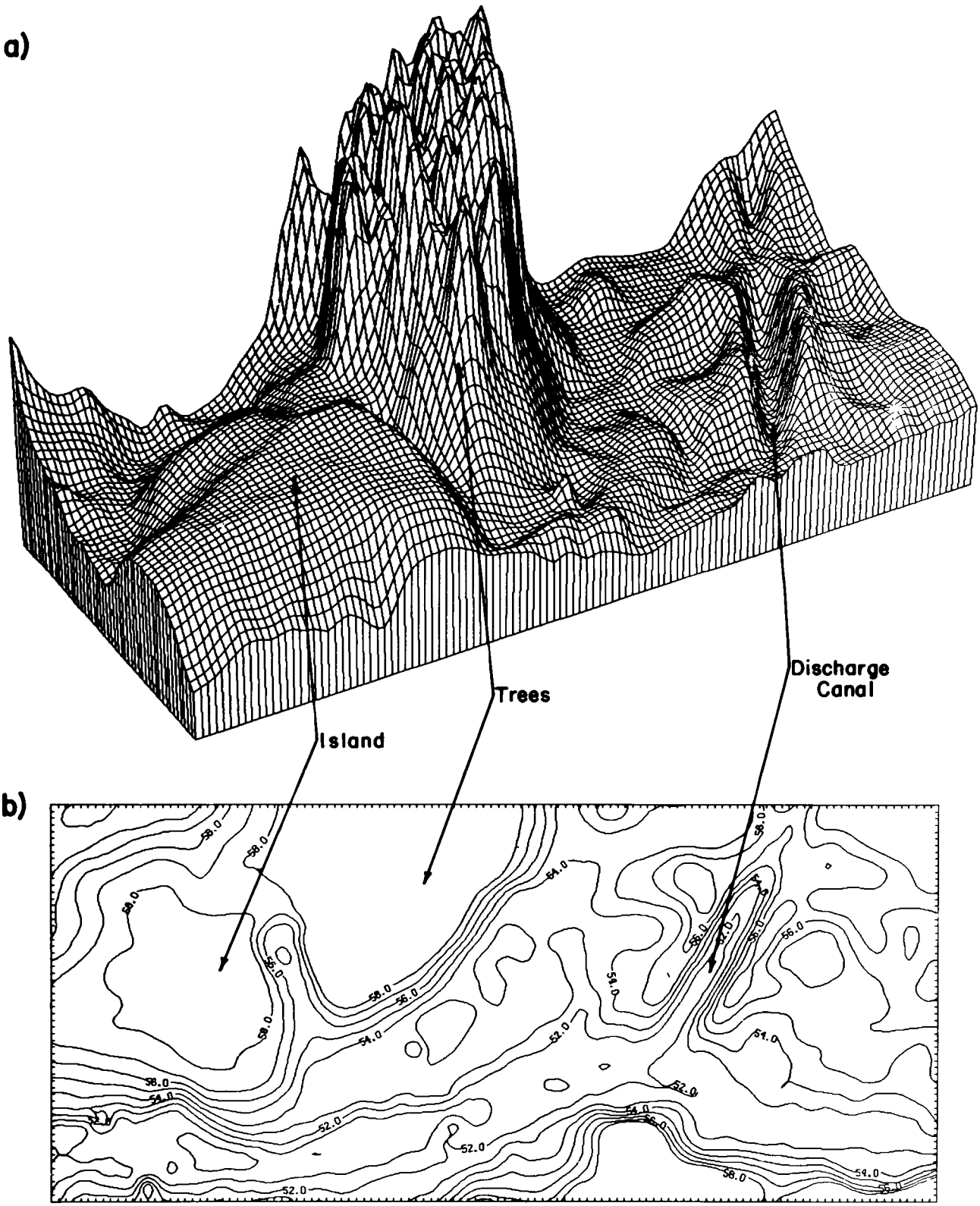

Figure 13. Examples of two types of final data products available from the merged topographic data sets. The upper diagram in the figure is a 3-dimensional isometric projection. A contoured projection of the same area is shown in the lower diagram.

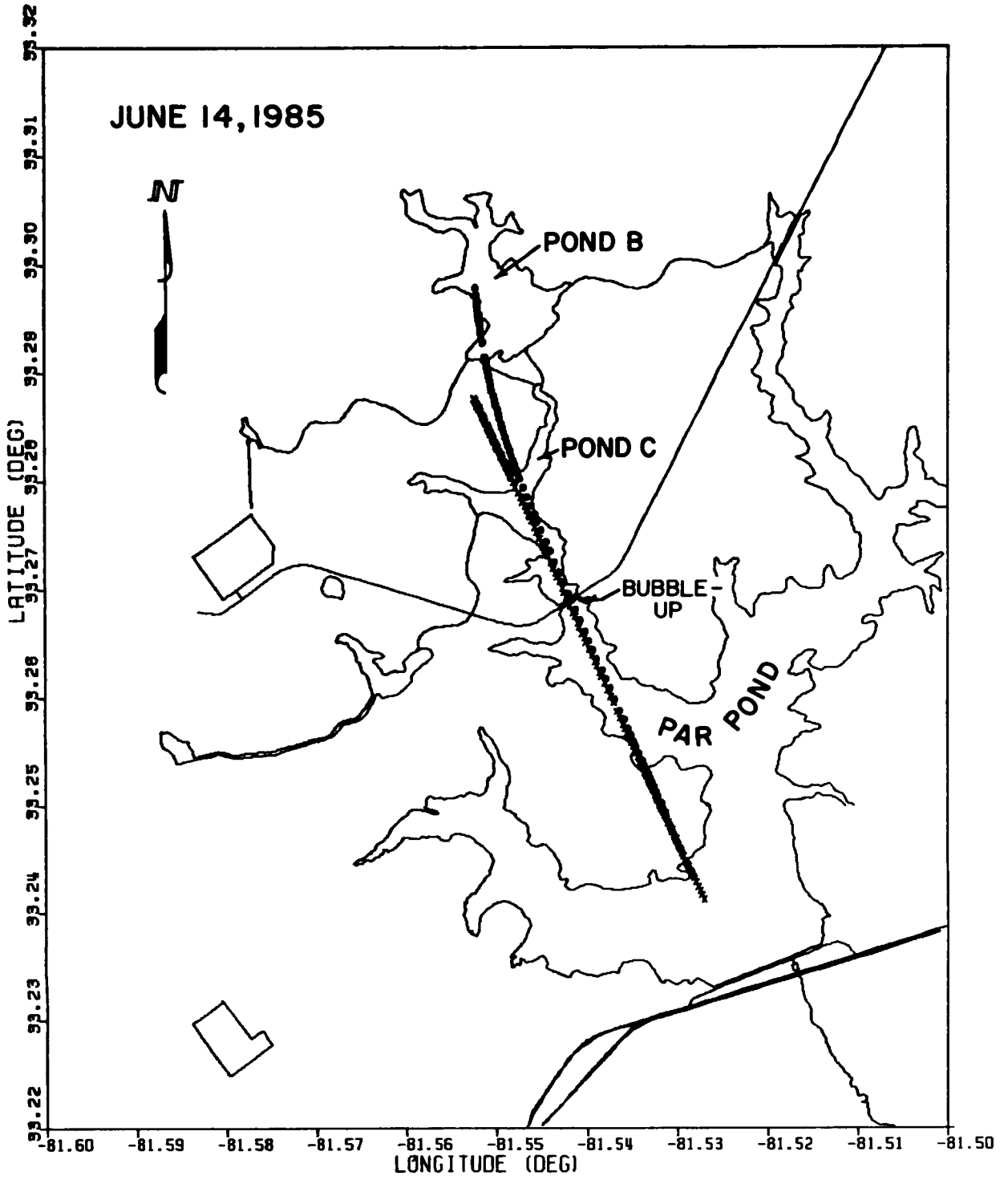

Figure 14. Map showing the ground tracks of the final two passes from the June 14th dye mapping investigation. The three ponds are labelled within the figure. Various cultural features are also shown.

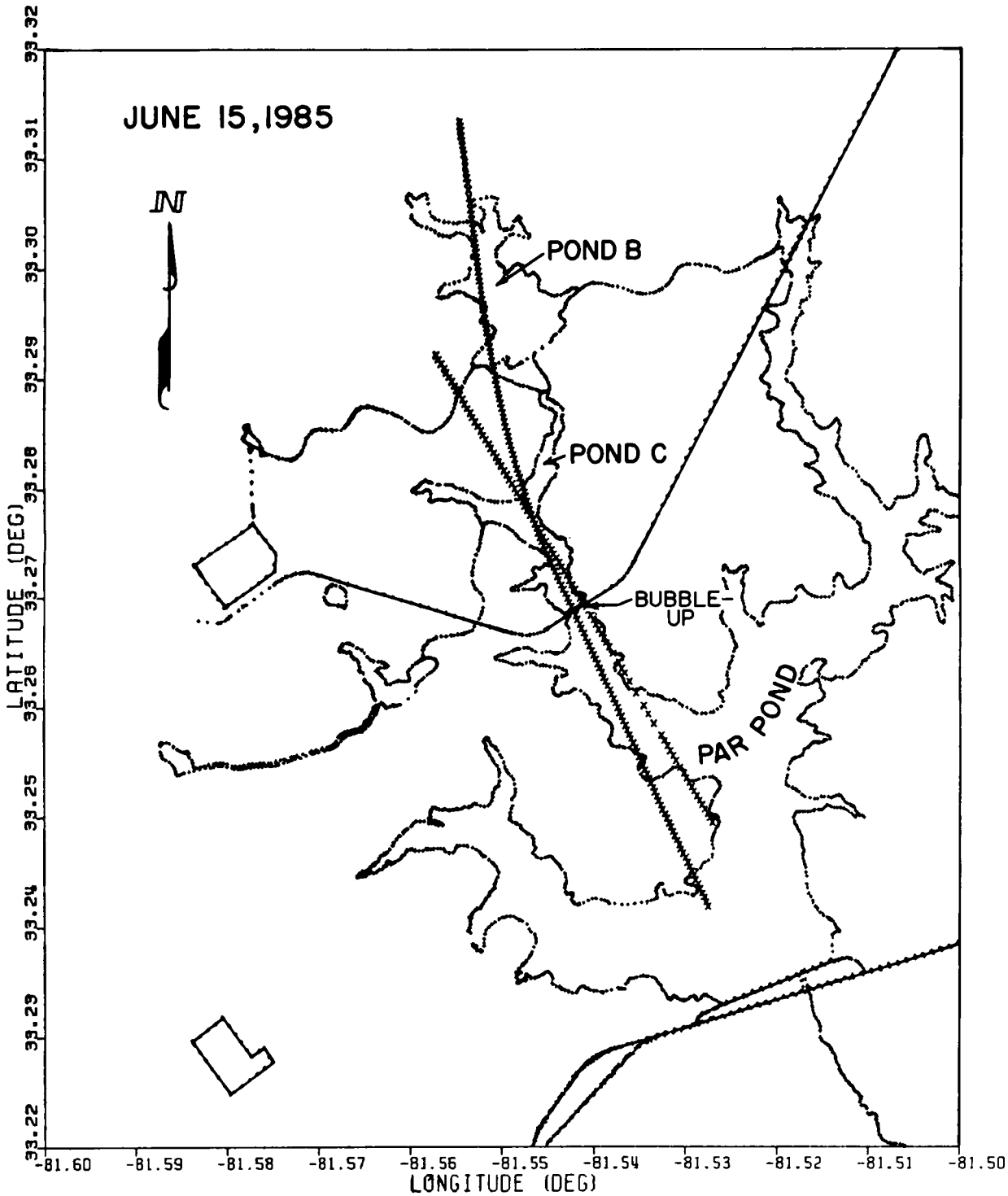

Figure 15. Map showing the ground tracks of the two passes from the June 15th dye mapping investigation. The three ponds are labelled within the figure. Various cultural features are also shown.

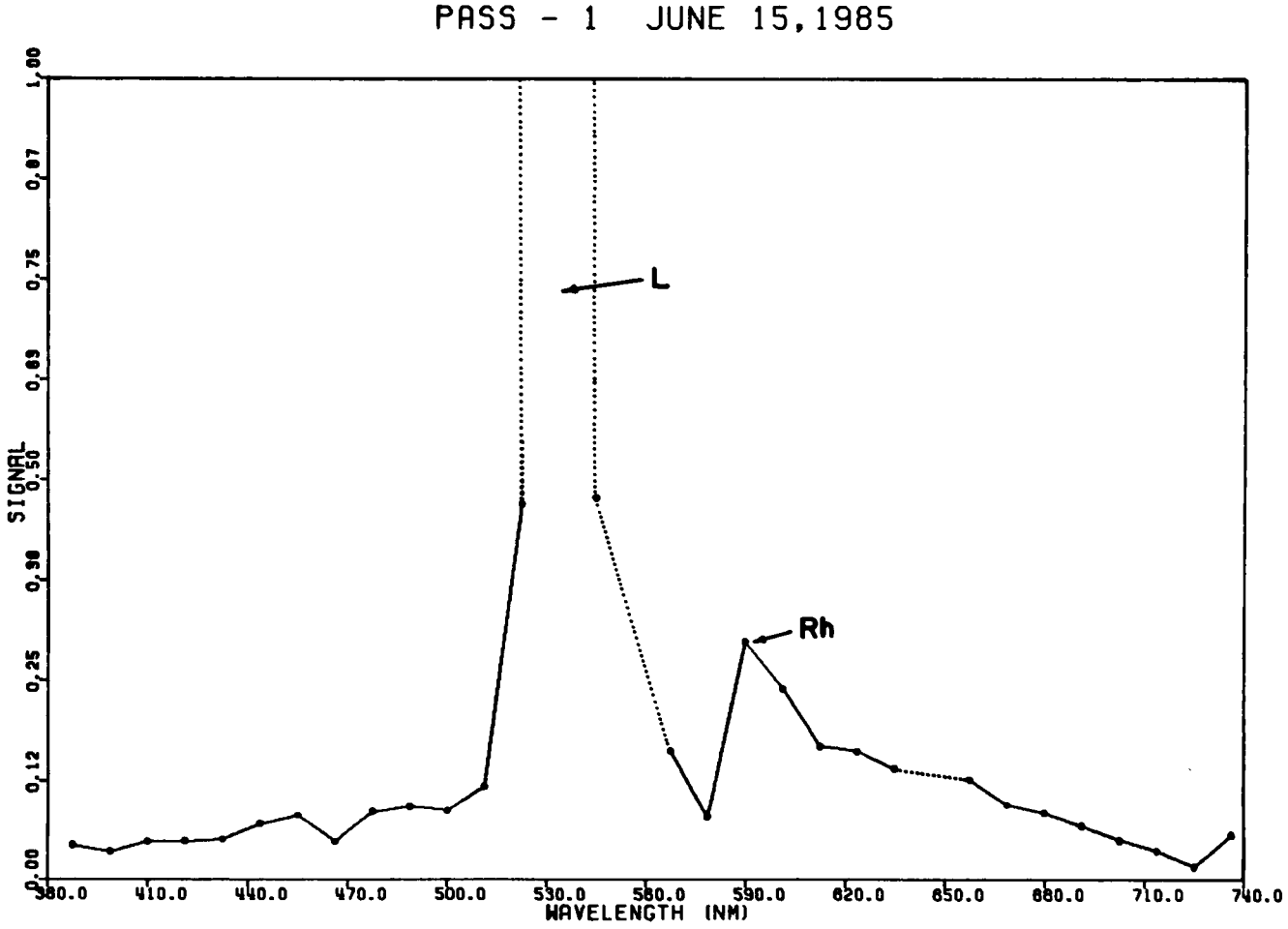

Figure 16. Laser induced Rhodamine WT fluorescence spectrum obtained with the aircraft system. The on-wavelength laser line "L" and peak dye fluorescence channel "Rh" are labelled in the figure.

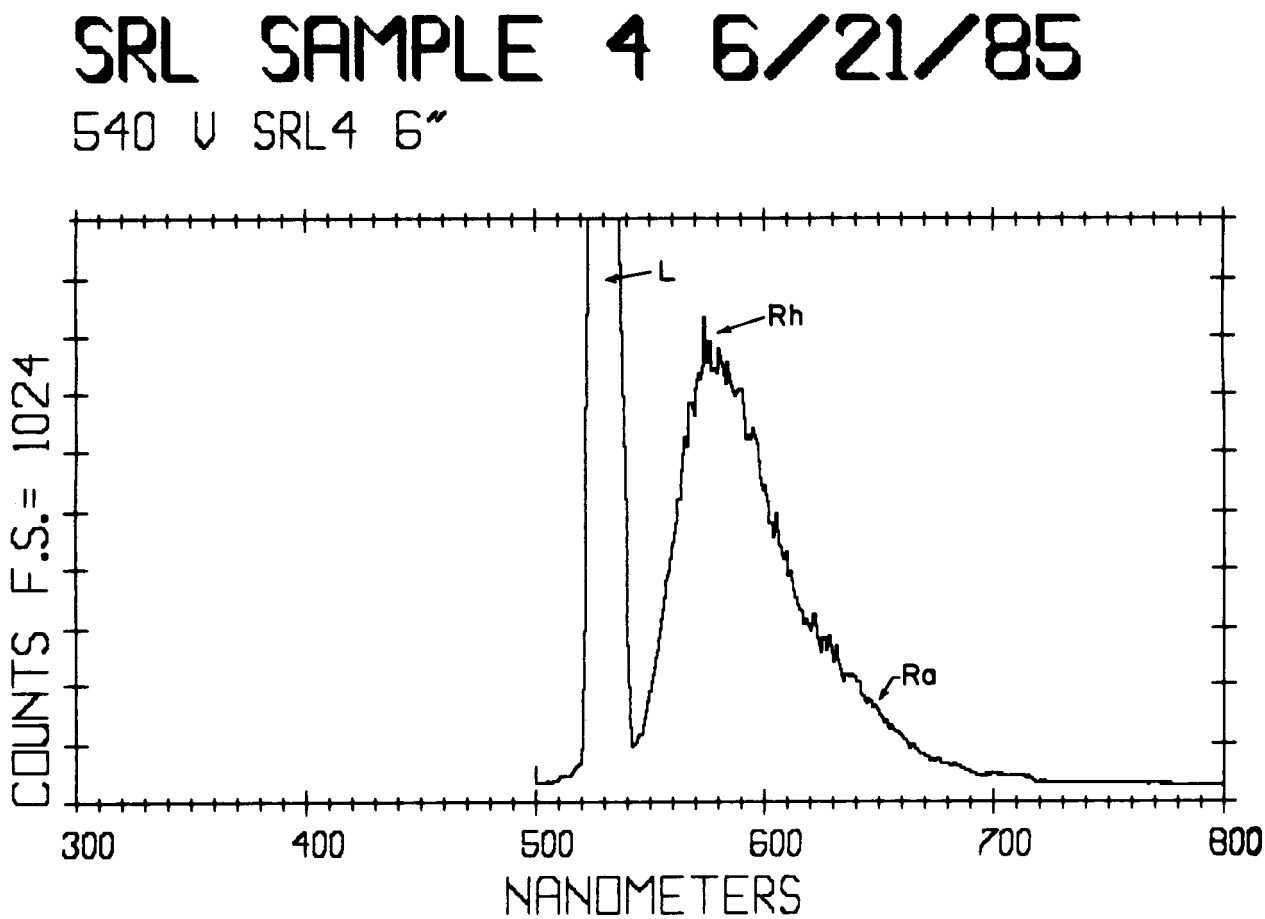

Figure 17. Laser induced Rhodamine WT fluorescence spectrum obtained with the Wallops Flight Facility Laser Laboratory system. The on-wavelength laser line "L" and peak dye fluorescence channel "Rh" are labelled in the figure.

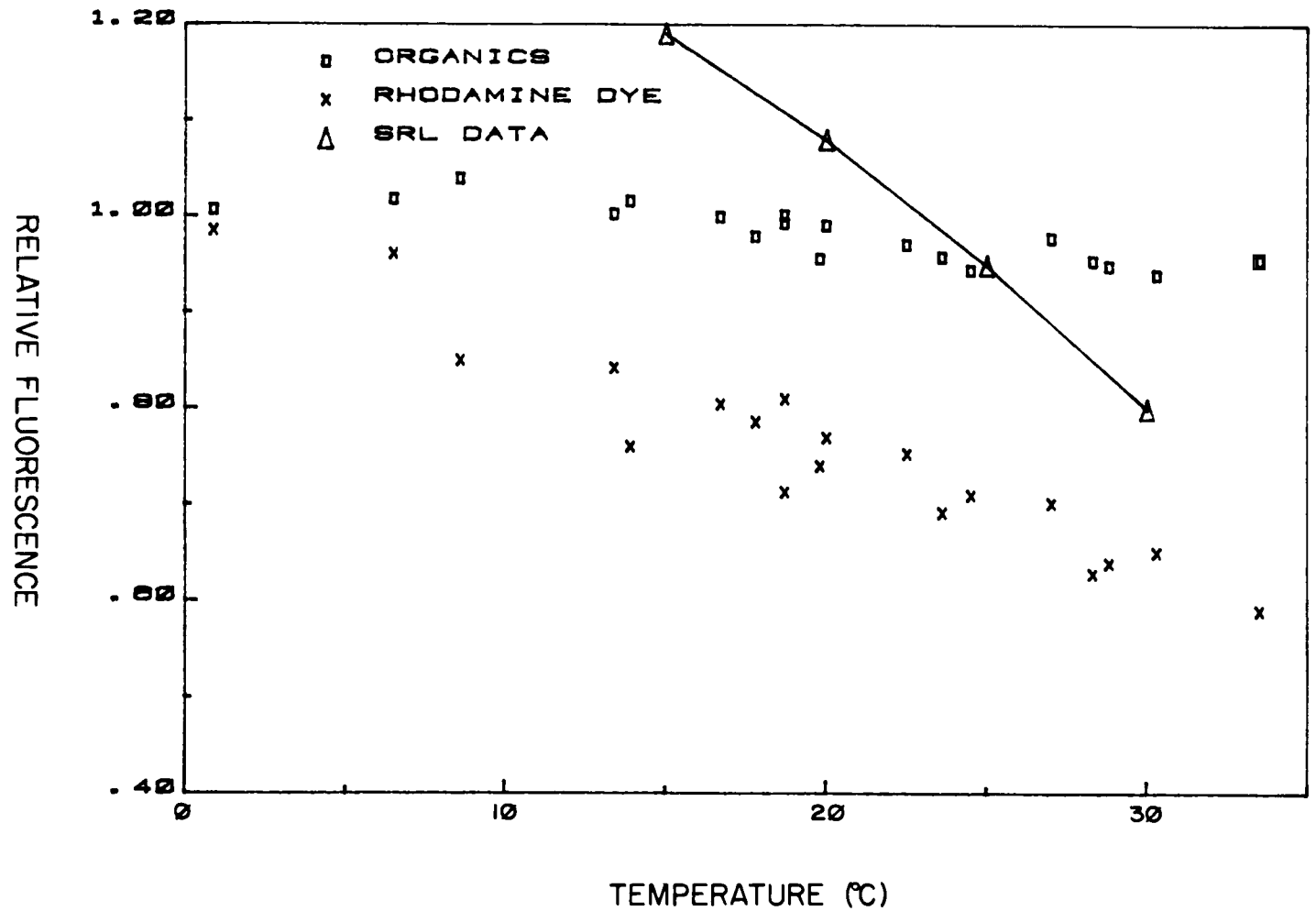

Figure 18. Plot illustrating the effect of temperature on relative fluorescence intensity. Shown in the plot are the laser induced fluorescence from dissolved organic matter "small squares" and Rhodamine dye "x's" both obtained on two sampling runs in the Wallops Flight Facility Laser Laboratory. Also shown is a plot of relative Rhodamine dye fluorescence obtained by SRP using a laboratory fluorometer.

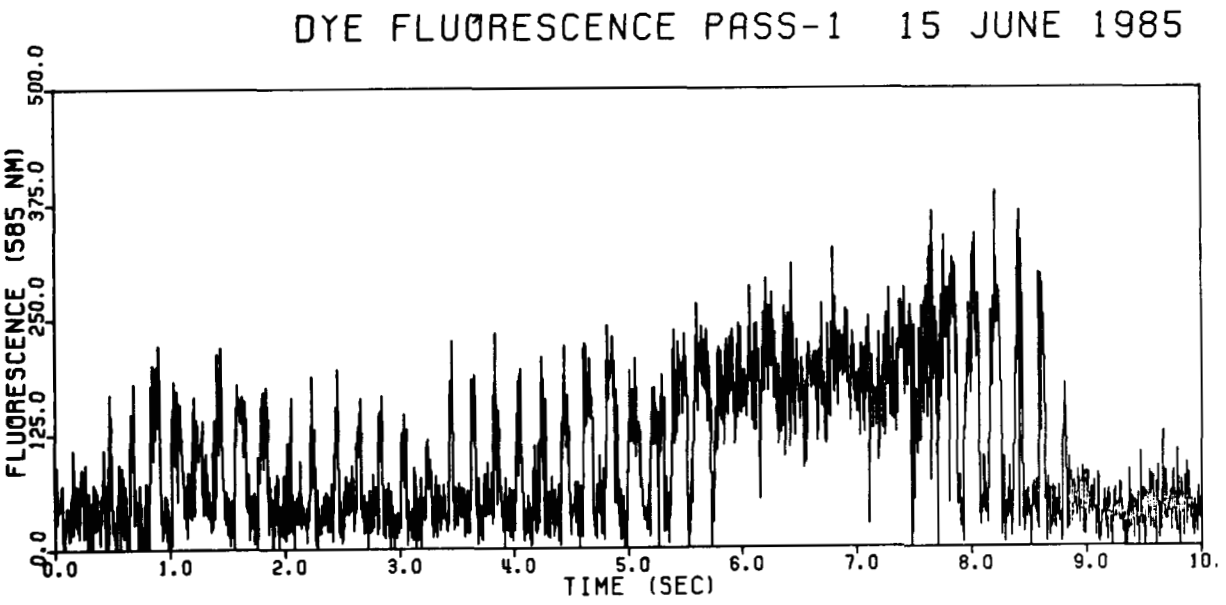

Figure 19. A cross-sectional plot of the peak laser induced fluorescence from Rhodamine dye plotted as a function time. The data was obtained during the first pass on June 15th. The modulation in the fluorescence signal from the scanner is apparent in the data. This effect is produced as the laser beam is swept alternately in and out of the dye plume.

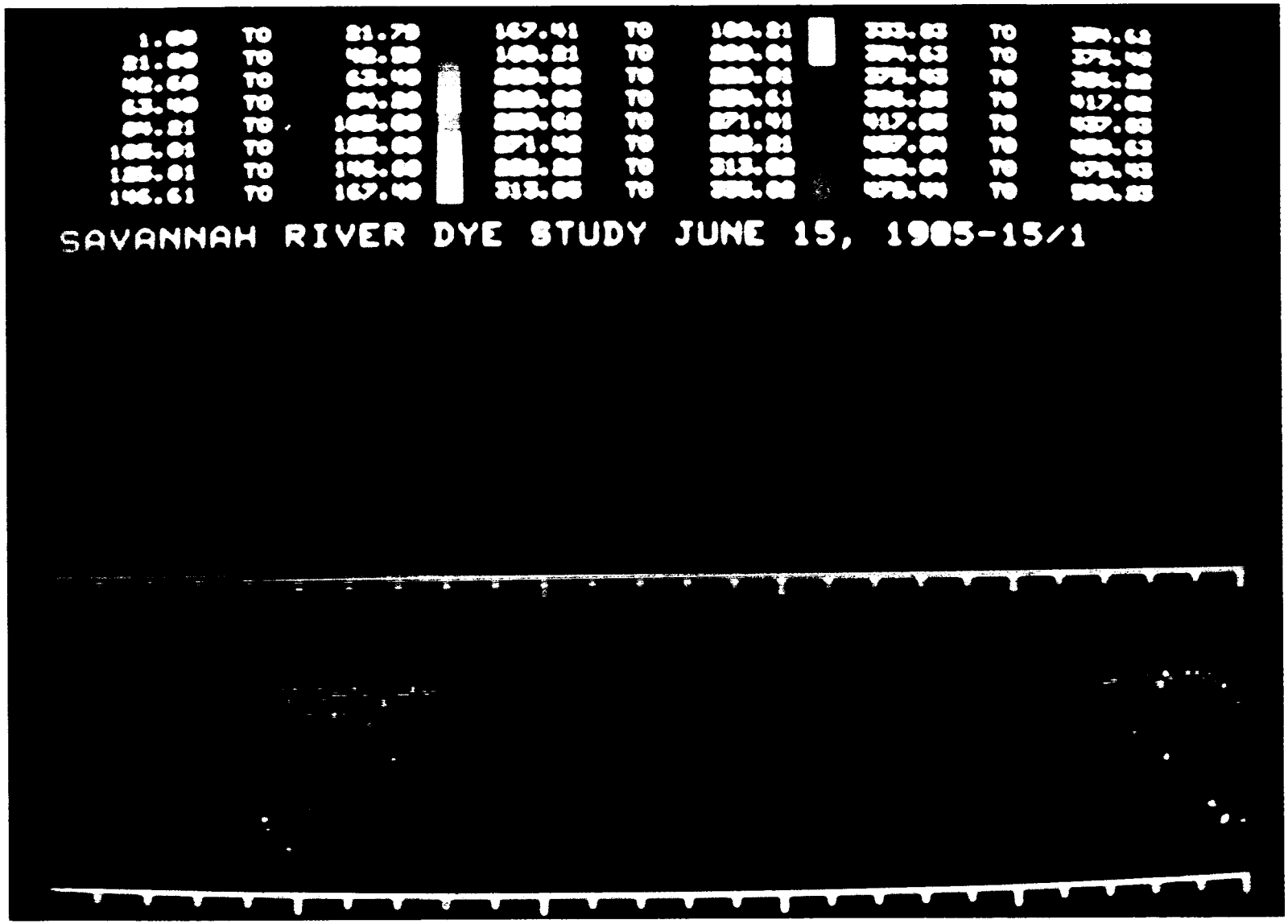

ORIGINAL PAGE
COLOR PHOTOGRAPH

Figure 20. A color plot of the dye fluorescence intensity at the individual laser footprints during the first pass on June 15th. The strength of the fluorescence is indicated by the color of the individual dots which are keyed to the inset above the diagram.

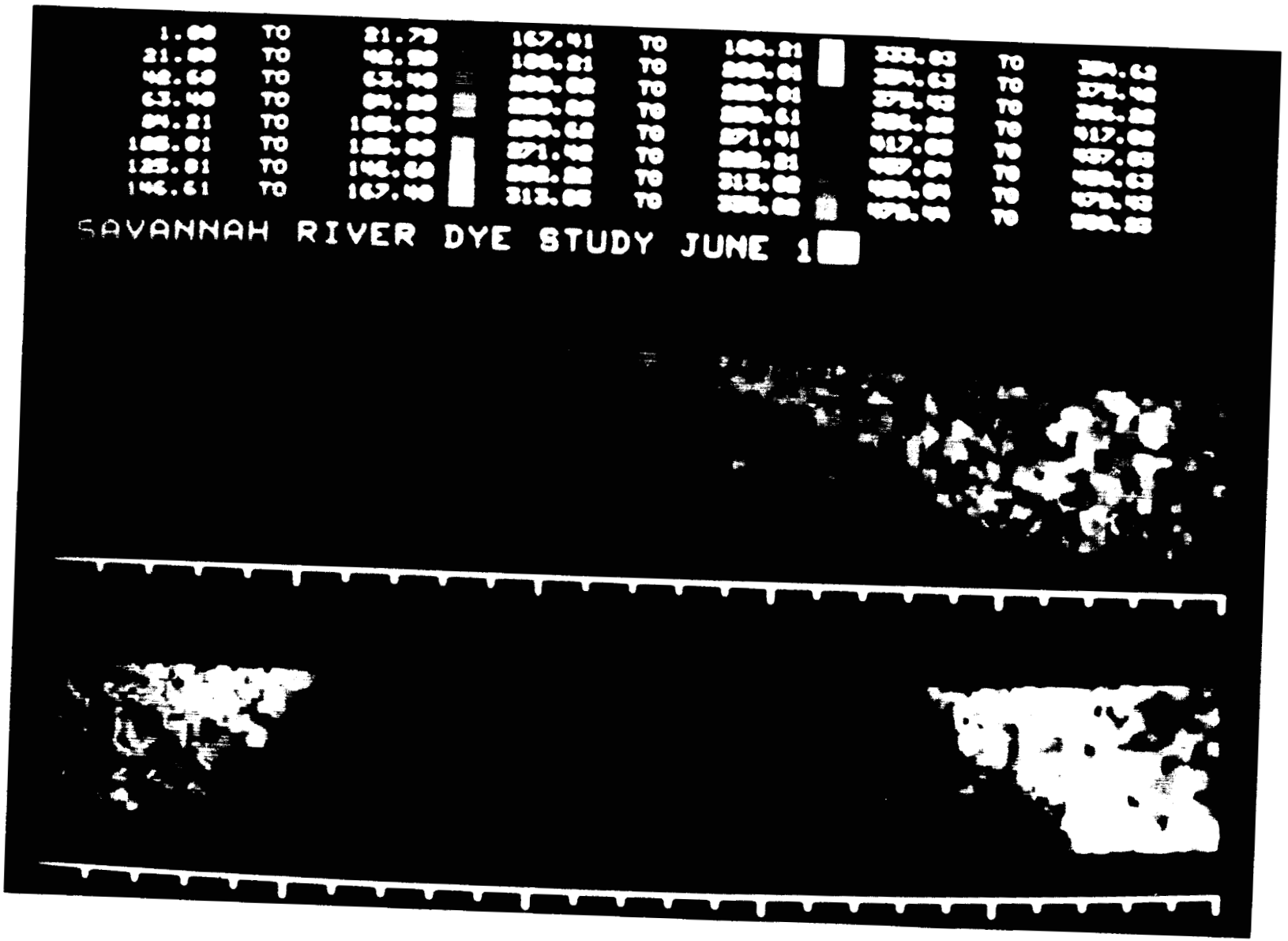

Figure 21. A color plot of the dye fluorescence intensity for the same pass shown in Figure 20. Here the data have been put into an evenly gridded format, filled and smoothed.

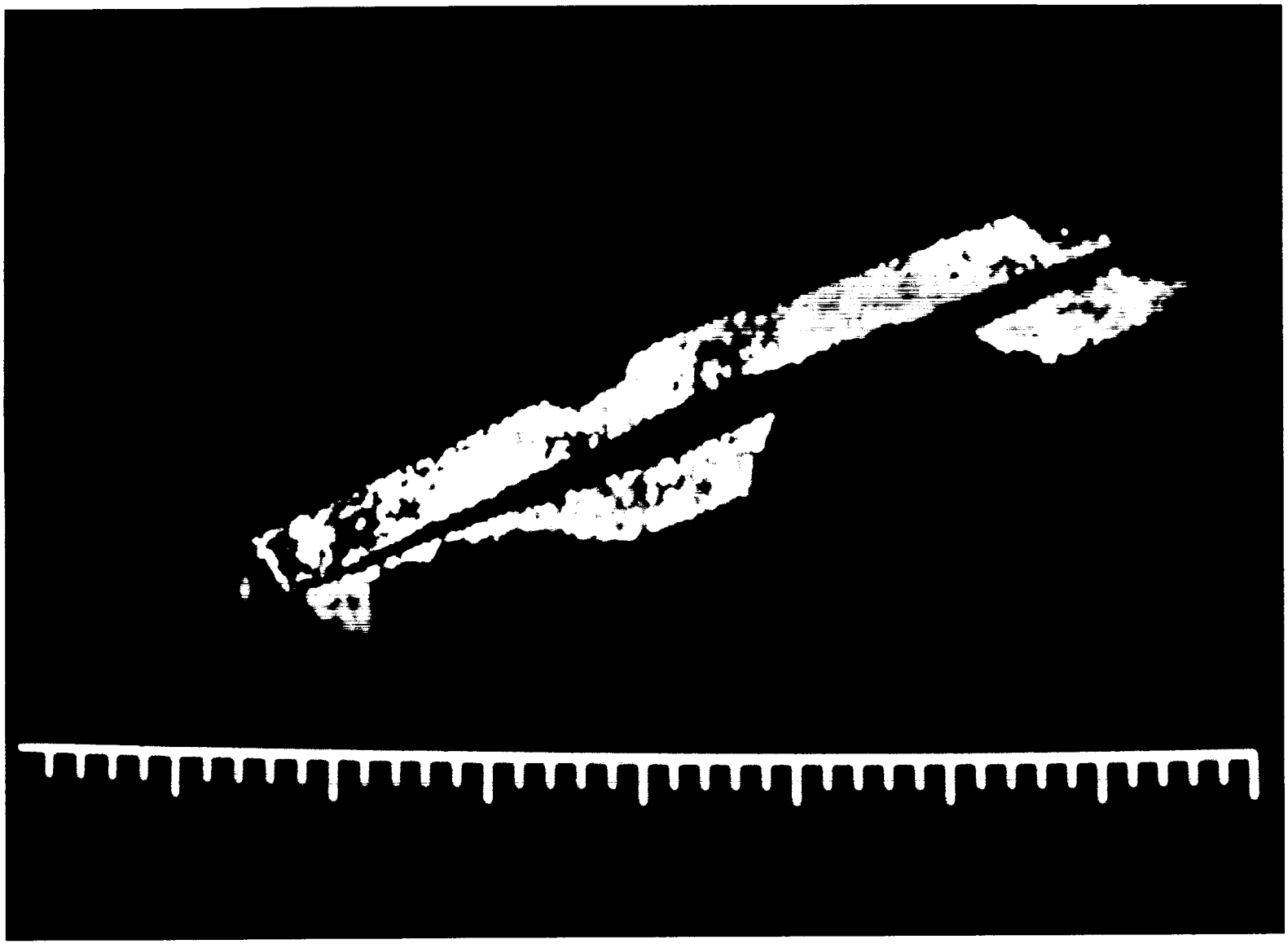

ORIGINAL PAGE
COLOR PHOTOGRAPH

Figure 22. A color plot of both passes from the June 15th mission. The data have been put into an evenly gridded format, filled, smoothed, and registered in the standard north/south coordinate system.

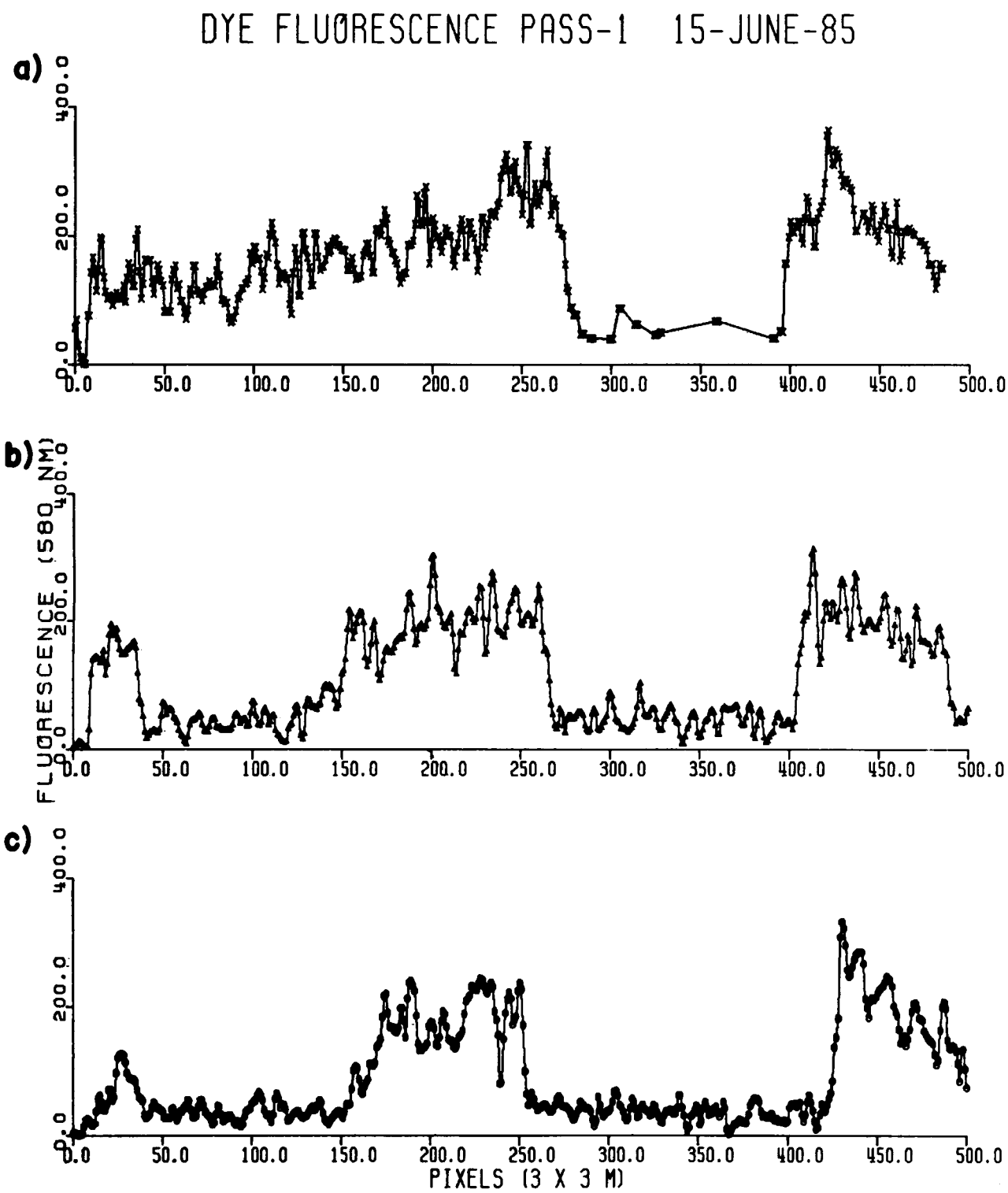

Figure 23. Cross-sectional plots of laser induced Rhodamine dye fluorescence from the left, center, and right portions of Pass 1 on June 15th. The data were put into an evenly gridded format, filled, and smoothed prior to extracting the cross-sections. This is an example of one of several analytical products that can be produced from the processed lidar data.

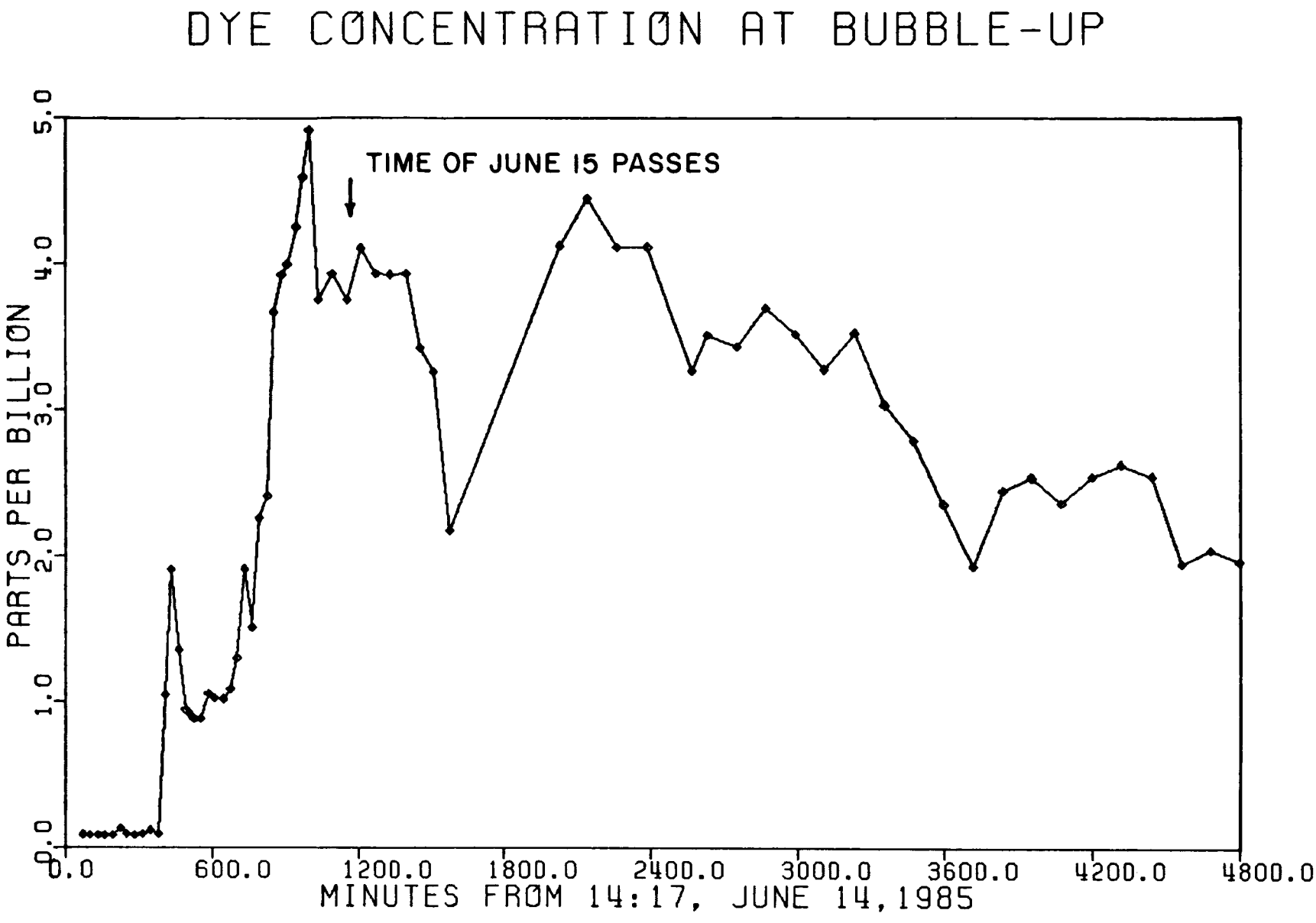

Figure 24. Graph of Rhodamine WT concentration at the "bubble-up" in the warm arm of Par Pond plotted as a function of time. Notice that the concentration at the time of the June 15th passes was ~4 μg/l, thus the dye concentration detected with the lidar system below the bubble-up was 4 μg/l or less. The dye concentration measurements were furnished by SRP.

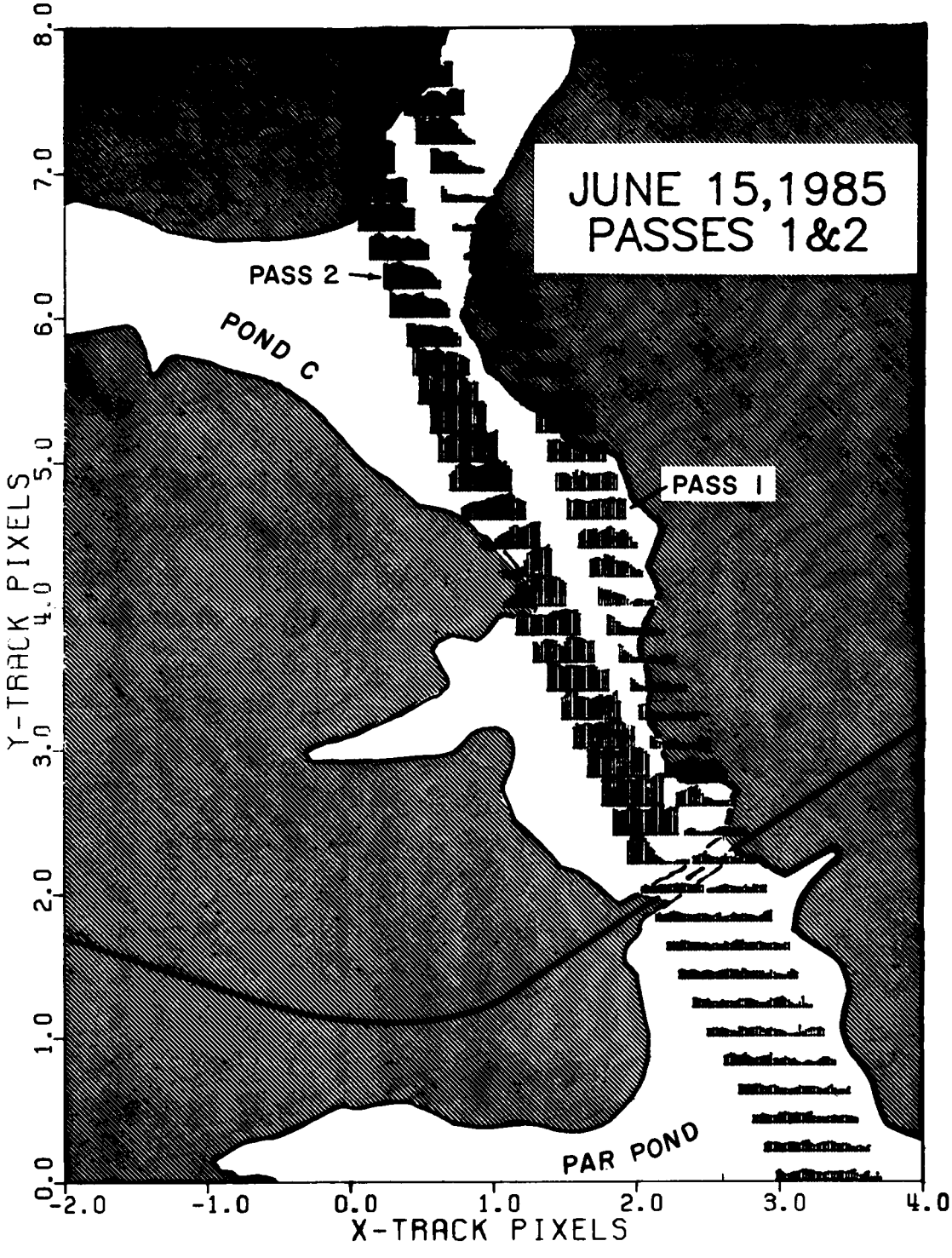

Figure 25. A "stick" projection of laser induced Rhodamine WT dye fluorescence produced from Passes 1 and 2 of the June 15th mission. Prior to plotting, the data were placed into an evenly gridded format, filled, smoothed, and registered into the standard north/south coordinate system. This is an example of one of several analytical products that can be produced from the processed lidar data.

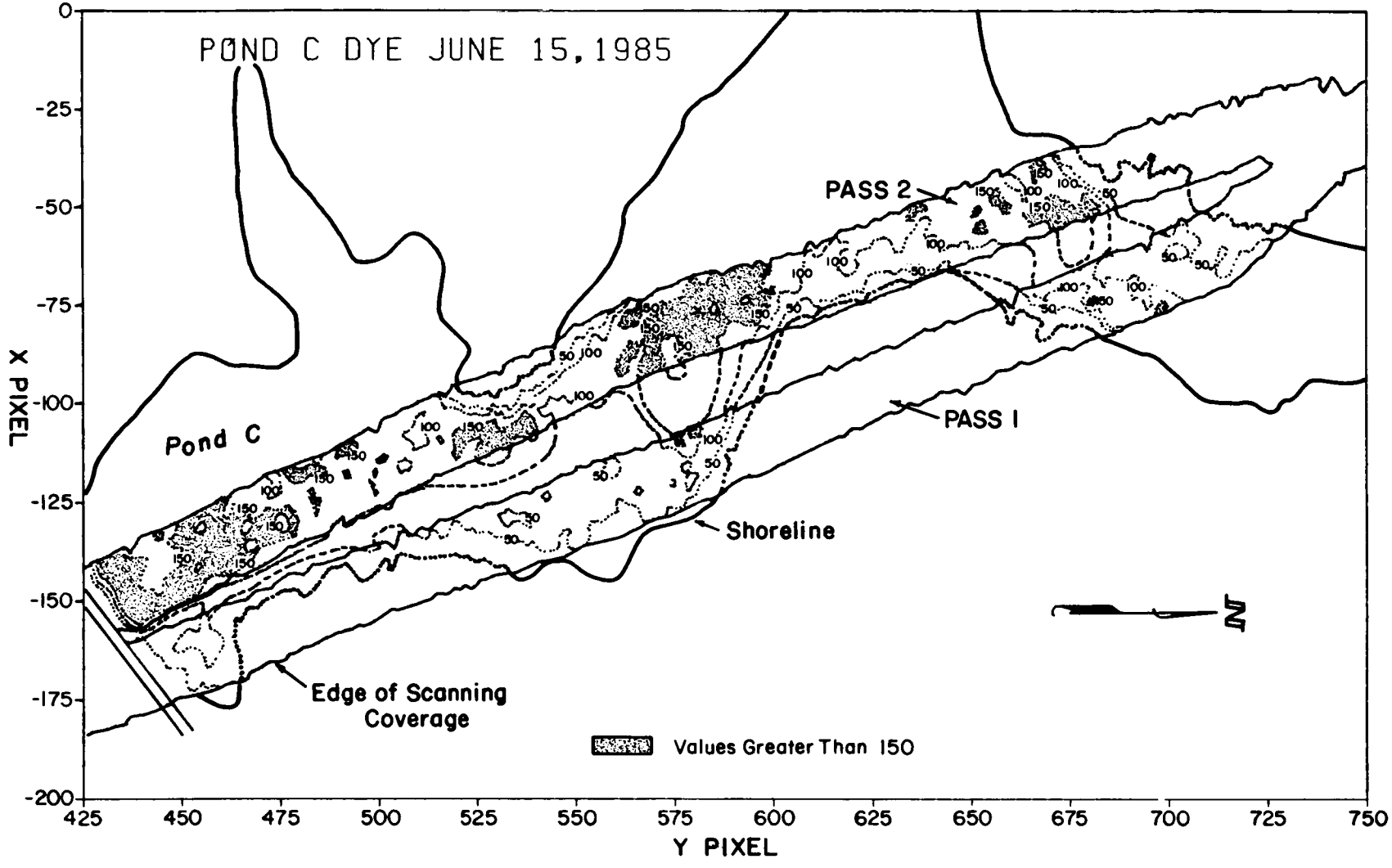

Figure 26. A contour projection of laser induced Rhodamine WT dye fluorescence produced from Passes 1 and 2 from the June 15th mission. Prior to plotting, the data placed into an evenly gridded format, filled, smoothed, and registered in the standard north/south coordinate system. This is an example of one of several analytical products that can be produced from the processed lidar data.

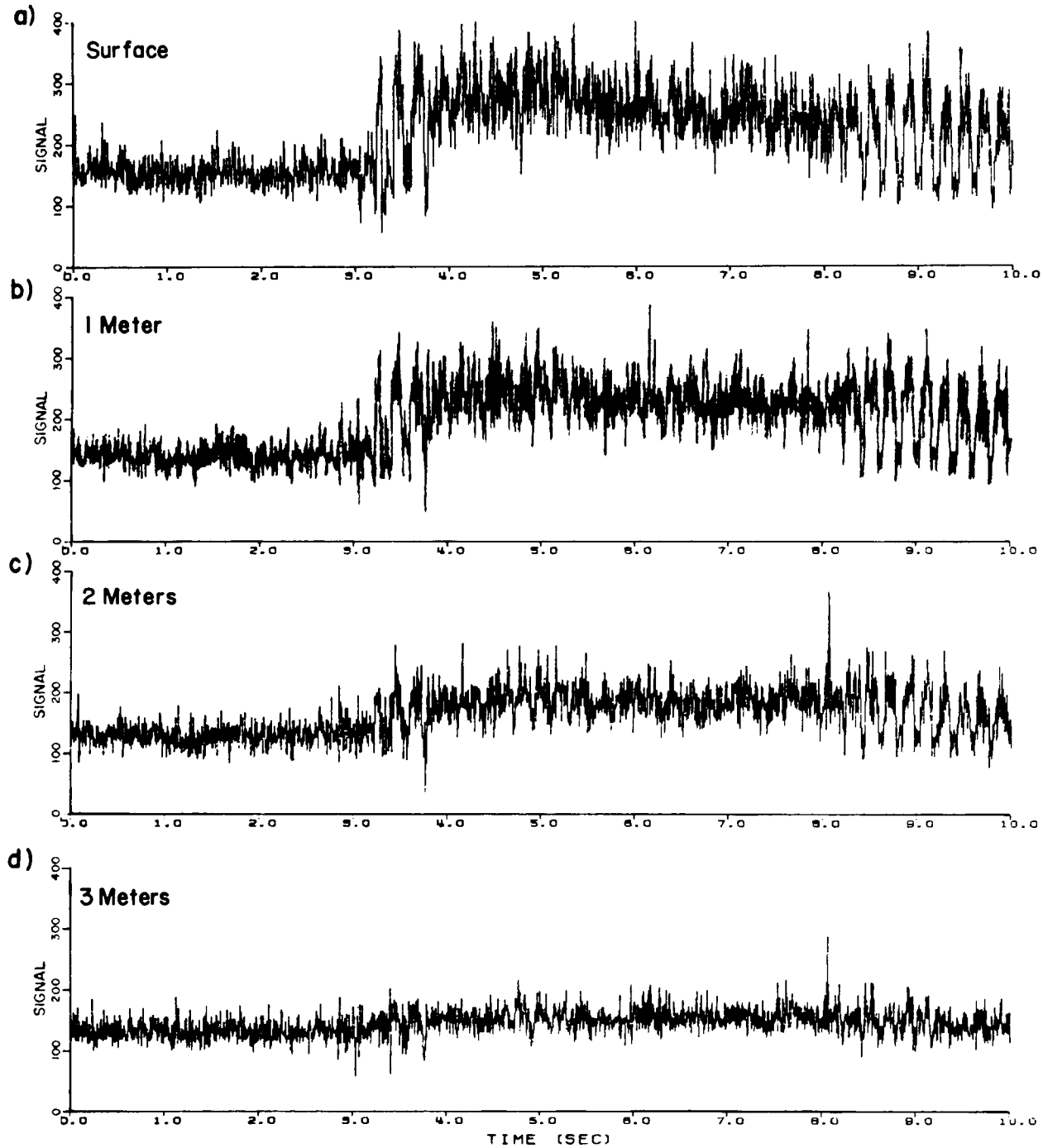

Figure 27. Cross-sections of laser induced Rhodamine WT dye fluorescence at the surface and at depths of 1, 2, and 3 m water depth obtained on Pass 1 from the June 15th mission. The data have not been evenly gridded. Accordingly, the modulation in the fluorescence signal produced as the scanner sweeps the laser beam alternately into and out of the dye plume is apparent in the cross-sectional profiles.

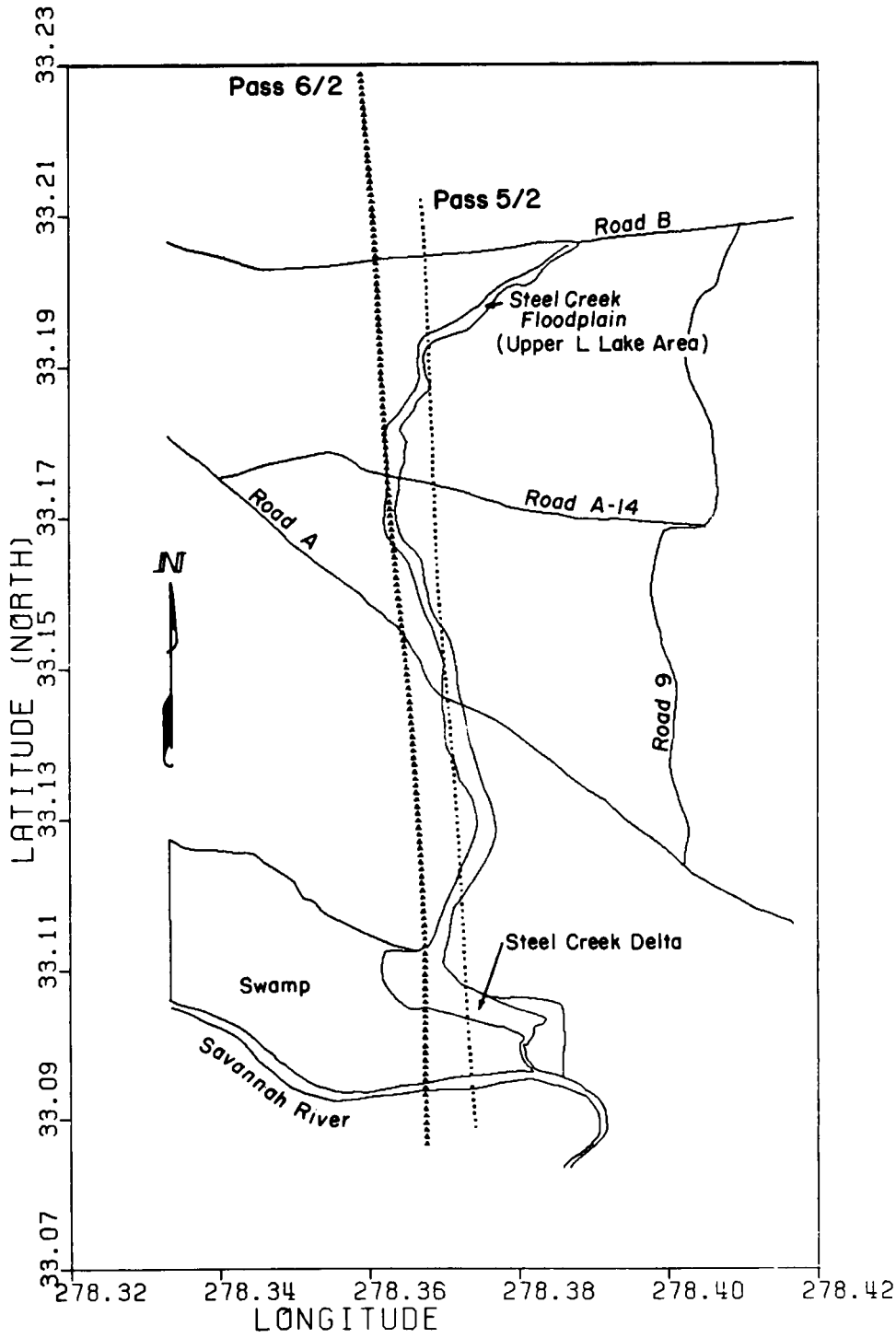

Figure 28. An enlarged plot of the Steel Creek Corridor showing the locations for the two wetlands mapping passes. Various cultural features are labelled within the figure.

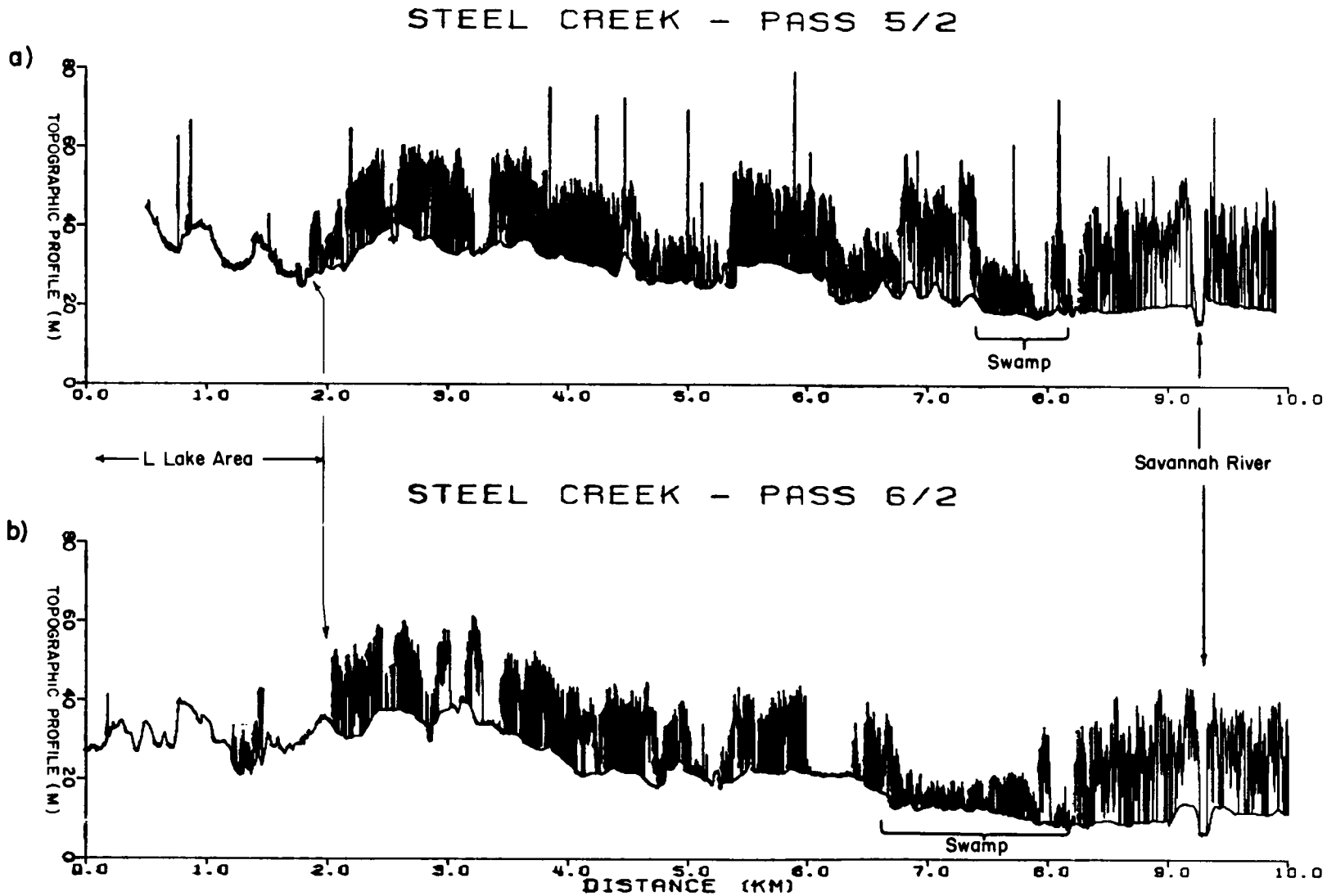

Figure 29. An elevation cross-section of both wetlands mapping passes plotted as a function of along-track distance. The location of the Savannah River, swamp, and L-Lake areas are indicated in the figures. This illustration should be referred to when studying the enlarged elevation cross-sections presented in Figures 30 - 39.

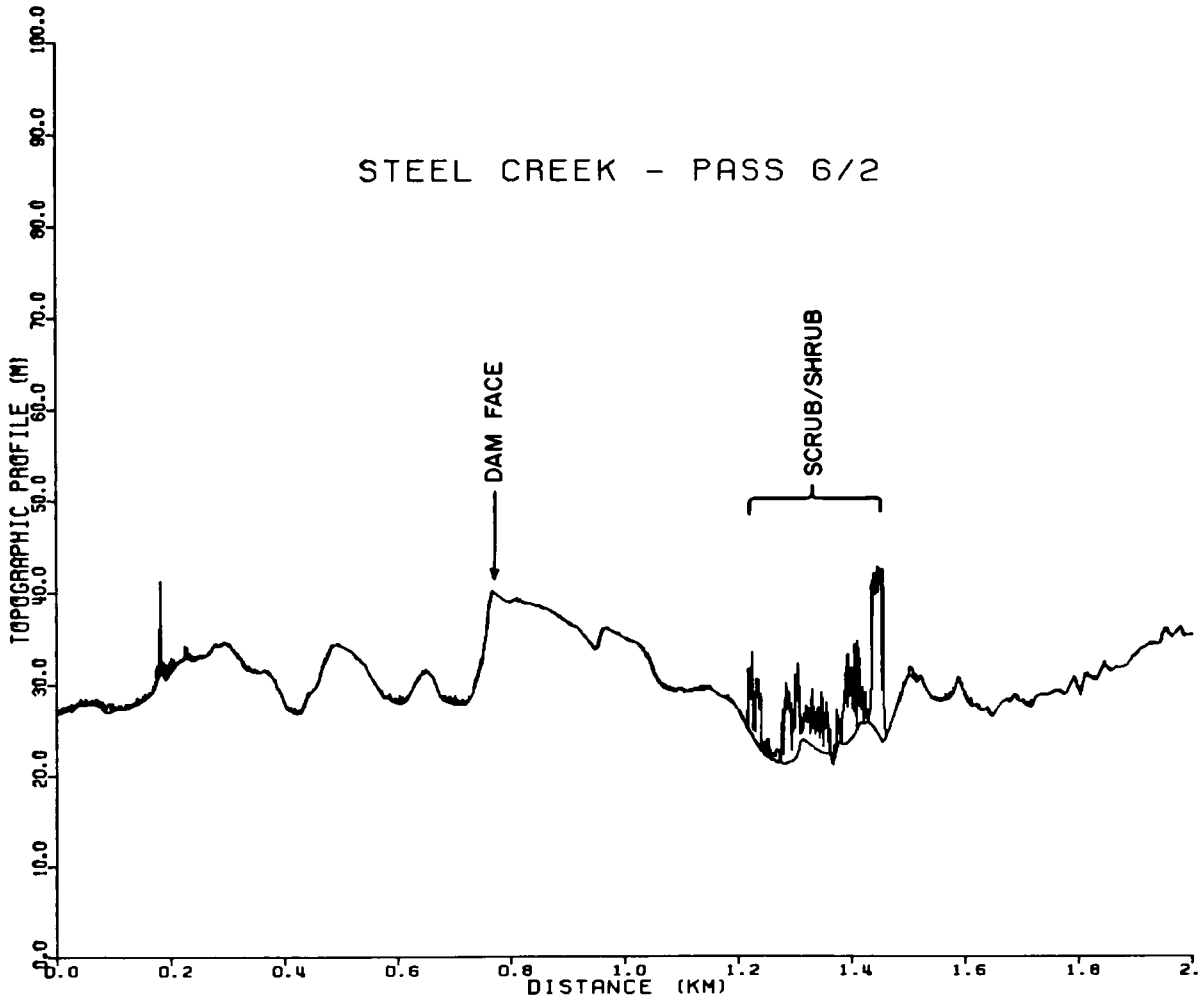

Figure 30. An enlargement of a portion of the elevation profile from Pass 6/2 acquired over the Steel Creek Wetlands. The location of various features of interest are labelled within the figure. The along-track distance (x-axis label) can be used to find the location of the plot in the overall cross-section of Pass 6/2 shown in Figure 29.

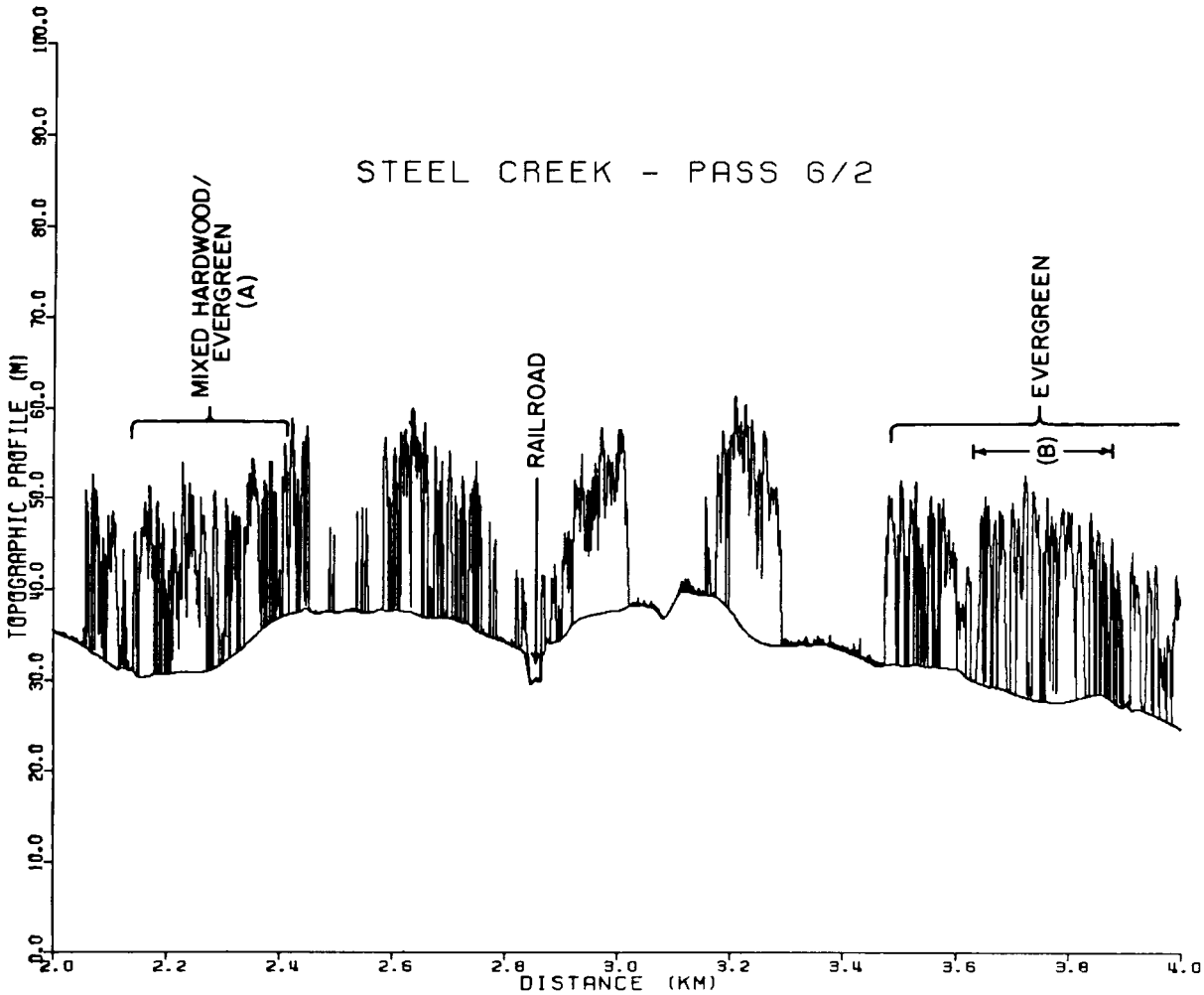

Figure 31. An enlargement of a portion of the elevation profile from Pass 6/2 acquired over the Steel Creek Wetlands. The location of various features of interest are labelled within the figure. The along-track distance (x-axis label) can be used to find the location of the plot in the overall cross-section of Pass 6/2 shown in Figure 29.

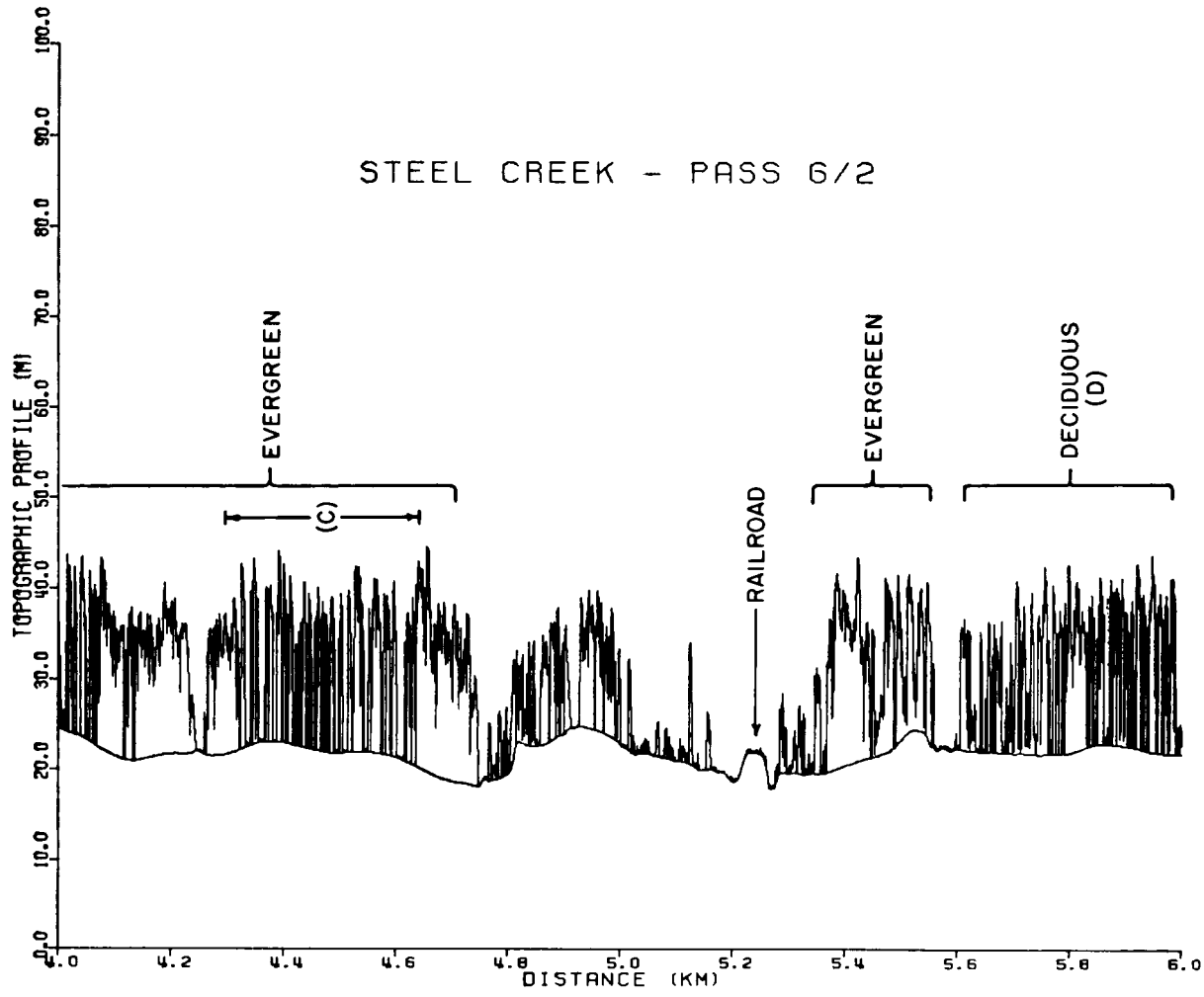

Figure 32. An enlargement of a portion of the elevation profile from Pass 6/2 acquired over the Steel Creek Wetlands. The location of various features of interest are labelled within the figure. The along-track distance (x-axis label) can be used to find the location of the plot in the overall cross-section of Pass 6/2 shown in Figure 29.

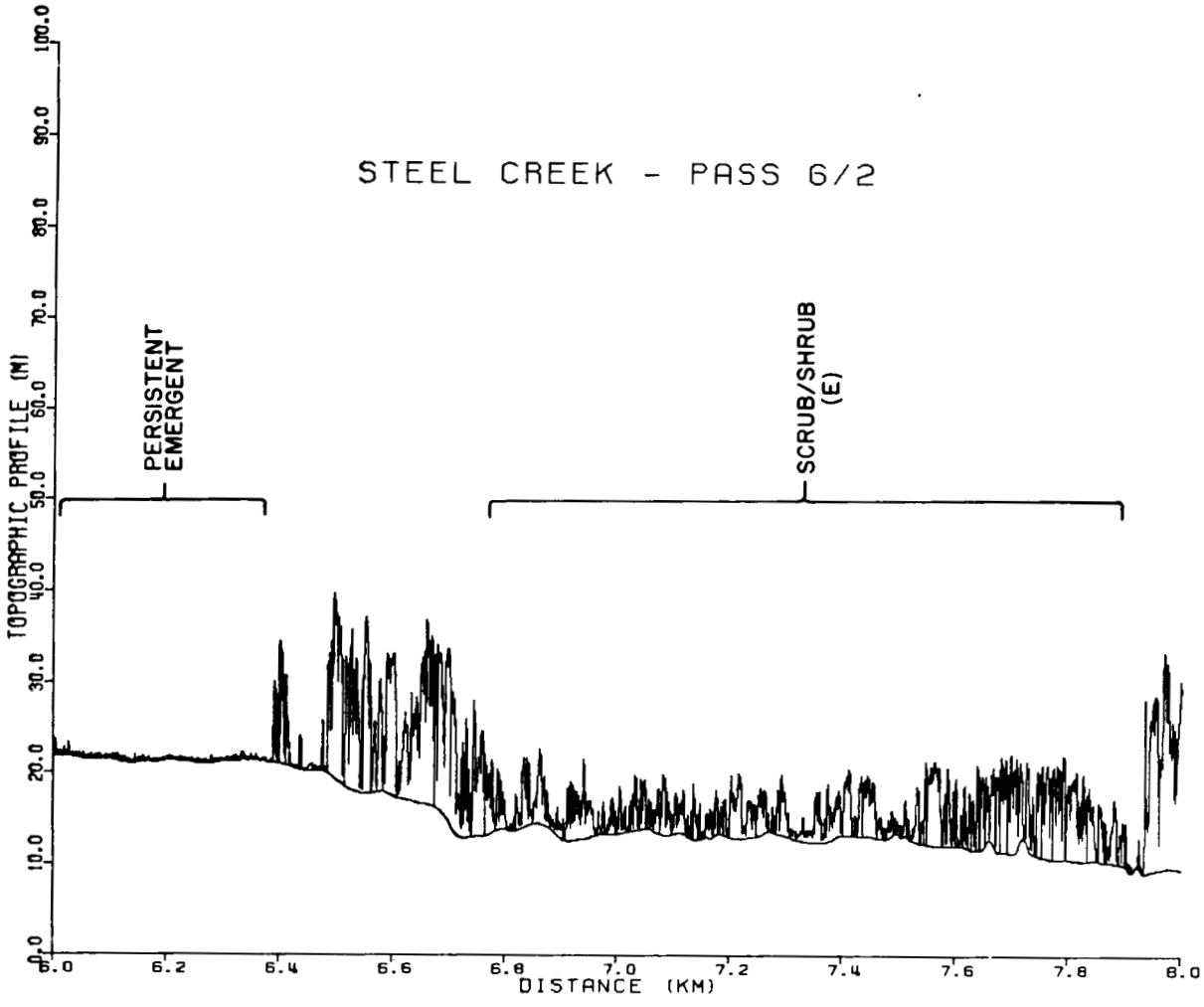

Figure 33. An enlargement of a portion of the elevation profile from Pass 6/2 acquired over the Steel Creek Wetlands. The location of various features of interest are labelled within the figure. The along-track distance (x-axis label) can be used to find the location of the plot in the overall cross-section of Pass 6/2 shown in Figure 29.

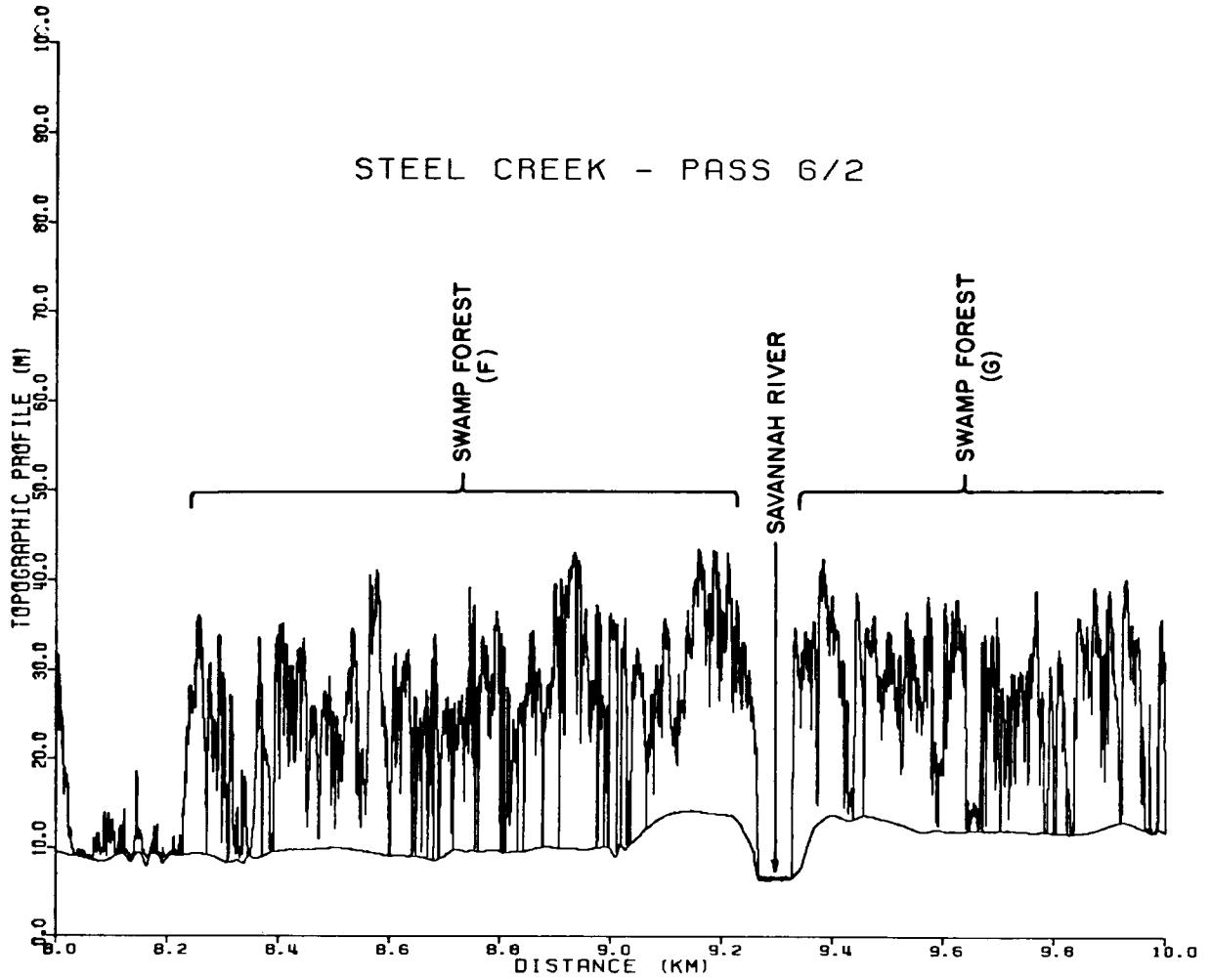

Figure 34. An enlargement of a portion of the elevation profile from Pass 6/2 acquired over the Steel Creek Wetlands. The location of various features of interest are labelled within the figure. The along-track distance (x-axis label) can be used to find the location of the plot in the overall cross-section of Pass 6/2 shown in Figure 29.

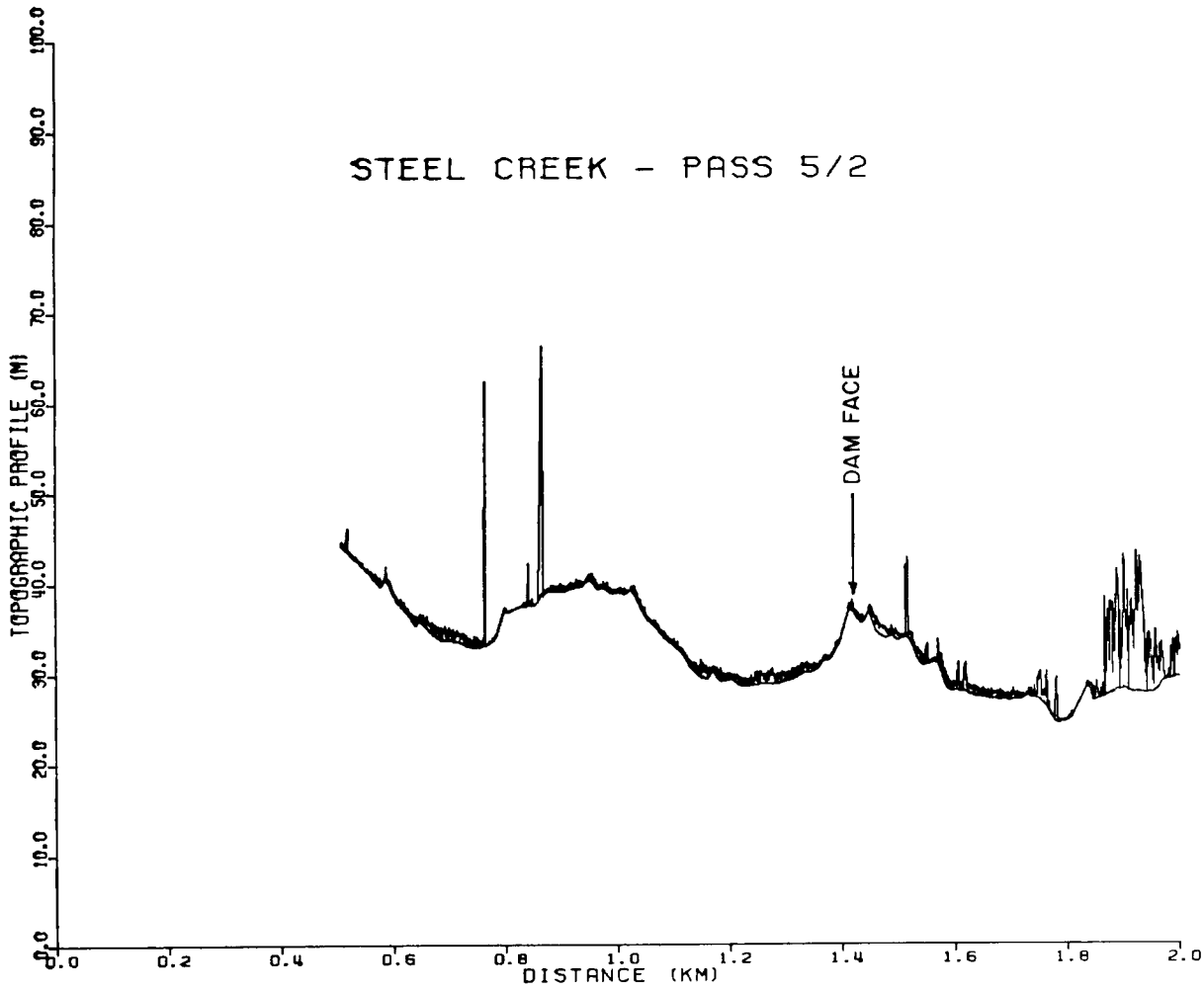

Figure 35. An enlargement of a portion of the elevation profile from Pass 5/2 acquired over the Steel Creek Wetlands. The location of various features of interest are labelled within the figure. The along-track distance (x-axis label) can be used to find the location of the plot in the overall cross-section of Pass 5/2 shown in Figure 29.

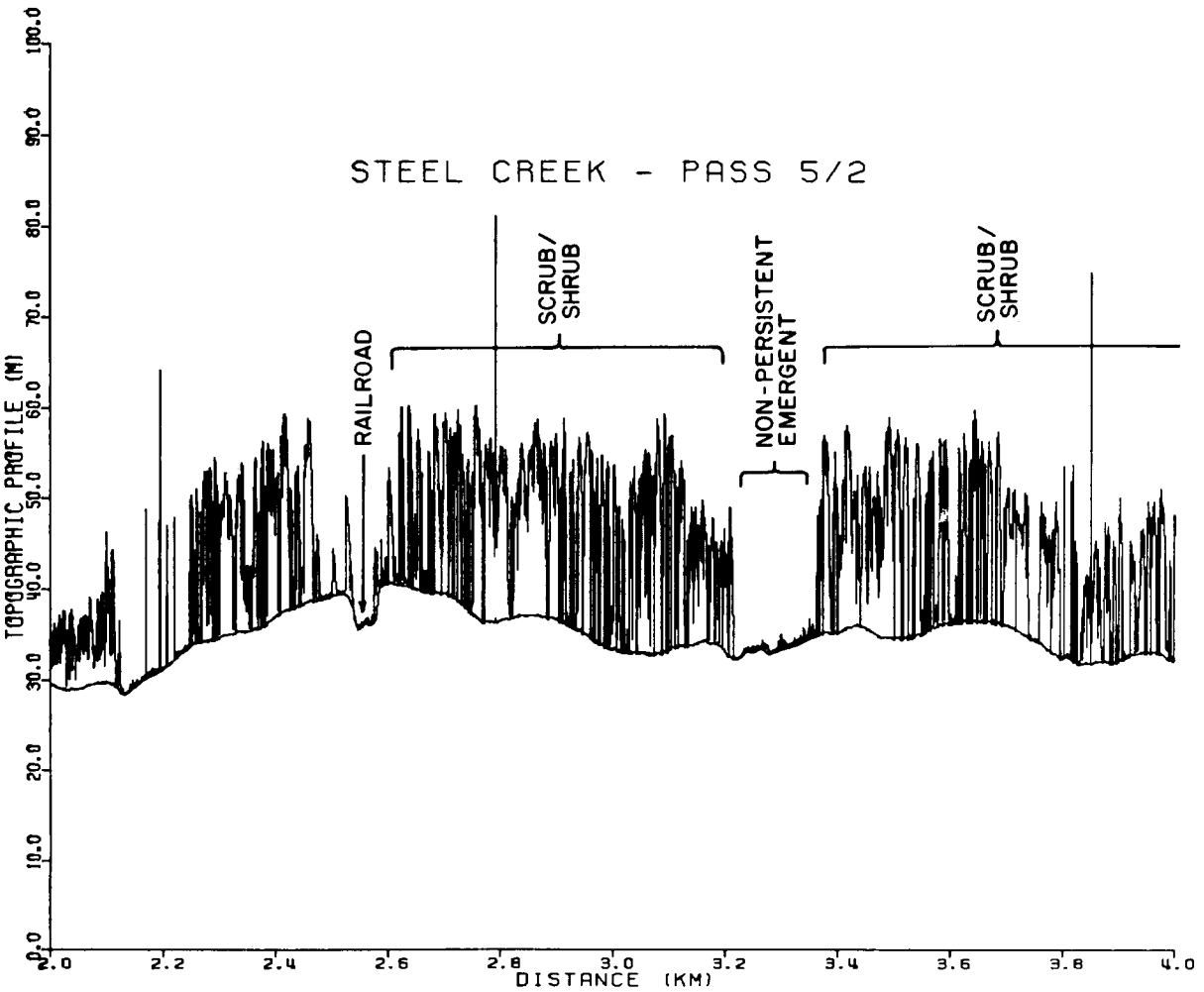

Figure 36. An enlargement of a portion of the elevation profile from Pass 5/2 acquired over the Steel Creek Wetlands. The location of various features of interest are labelled within the figure. The along-track distance (x-axis label) can be used to find the location of the plot in the overall cross-section of Pass 5/2 shown in Figure 29.

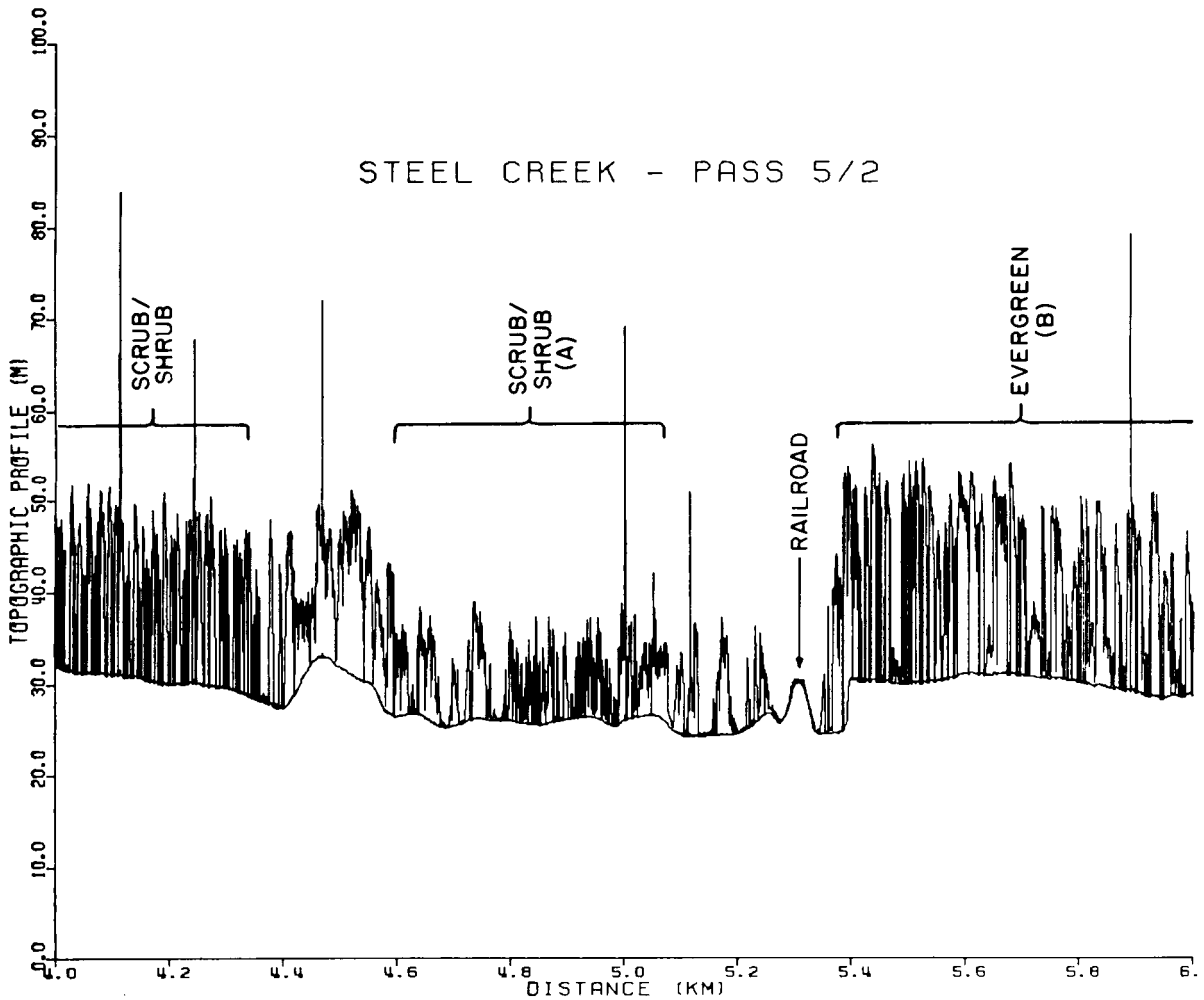

Figure 37. An enlargement of a portion of the elevation profile from Pass 5/2 acquired over the Steel Creek Wetlands. The location of various features of interest are labelled within the figure. The along-track distance (x-axis label) can be used to find the location of the plot in the overall cross-section of Pass 5/2 shown in Figure 29.

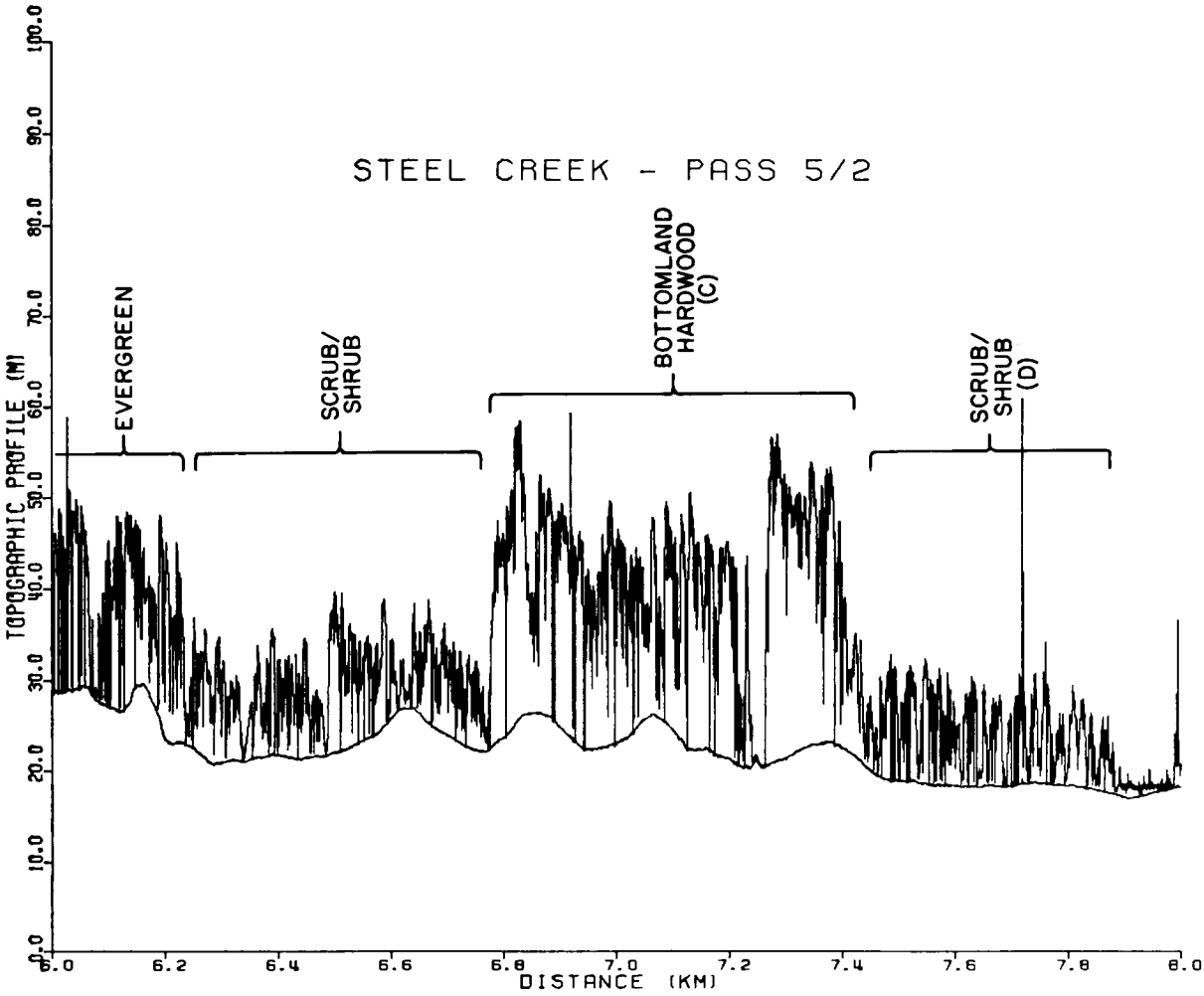

Figure 38. An enlargement of a portion of the elevation profile from Pass 5/2 acquired over the Steel Creek Wetlands. The location of various features of interest are labelled within the figure. The along-track distance (x-axis label) can be used to find the location of the plot in the overall cross-section of Pass 5/2 shown in Figure 29.

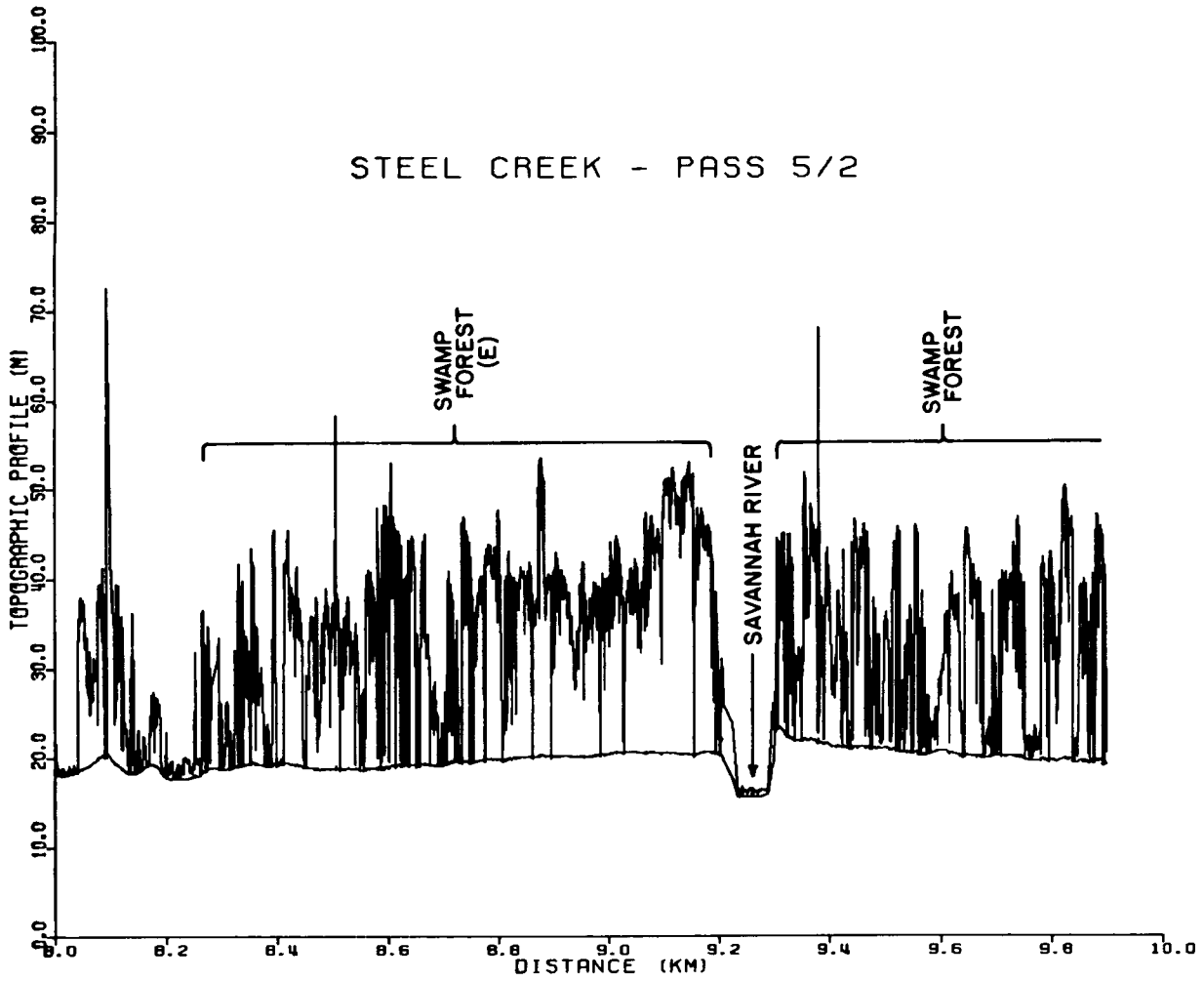

Figure 39. An enlargement of a portion of the elevation profile from Pass 5/2 acquired over the Steel Creek Wetlands. The location of various features of interest are labelled within the figure. The along-track distance (x-axis label) can be used to find the location of the plot in the overall cross-section of Pass 5/2 shown in Figure 29.

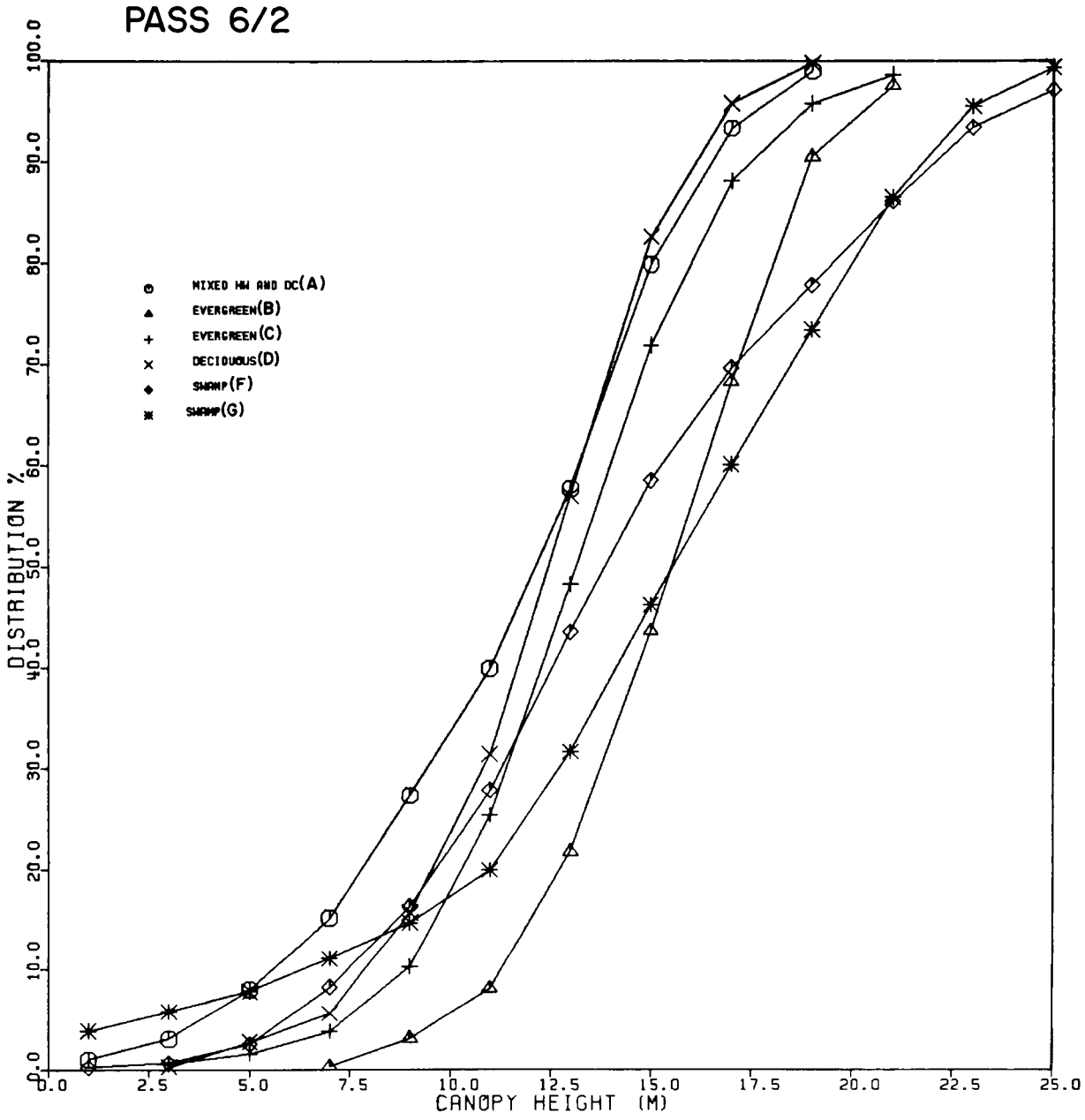

Figure 40. Plot indicating the height distribution for various vegetative cover types in the Steel Creek Corridor. The locations of the areas from which the distributions were calculated are designated by letters which can be found on the enlarged elevation cross-sections plotted in Figures 30-34.

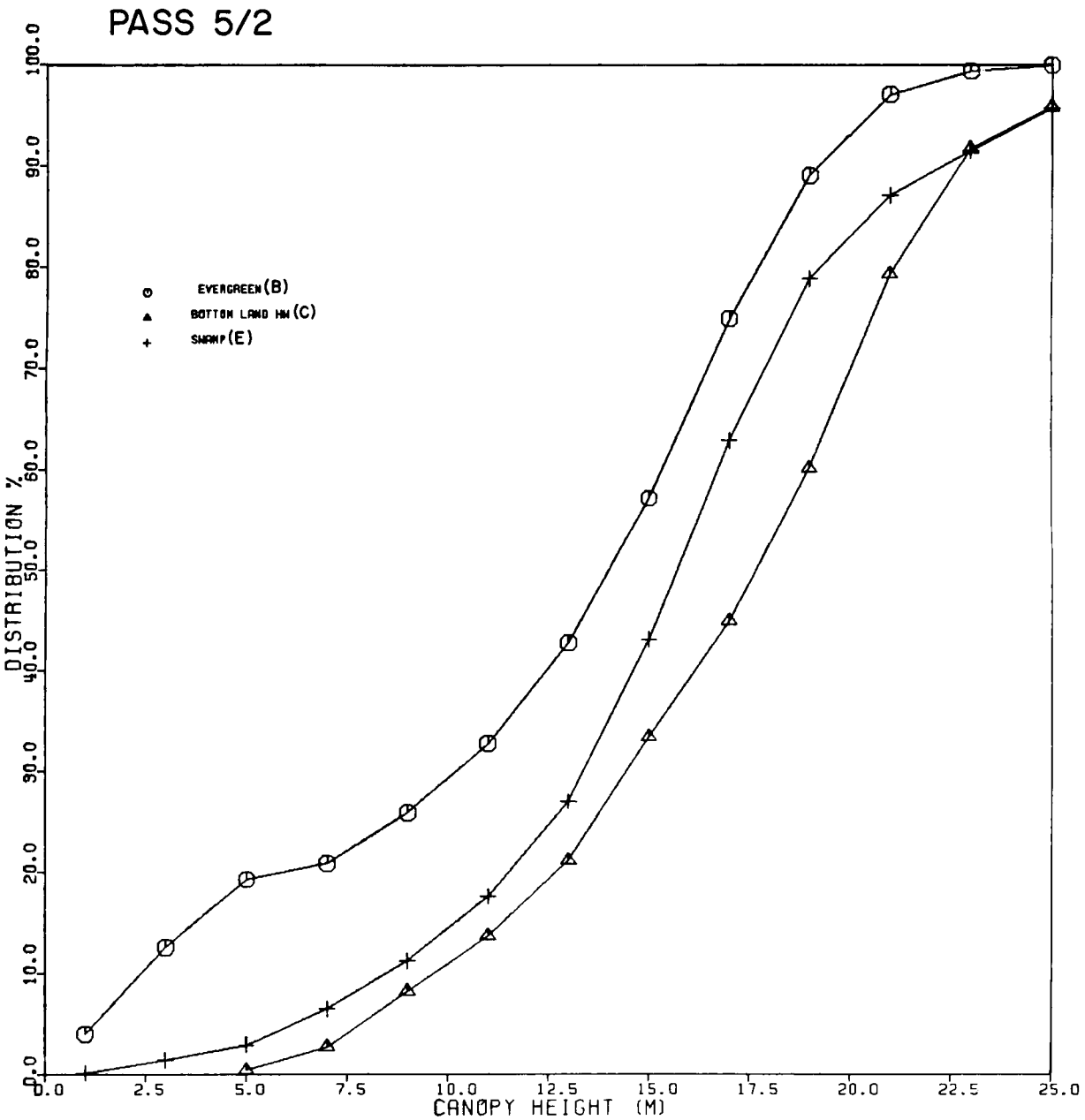

Figure 41. Plot indicating the height distribution for various vegetative cover types in the Steel Creek Corridor. The locations of the areas from which the distributions were calculated are designated by letters which can be found on the enlarged elevation cross-sections plotted in Figures 35-39.

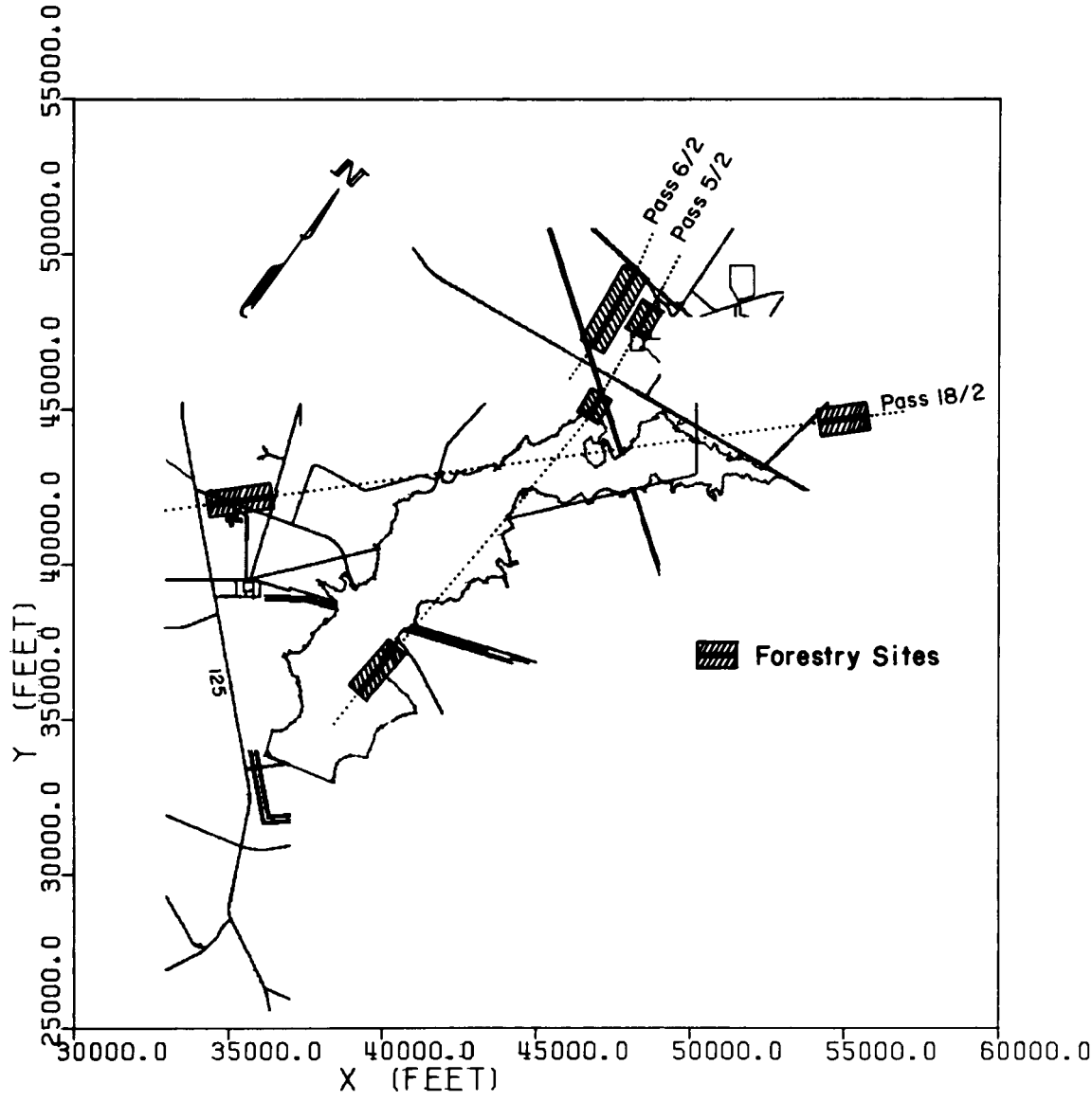

Figure 42. A map indicating the locations of passes where airborne lidar data was collected which will be utilized to produce information related to forestry and forest management. The specific regions along each of the passes where the analysis will be concentrated are shown as shaded areas.

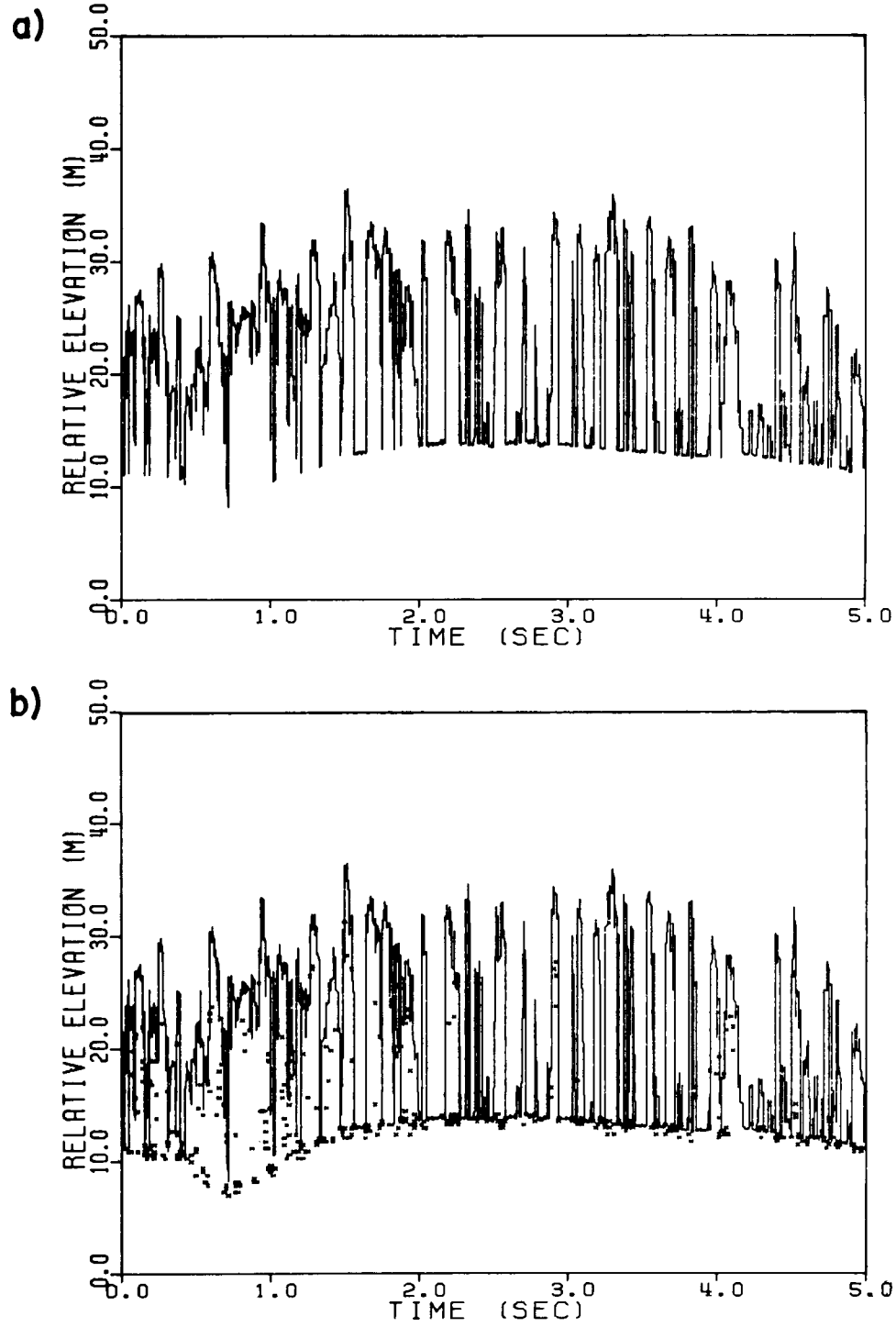

Figure 43. Elevation cross-section showing the detailed information available from the airborne lidar profiling data which is being utilized in the forestry analysis. In the upper profile (a) only the location determined from the initial surface return is plotted. In the lower profile (b) the location of the deepest return from the 8 channel multi-stop is plotted along with the profile shown in (a).

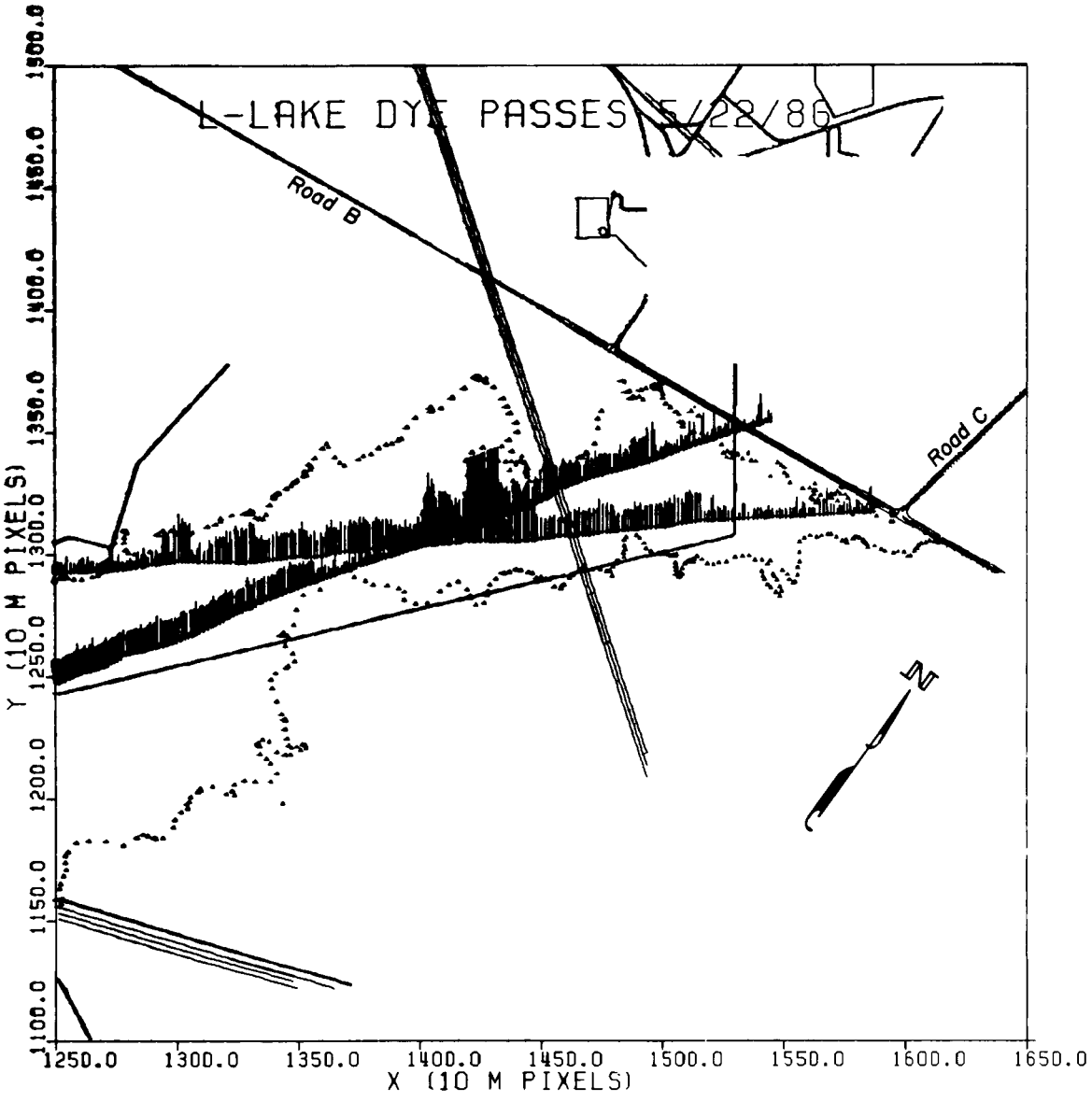

Figure 44. A "stick diagram" showing the relative laser induced Rhodamine dye fluorescence intensity on two of the passes flown over the upper portion of L-Lake during the May 22, 1986, survey. The location of the 190 ft lake surface contour is shown as a series of small, unconnected triangles. The major cultural features are identified in the figure.

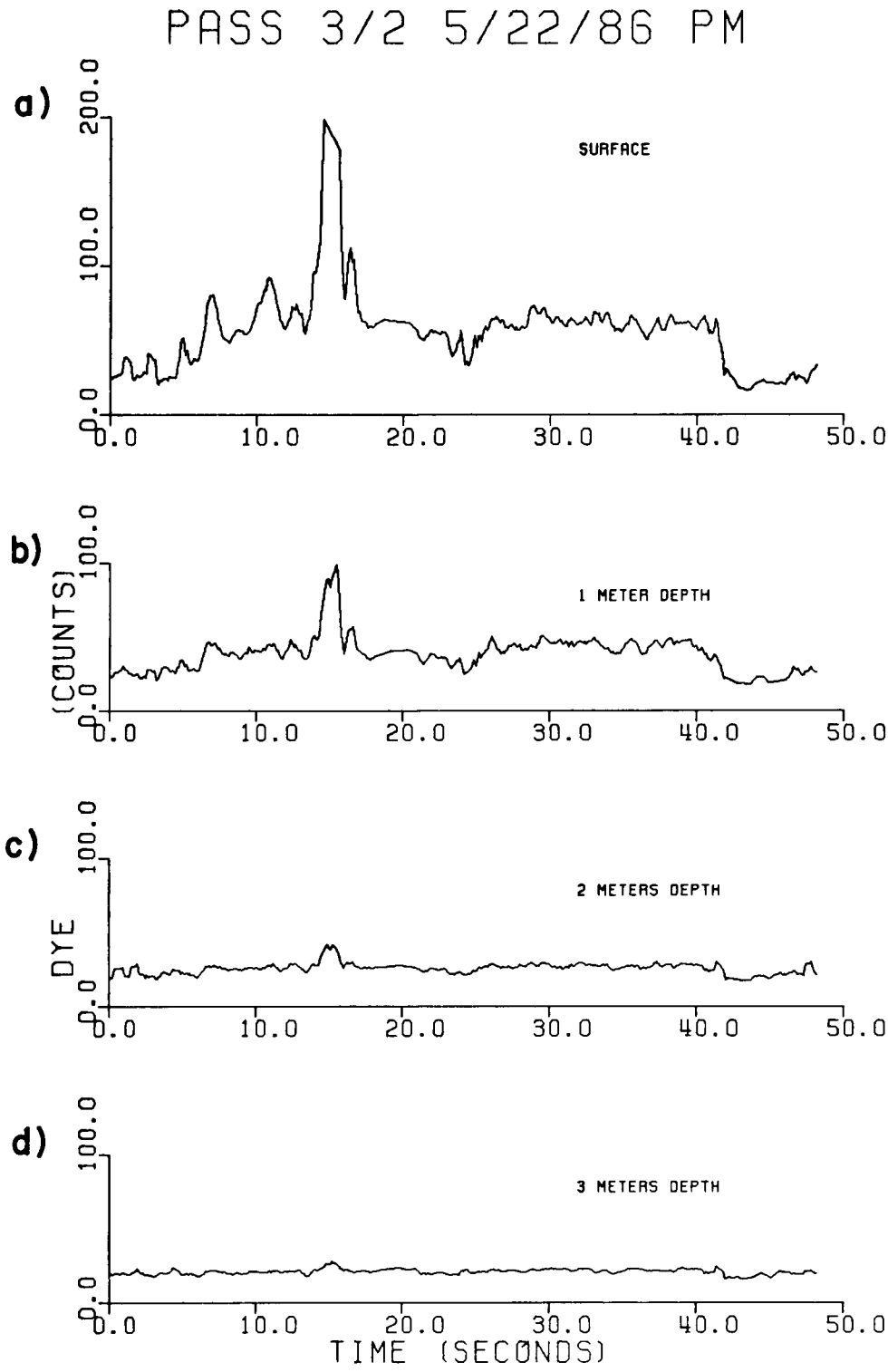

Figure 45. Cross-sectional profiles of relative laser induced Rhodamine dye fluorescence intensity plotted as a function of time. The dye intensity profiles are shown for surface and depths of 1, 2, and 3 m.

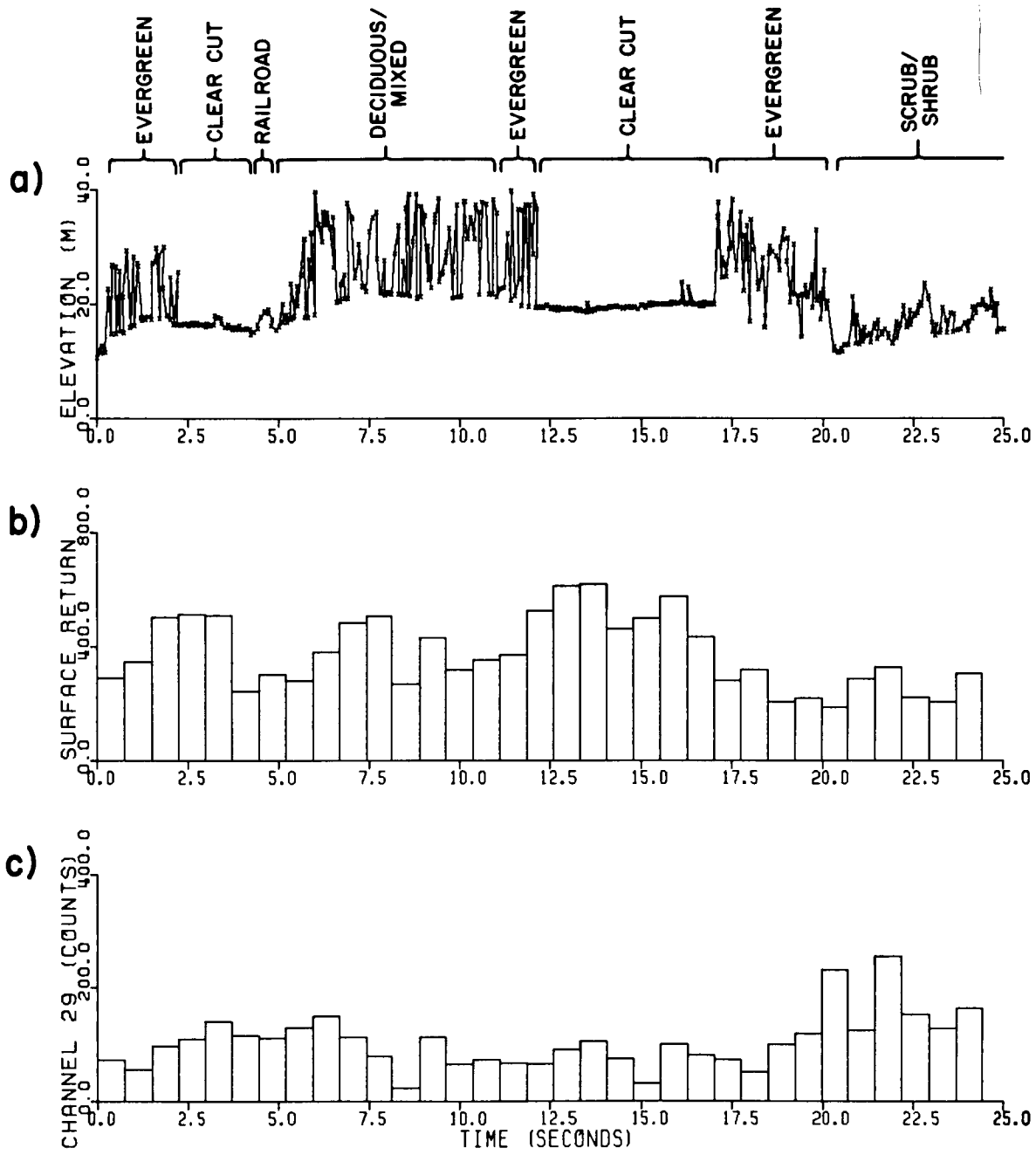

Figure 46. Preliminary results from data collected over the Steel Creek Corridor during the 1986 survey. The upper profile (a) is an elevation cross-section of a pass flown from north to south through the corridor. The mean surface return (b) or reflectivity at 355 nm is plotted in the middle profile. The lower profile (c) is a plot of the mean backscattered signal at 685 nm where chlorophyll fluorescence is centered.

NASA
National Aeronautics and Space Administration

Report Documentation Page

1. Report No.	2. Government Accession No.	3. Recipient's Catalog No.
NASA TM-4007 DOE/SR/14075-1		

4. Title and Subtitle

Airborne Lidar Experiments at the Savannah River Plant - June 1985

5. Report Date

September 1987

6. Performing Organization Code

672

7. Author(s)

William B. Krabill(1) and Robert N. Swift(2)

8. Performing Organization Report No.

10. Work Unit No.

9. Performing Organization Name and Address

(1) NASA Goddard Space Flight Center/Wallops Flight Facility, Wallops Island, VA 23337
(2) EG&G Washington Analytical Services Center Wallops Island, VA 23337

11. Contract or Grant No.

13. Type of Report and Period Covered

Technical Memorandum

12. Sponsoring Agency Name and Address

National Aeronautics and Space Administration
Washington, DC 20546

14. Sponsoring Agency Code

15. Supplementary Notes

16. Abstract

The results of remote sensing experiments at the Department of Energy (DOE) Savannah River Nuclear Facility utilizing the NASA Airborne Oceanographic Lidar (AOL) are presented. The flights were conducted in support of the numerous environmental monitoring requirements associated with the operation of the facility and for the purpose of furthering research and development of airborne lidar technology. Areas of application include airborne laser topographic mapping, hydrologic studies using fluorescent tracer dye, timber volume estimation, baseline characterization of wetlands, and aquatic chlorophyll and photopigment measurements. Conclusions relative to the usability of airborne lidar technology for the DOE for each of these remote sensing applications are discussed.

17. Key Words (Suggested by Author(s))	18. Distribution Statement
Airborne Lidar Topographic Mapping Hydrology	Unclassified - Unlimited STAR Category 43

19. Security Classif. (of this report)	20. Security Classif. (of this page)	21. No. of pages	22. Price
Unclassified	Unclassified	97	A05